Southwest Washington Ozone Study

Final Report

Publication No.99-203

Printed on Recycled Paper

Southwest Washington Ozone Study

Final Report

Prepared by:

Mike Barna, Brian Lamb, Susan O'Neill, and Hal Westberg
Laboratory for Atmospheric Research
Department of Civil & Environmental Engineering
Washington State University

Clint Bowman, Jennifer DeMay, Cris Figueroa-Kaminsky, Sally Otterson,
Washington State Department of Ecology
Air Quality Program

Publication No. 99-203

For additional copies of this document, contact:

Department of Ecology
Publications Distribution Center
PO Box 47600
Olympia, WA 98504-7600
Telephone: (360) 407-7472

For more information or if you have special accommodation needs, please contact Tami Dahlgren at the Air Quality Program at (360) 407-6830 (voice); or (360) 407- 6006 (TDD only).

Acknowledgement

The study team would like to acknowledge the contributions from Weimin Jiang and Don Singleton Canadian National Research Council, Steve Albers and Monica Russell of the Oregon Department of Environmental Quality, and Jennifer Brown of the Southwest Air Pollution Control Authority. We would also like to thank Reynold Metals, Longview Fibre, Weyerhaeuser, B.F. Goodrich Kalama, and numerous individuals, industries, and government agencies that provided emissions inventory information. Finally, we would like to acknowledge Chris Geron and Tom Pierce, US EPA, for their contributions in the development of the biogenic emission inventory.

Table Of Contents

Executive Summary

During the development of the Portland/Vancouver air quality maintenance plan, point sources north of the maintenance area, in Longview, were identified as potentially important contributors of NOx and VOC that might significantly enhance ozone formation within the maintenance area. The Washington Department of Ecology (Ecology), in coordination with the Southwest Washington Air Pollution Control Agency (SWAPCA), contracted with Washington State University (WSU) to conduct a photochemical modeling study to investigate the impact of emissions from Longview on the Portland/Vancouver maintenance area. Ecology and WSU collaborated on this study. This report contains the findings of the WSU and Ecology modeling team.

The approach employed in this study involves the use of a photochemical modeling system with the following components:
a) the Mesoscale Model, Version 5 (MM5), a numerical weather model,
b) a detailed anthropogenic and biogenic emission inventory, specific for the region,
c) CALMET, a diagnostic wind field and boundary layer model that merges wind fields from MM5 with available observations, and
d) CALGRID, a numerical photochemical model that uses the emission inventory and the CALMET meteorological fields to predict ambient ozone and other pollutant concentrations throughout the model domain.

The main objective of this study was to address the question: What is the impact of the emissions from the major industrial point sources in Cowlitz County on the ozone levels in the Portland/Vancouver maintenance area? This objective includes an investigation of the impact of a reduction of VOC emissions, a reduction of NOx emissions, and reductions of both VOC and NOx emissions for the identified major point sources. In this case, the reduction of VOC emissions includes a reduction of CO emissions.

A second objective of this work was to improve the regional photochemical modeling system and to evaluate the performance of the model compared to ambient observations. A key aspect of this objective was to run the MM5 prognostic weather model with a fine resolution grid in order to improve the meteorological fields used in the chemical transport model.

An ozone episode which occurred during 11-14 July 1996 was selected for simulation due to the availability of ambient measurements and because it appeared to be generally representative of the synoptic weather patterns conducive to ozone formation in the Pacific Northwest. The event was simulated by running the MM5 model with a relatively fine grid resolution of 5 km, passing the MM5 results to the CALMET diagnostic model to merge available observations with the predicted wind fields, and using CALGRID to predict ozone concentrations throughout the Portland/Vancouver area during the event. In the process of simulating this event, a very considerable amount of effort was required to obtain a representative MM5 solution with reduced surface wind speeds at the 5 km grid scale. In turn, considerable work was also required to merge the MM5 solution with observations in CALMET to obtain wind fields which agreed with

surface wind observations and which produced ozone concentration patterns in agreement with the available monitoring data in the Portland/Vancouver region. In both instances, the amount of effort was far more than originally anticipated. As a result, original plans to model two or even three separate ozone episodes were set back, and other models runs to investigate overall model sensitivity were greatly reduced. Thus, the results of this analysis are based upon a successful simulation of the 11-14 July 1996 event.

Given the complicated terrain and associated wind patterns in the area, the model performance appears to be within an acceptable range, although it is clear that the model has a tendency to underestimate observed ozone concentrations for the base case simulation. The normalized bias in ozone at the four monitoring stations in the area ranged from -7% to -41%, while the differences between the average of the daily maximum ozone at each site was approximately 10% at three sites and 30% at a fourth site. As indicated previously, one objective of this work was to improve the overall performance of the regional modeling system. This was primarily accomplished through changes in the method used to generate the input meteorological fields. No changes in the emission inventory were required to obtain a reasonable level of agreement between observed and predicted ozone concentrations, which suggests that the emission inventory is not in significant error.

The major industrial sources in Cowlitz County consist of two pulp mills (Longview Fibre and Weyerhaeuser), an aluminum smelter (Reynolds Metals), and a synthetic chemical manufacturing facility (B.F. Goodrich Kalama). During the 11-14 July 1996 episode, the Longview Fibre facility was operating at 60% of normal operating levels. The emission inventory reflected this situation. However, to address changes in emissions corresponding to possible control levels, it is appropriate to employ the normal operating situation as the base emissions. Consequently, two different base case runs were completed. The first reflected the actual conditions during the episode. The results from this base case were used to evaluate model performance relative to available ozone observations. In the second base case, emissions from Longview Fibre were increased to simulate normal operating conditions. This adjusted base case was then used as the basis for comparison to the following sensitivity runs:

1. Modification of point source VOC/CO emissions to reflect 90%, 80%, and 60% of actual emissions;
2. Modification of point source NOx emissions to reflect 90%, 80%, and 60% of actual emissions;
3. Modification of point source VOC/CO, and NOx emissions to reflect 90%, 80%, and 60% of actual emissions; and
4. Modification of point source emissions to reflect zero NO_x emissions, zero VOC/CO emissions, and zero VOC/CO and NO_x emissions.

Thus, two base case runs and twelve sensitivity runs were completed for this study. The purpose of these sensitivity runs was to provide an estimate of the change in ozone levels experienced in the ozone maintenance region as a result of changes in point source emissions in Cowlitz County.

When comparing the base case scenario with the series of sensitivity runs, the following observations are relevant:

- Maximum predicted ozone concentrations occur south of Portland during the 11-14 July 1996 episode. A maximum ozone concentration of 172 ppb was predicted 50 km south of Portland at 1600 LST, 14 July 1996. Both reductions and enhancements of ozone concentrations occurred in different locations within the study region when emissions from the Longview industrial sources were reduced. The region of maximum predicted ozone concentrations does not coincide with the area affected by reduction in emissions from the industrial facilities, nor does it coincide with the current ozone monitoring site locations.

- Reducing NOx emissions, either alone or with VOC emission reductions, causes an increase in ozone concentrations within the immediate vicinity of the industrial sources. The increase is due to a decrease in the amount of ozone titrated by NO emissions. However, the increase tends to be most significant at night, and occurs in an area with low ambient ozone concentrations. The enhancement was approximately 5 ppb ozone for the 60% of normal NOx emission cases.

- Reducing NOx emissions, either alone or with VOC emission reductions, causes a decrease in ozone concentrations further downwind of the sources, with the maximum effect in a region to the southwest of Portland during late afternoon. The reduction was approximately 11 ppb for the 60% of normal NOx emissions cases. The location of the maximum reduction occurs approximately 70 km downwind of the Cowlitz County. point sources, in an area where the predicted ambient ozone levels are approximately 90 ppb.

- Reducing VOC emissions has a much smaller effect on ambient ozone concentrations compared to cases with reduced NOx emissions. For the 60% of normal VOC emissions case, the reduction in ozone is approximately 2 ppb.

- At the monitoring sites, the largest enhancement equaled 5 ppb at Sauvie Island. The enhancement occurred at night when the ozone base case concentration was 35 ppb. The largest reduction equaled 11 ppb at Milwaukee, and it occurred in late afternoon when the ozone base case concentration was 85 ppb. Both of these maximum differences were obtained for the zero VOC/CO and NOx emissions run.

- About two times greater ozone concentration reductions were achieved per ton of NOx reduced than per ton of VOC reduced from the emissions of the Longview industrial sources. In contrast, about five times higher ozone concentration enhancements were obtained in the vicinity of the industrial complex per ton of NOx reduced than per ton of VOC reduced. For both enhancements and reductions, the trend of differences in the ozone concentrations versus changes in emissions is essentially linear.

In summary, modeled emission reductions from the four Longview industrial sources showed that ozone levels can be increased immediately downwind of the sources. At the same time,

ozone levels are reduced compared to the base case further downwind of the industrial sources. The reduced ozone levels do not occur in the region where the maximum ozone levels are predicted to occur. As a result, it does not appear from this analysis that changes in emissions at the industrial sources in Cowlitz County will have a significant impact upon the maximum levels of ozone produced in the Portland/Vancouver airshed. It should be emphasized, however, that these results are based upon only one simulation, and that simulations of other ozone events may yield different results.

Introduction

Tropospheric ozone, a component of photochemical smog, is formed in the atmosphere through a complex series of reactions involving volatile organic compounds (VOC), oxides of nitrogen (NOx), and sunlight. Ozone is a strong oxidizing agent. It can irritate the lung passages and reduce lung function. The Federal Clean Air Act directed the Environmental Protection Agency (EPA) to identify limits on the amount of ozone that can be present in the air without harming human health or the environment. A new federal standard for ozone was announced on June 25, 1997. To determine whether an area is in compliance of this new ozone standard, over three consecutive years, the fourth highest eight-hour average measurement reported each year is averaged over the three years. If this three year average is greater than 85 ppb, the federal standard is exceeded.

Motor vehicle exhaust is generally the largest source of nitrogen oxides. There are many sources of VOC. VOC sources can either be anthropogenic, such as motor vehicle exhaust, consumer solvents and gasoline vapor, or biogenic, such as isoprene and terpene emissions from vegetation.

Maintenance plans have been approved for two areas in the State of Washington that were previously not meeting the federal ozone standard. One maintenance area is in the Puget Sound region, and roughly consists of Pierce, King and Snohomish counties. Another area contains Vancouver, WA and includes Portland, OR. These plans describe control measures designed to reduce ozone formation.

During the development of the Portland/Vancouver maintenance plan, it was recognized that the effect of point sources in the maintenance area needed to be better understood. In particular, point sources north of the maintenance area, in Longview, were identified as potentially important sources for NOx and VOCs that might significantly enhance ozone formation within the maintenance area. The Washington Department of Ecology (Ecology), in coordination with the Southwest Washington Air Pollution Control Agency (SWAPCA), contracted with Washington State University (WSU) to conduct photochemical modeling to investigate the impact of emissions from Longview on the Portland/Vancouver maintenance area. Ecology and WSU collaborated on this study. This report contains the findings of the WSU and Ecology modeling team.

The approach employed in this study involves the use of a photochemical modeling system with the following components:

- MM5 (Mesoscale Model, Version 5), a numerical prognostic weather model which provides detailed wind fields for the selected ozone episode period,
- A detailed anthropogenic and biogenic emission inventory, specific for the Cascadia region, that provides hourly, gridded emissions of 21 different model species, including 17 lumped VOC species,

- CALMET, a diagnostic wind field and boundary layer model that interpolates wind fields from MM5 with available surface and upper air observations to produce hourly, gridded, three-dimensional wind and boundary layer parameter fields for the modeling period, and
- CALGRID, a regional photochemical air quality model that uses the detailed emission inventory, a version of the SAPRC90 chemical kinetic mechanism optimized for the Cascadia region, and the CALMET meteorological fields to predict ambient ozone and other pollutant concentrations throughout the model domain.

This report describes the second phase in the overall development of a regional photochemical modeling system for the Pacific Northwest. In the first phase, the various components of the modeling system were assembled, the necessary input data were compiled, and an initial simulation of an ozone event which occurred during 11-14 July 1996 were completed (Ecology, 1997). This first phase of model development was conducted within the framework of a study aimed at the investigation of the impact of Stage II vapor recovery systems employed at gasoline stations within Washington counties. Predicted ozone concentrations from this initial simulation were typically less than observed, and in some cases, the differences were significant. In an analysis of these results, it was determined that the meteorological wind fields did not appear to produce the correct transport compared to observations; in addition, a few missing sources or other inconsistencies in the emission inventory were identified, and other sources of uncertainty were documented. In the second phase of this work, the intent was to continue the development of the regional modeling system by addressing these problem areas. This work was pursued within the context of the present study which addresses the impact of industrial point sources within the southern portion of the Cascadia domain.

Objectives

The main objective of this study was to address the question:

What is the impact of the emissions from the major industrial point sources in Cowlitz County on the ozone levels in the Portland/Vancouver maintenance area?

This objective includes the investigation of the impact of reductions in VOC emissions, reduction of NOx emissions, and reduction of both VOC and NOx emissions for the identified major point sources in Cowlitz County. In this case, a reduction of VOC emissions includes a reduction of CO emissions.

A second objective of this work was to improve the regional photochemical modeling system and to evaluate the performance of the model with respect to ambient observations. A key aspect of this objective was to run the MM5 prognostic weather model with a fine resolution grid (i.e., 5 km) in order to improve the meteorological fields used in the chemical transport model.

Study Design

The original study design included two separate tasks. First, improvements in the simulation of the base case ozone event, 11-14 July 1996, were to be obtained by running the MM5 model with greater resolution and using four-dimensional data assimilation (FDDA), correcting various

portions of the emission inventory, and conducting the simulation over a slightly larger domain than was used in the first phase of the model development. After a suitable base simulation was achieved, a series of sensitivity runs were to be completed that addressed the impact upon ozone formation of VOC and NOx emissions from the four large industrial sources located in Cowlitz County. Finally, if time and resources allowed, this two step process was to be repeated for a second ozone episode, which occurred 22-28 July 1996.

To assess the accuracy of the overall photochemical modeling system, the study included an evaluation of the predicted meteorological fields using available surface and upper air observations, and an evaluation of predicted surface ozone concentrations using available surface measurements. Thus, the study consisted of four sub-tasks: (1) development of the emission inventory and modeling input data, (2) performing MM5/CALMET/CALGRID simulations of the base case scenario, (3) running a series of sensitivity runs that involved modifying the emissions from the point sources in Cowlitz County and, subsequently, comparing each one to the base case, and (4) quality assurance and model validation.

Model Input Development

Model Domain

As part of the overall improvement to the regional modeling system, the CALMET/CALGRID modeling domain was enlarged from 60 x 114 grids to 74 x 132 grids. The horizontal grid size was not changed from the original resolution of 5 km x 5 km. The domain size was increased to account for air flow across the crest of the Cascades and through the Columbia River Gorge, and the domain origin was shifted south to address the possibility of contributions from Salem and other urban areas south of Portland. The number of vertical layers in MM5 was kept at 32, and the number of vertical layers in CALMET/CALGRID was kept at 10 as described in Appendices B and C. Three nested domains were used in the MM5 simulation with grid sizes of 45 km, 15 km and 5 km. The inner MM5 domain was selected to match the CALMET/CALGRID domain as closely as possible. The MM5 domains are shown in Appendix B. The topography of the new domain is shown in Figure 1. New MM5 land use data were obtained from the University of Washington at a 1 km scale and includes minor modifications to the standard set of MM5 land use classes to include mixed forest and agricultural areas. This land use distribution was employed in the MM5, CALMET, and CALGRID simulations.

While the domain size was increased for inventory development and for the original base case simulation, a smaller sub-domain (60 x 80 grids) was employed for the large number of iterative CALMET/CALGRID runs required to achieve an acceptable base case simulation and also for the large number of sensitivity runs for the industrial point source impact investigation. The use of a sub-domain was necessary since it involved significantly less computer execution time and disk storage space. Comparison of results from the large domain and the smaller sub-domain indicated there was effectively no change in predicted ozone concentrations in the Portland/Vancouver area for the base case simulation. A portion of the sub-domain and the meteorological and ozone monitoring stations in the Portland/Vancouver vicinity are shown in Figure 2.

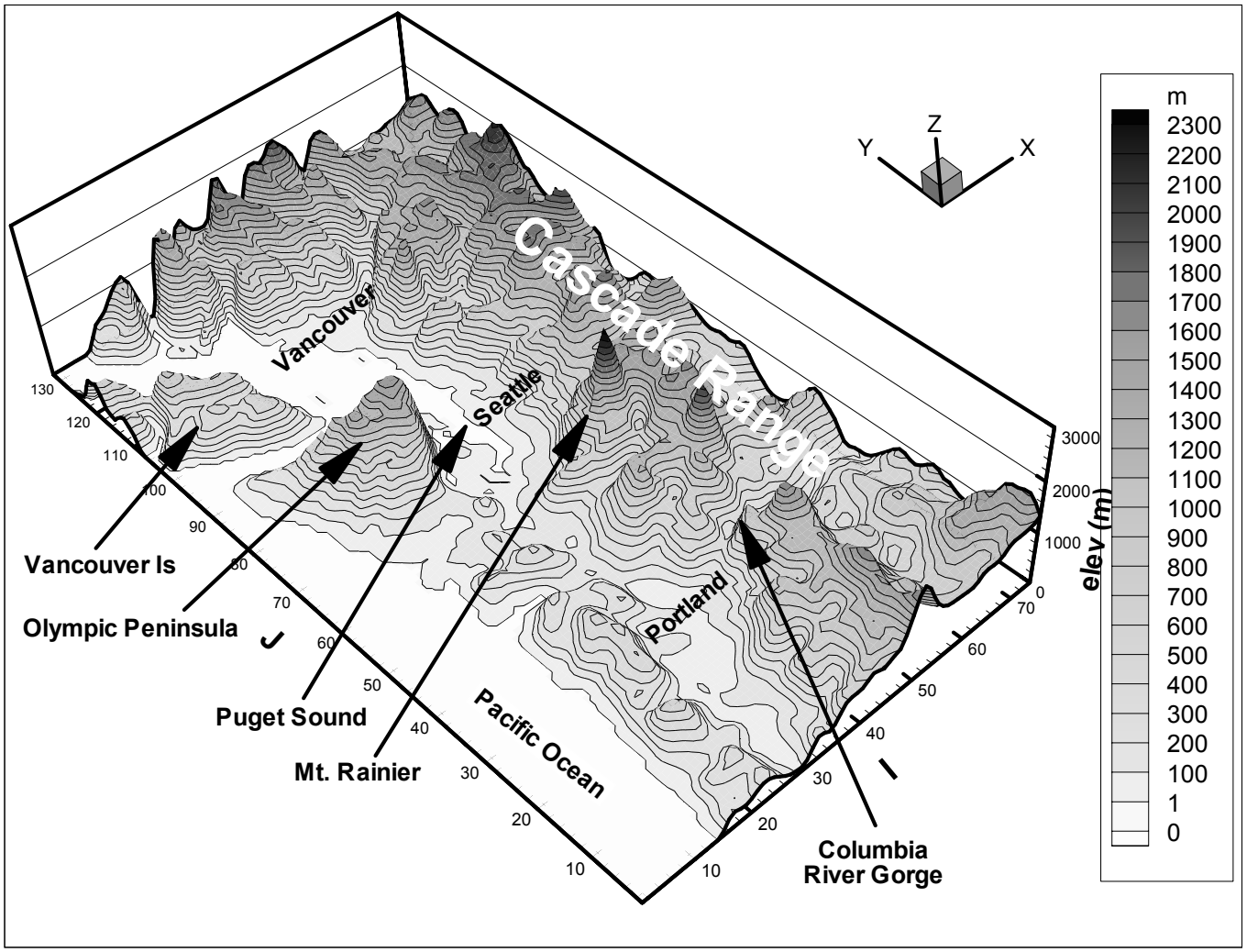

Figure 1. Topography of the enlarged modeling domain (74 x 132 grids); vertical scale is exaggerated.

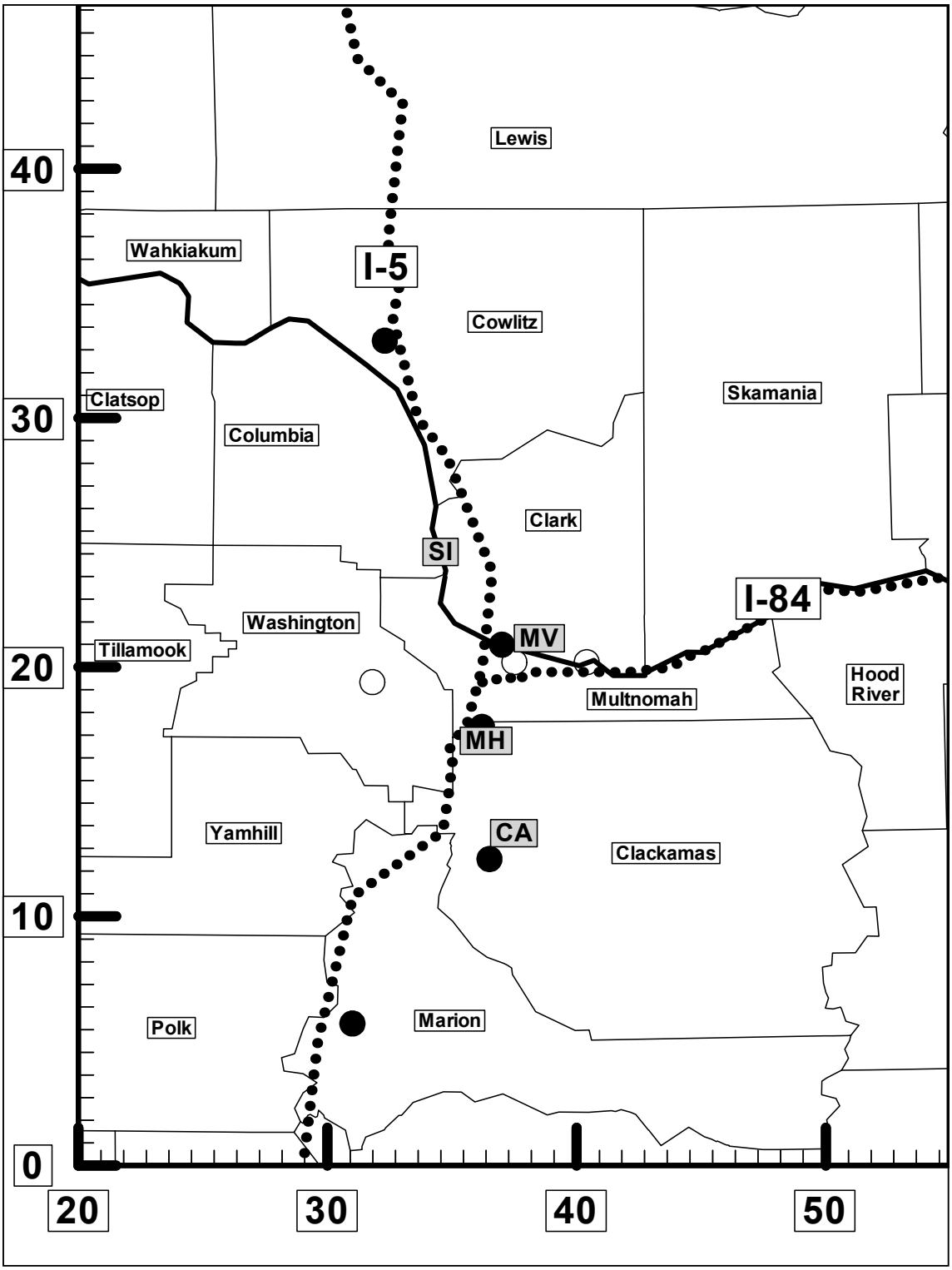

Figure 2. Portion of the Portland/Vancouver sub-domain used for iterative CALMET/CALGRID simulations. Surface meteorological sites (solid circles) and ozone monitors (squares with two character label) are shown.

Episode Selection

Three recent ozone events were selected for possible modeling based on the availability of ozone, VOC, and meteorological observation data. These events were believed to be representative of ozone episodes in the Portland/Vancouver area; concentrations measured during these episodes are shown in the following table.

Table 1. Observed Peak Ozone Concentrations in ppb

	MT. View		Milwaukee		Carus		Sauvie Island	
Date	1-Hr Avg.	8-Hr Avg.	1-Hr Avg.	8-Hr Avg.	1-Hr Avg.	8-Hr Avg.	1-Hr Avg.	8-Hr Avg.
7/13/96	90	82	91	85	124	106	94	84
7/14/96	112	97	145	120	108	102	90	79
7/24/96	85	73	no data	no data	110	86	61	54
7/25/96	86	72	no data	no data	89	83	83	68
7/26/96	108	87	119	94	149	113	88	77
7/27/96	95	75	90	67	111	99	87	70
7/19/97	59	53	65	55	77	65	59	52
7/20/97	77	62	101	73	73	68	48	38

Emission Inventory

Ecology developed the emission inventory for the CALGRID runs. An event-specific emission inventory was developed for the ozone episode that took place 11-14 July 1996. Speciated VOC, NOx, CO, and SO_2 emissions were calculated for point, area and mobile emission sources. The development of the emission inventory is described in Appendix A. The data generated from the emission models and calculations were gridded and temporally adjusted.

Contour maps of the anthropogenic area and mobile VOC and NOx emissions are shown in Figures 3 and 4, respectively, for 0800 on Friday, 12 July 1996. These emission maps reflect the distribution of roadways and population centers within the domain. Maximum VOC emissions equaled approximately 0.3 MT/hr/grid (MT = metric ton, each grid measures 5 km x 5 km), while maximum NOx emissions equaled 0.12 MT/hr/grid. Similar maps for the biogenic emissions of VOC and NOx for a mid-afternoon period are shown in Figures 5 and 6. In this case, the biogenic VOC emissions are more evenly distributed throughout the domain compared to the anthropogenic emissions. Higher emissions tend to occur in the southern portion of the domain; this pattern is due to the distribution of vegetation species and to the warmer temperatures that existed in this region. Maximum biogenic VOC emissions equaled approximately 1.4 MT/hr/grid, while maximum NOx emissions from soils were very small at less than 0.002 MT/hr/grid.

A time series of the anthropogenic emissions is shown in Figure 7 for the modeling period. The early morning and late afternoon peaks due to rush hour traffic are evident during the weekdays, but these peaks are missing on the weekends. Somewhat surprisingly, daytime VOC emissions are higher on the weekends compared to the weekdays, while NOx emissions are reduced on the weekends compared to the weekdays. The increased emissions of VOCs on the weekend are due to increased recreational boating and use of lawn/garden equipment. The decrease in NOx emissions on the weekend is due to the reduction of heavy duty diesel, commercial, industrial, and construction equipment use. A summary of the average daily emissions during the four day period is given in Table 2.

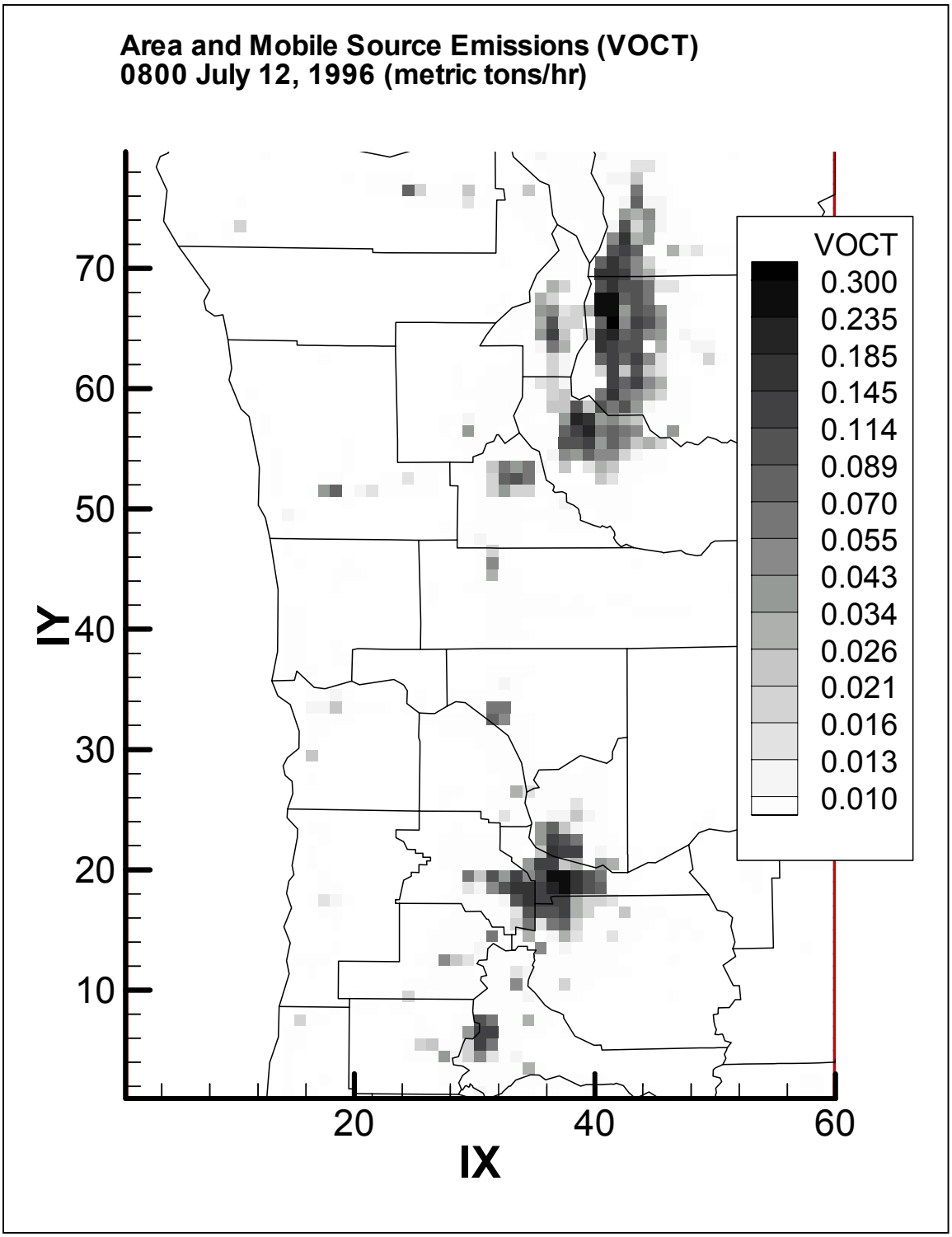

Figure 3. Spatial distribution of area and mobile VOC emissions from anthropogenic sources during 0800 on Friday, July 12, 1996.

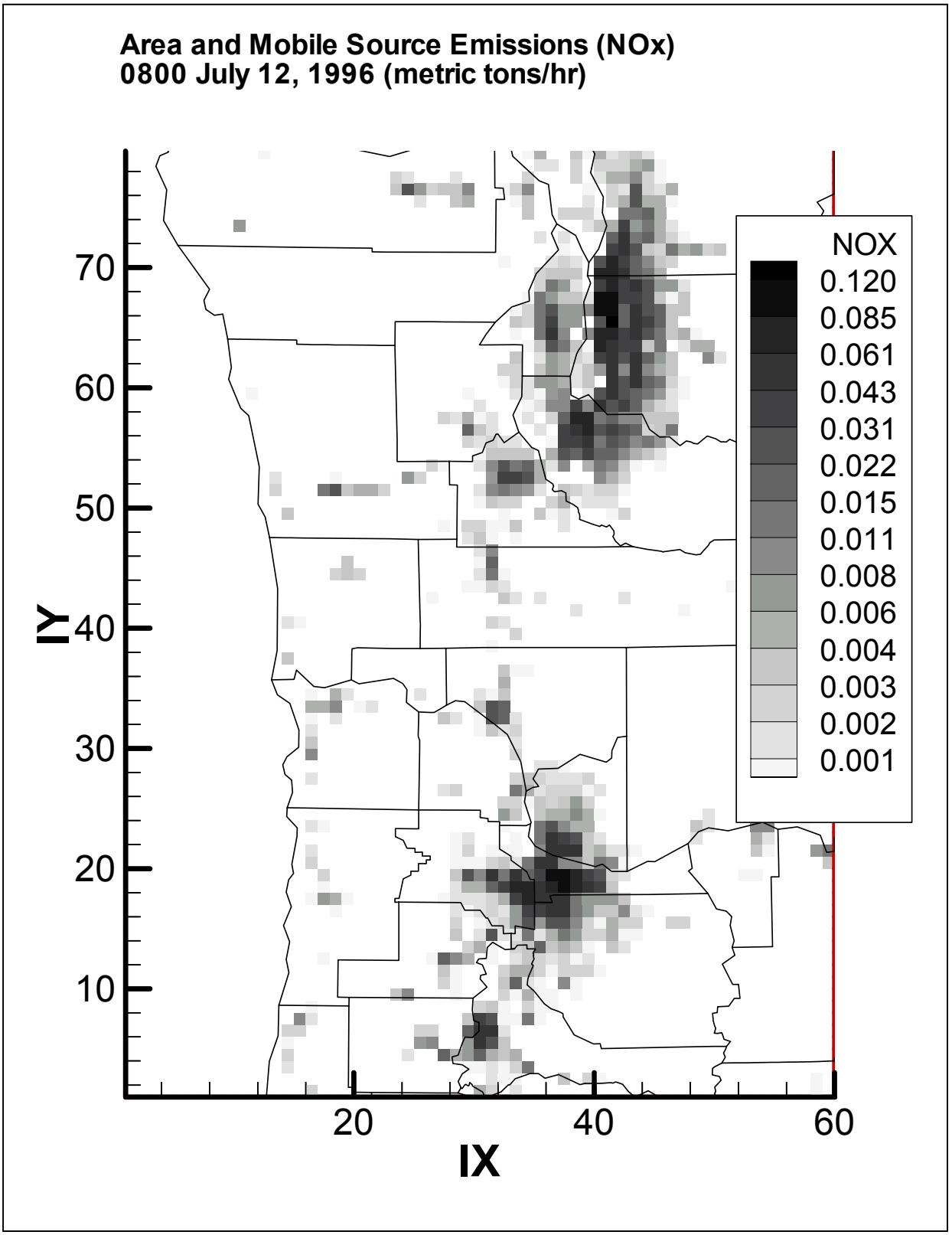
Area and Mobile Source Emissions (NOx)
0800 July 12, 1996 (metric tons/hr)
NOX
0.120
0.085
0.061
0.043
0.031
0.022
0.015
0.011
0.008
0.006
0.004
0.003
0.002
0.001
IY
70
60
50
40
30
20
10
20
40
60
IX

Figure 4. Spatial distribution of area and mobile NOx emissions from anthropogenic sources during 0800 on Friday, July 12, 1996.

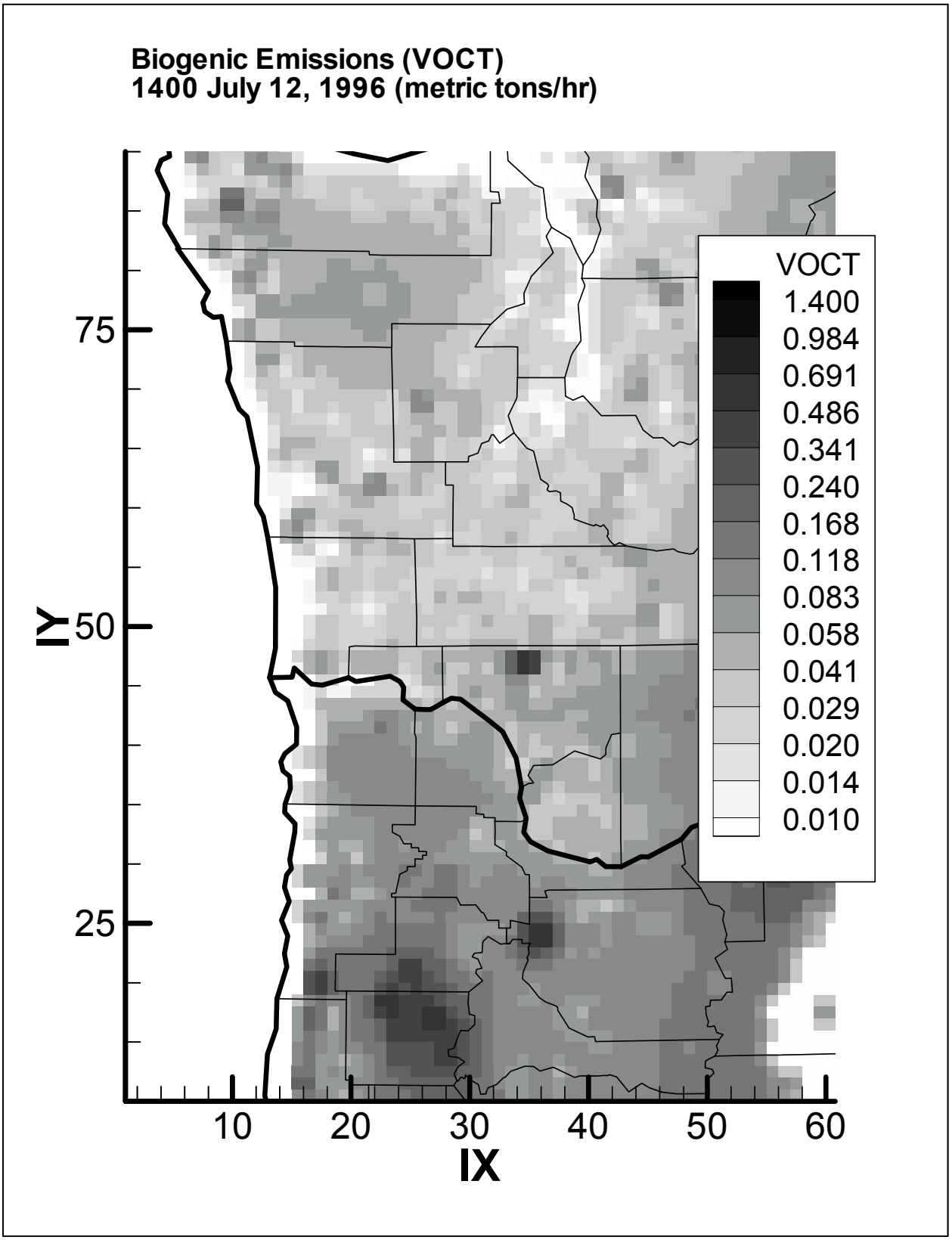

Figure 5. Spatial distribution of biogenic VOC emissions during 1400 on Friday, July 12, 1996.

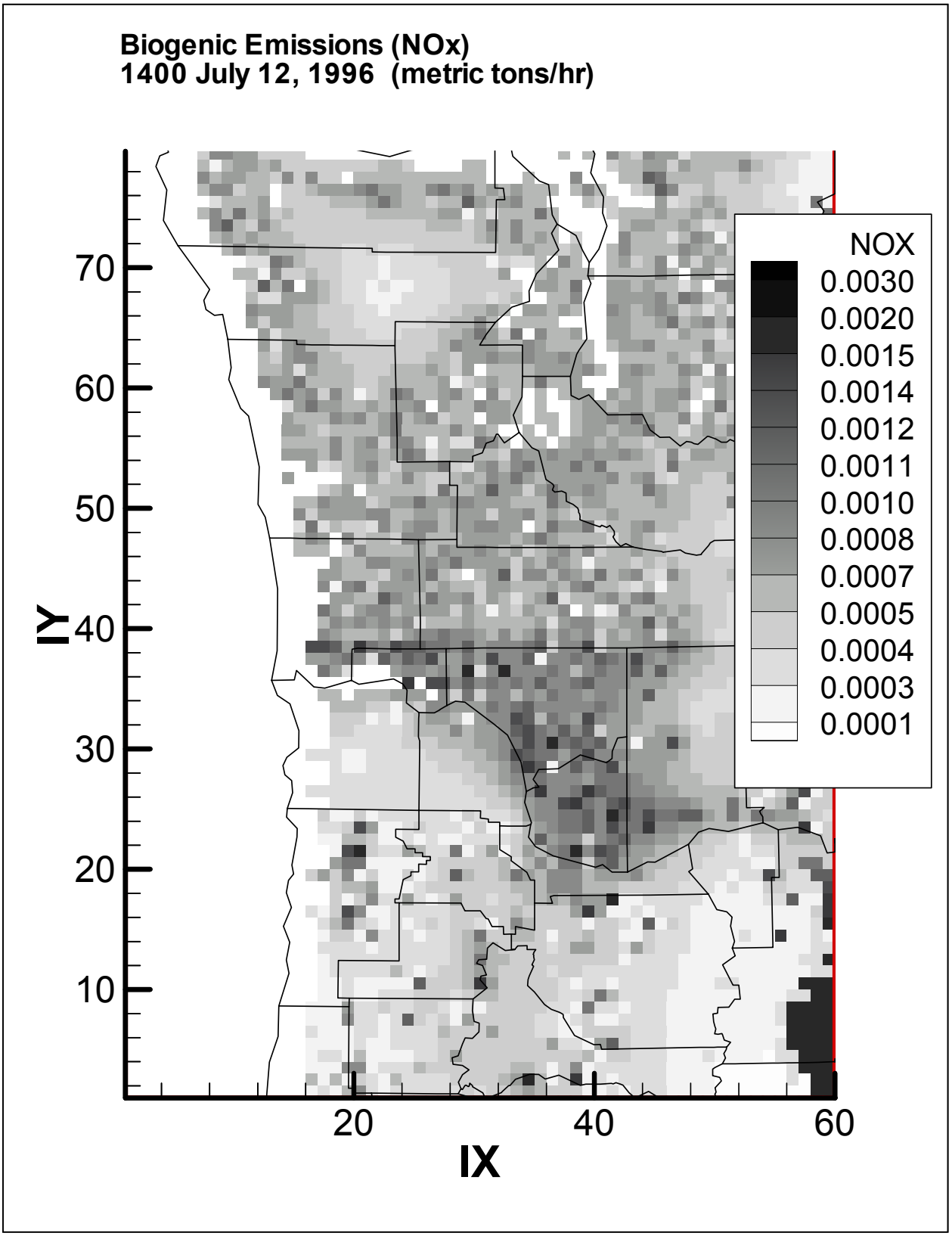

Figure 6. Spatial distribution of biogenic NOx emissions during 1400 on Friday, July 12, 1996.

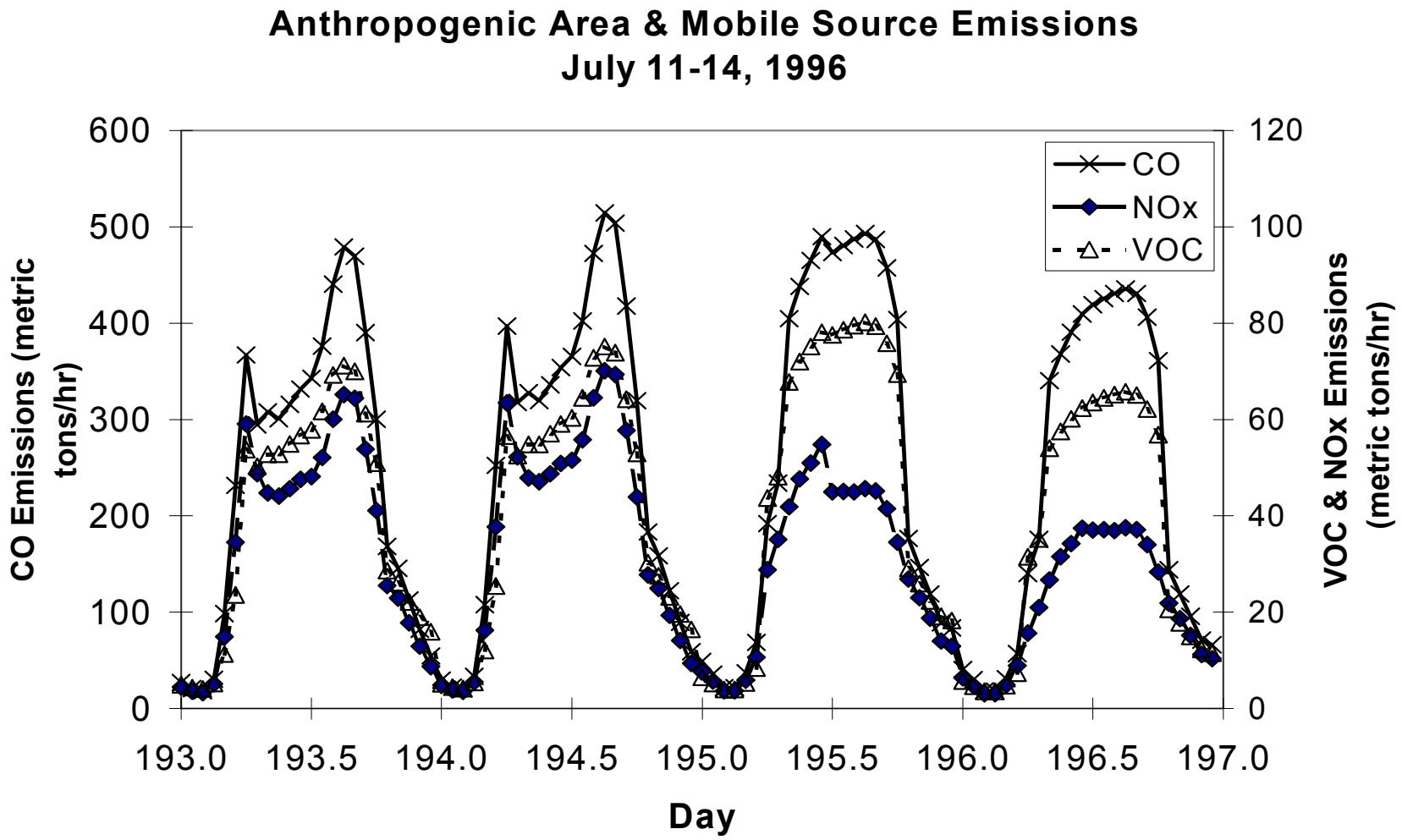

Figure 7. Time series of VOC, NOx, and CO area and mobile anthropogenic sources for the domain.

Table 2. Summary of anthropogenic and biogenic emissions in metric tons per day (MT/day) for the modeling domain.

Model Species	Point Sources	Area Sources	Mobile Sources	Total Anthropogenic Emissions	Biogenic Emissions	Total Emissions	Percent Anthropogenic (%)
ALK1	21	198	188	407	81	489	83.4
ALK2	11	107	49	167	0	167	100.0
ARO1	9	61	55	125	0	125	100.0
ARO2	6	52	46	104	0	104	100.0
CCHO	9	2	3	14	374	388	3.5
CRES	1	0	0	1	0	1	100.0
ETHE	2	13	21	35	0	35	100.0
ETOH	2	32	1	35	217	253	14.0
HCHO	3	4	7	15	510	525	2.8
MEK	3	21	3	27	324	351	7.6
MEOH	2	4	2	8	0	8	100.0
MGLY	0	0	0	0	0	0	100.0
MTBE	6	0	0	6	0	6	100.0
OLE1	3	16	25	44	176	219	19.9
OLE2	1	15	27	43	70	113	37.8
OLE3	6	0	0	6	4117	4124	0.2
RCHO	2	2	1	6	55	61	9.5
Total VOC	86	528	428	1042	5926	6968	15.0
SO2	641	10	36	687	0	687	100.0
NOx	162	105	629	896	94	990	90.5
CO	616	1651	4252	6519	0	6519	100.0

The main features of the emission inventory include:

- a relatively small contribution from the point sources to the total anthropogenic VOC emissions (8%),
- a slightly higher contribution of area VOC emissions (51%) compared to mobile (41%) VOC emissions to the total anthropogenic emissions,
- an approximately 18% contribution of NOx point sources to the total anthropogenic NOx emissions,
- a much higher contribution of mobile NOx sources (70%) compared to area NOx emissions (12%) to the total anthropogenic NOx emissions, and
- biogenic VOC emissions account for 85% of the domain-wide total VOC emissions, but biogenic NOx emissions account for only 10% of the domain wide total NOx emissions.

The biogenic emission inventory for this second phase of the model development was significantly revised. Revisions include the incorporation of additional tree genus distribution

data in Washington, Oregon and British Columbia, and correction of the compound-specific breakdown of emissions of the "Other VOC" (OVOC) category in BEIS. The distribution of model species emissions is given in Table 3. The lumped species OLE3, which includes isoprene and terpenes, accounts for 70% of the biogenic total VOC emissions. The remainder are distributed among oxygenated VOCs (25%), other olefins (4.2%), and alkanes (1.4%).

Table 3. Summary of biogenic emissions (metric tons/day)

Model Species	Biogenic Emissions	Percent of Total VOC Biogenics
ALK1	81	1.4
CCHO	374	6.3
ETOH	217	3.7
HCHO	510	8.6
MEK	324	5.5
OLE1	176	3.0
OLE2	70	1.2
OLE3	4117	69.5
RCHO	55	0.9
Total Biogenic VOC	5926	100.0
NOx	94	

It is important to note that while biogenic VOC emissions dominate the total VOC inventory on a domain-wide basis, there are two aspects of biogenic VOC emissions that reduce their importance in urban ozone production: 1) anthropogenic VOC emissions occur in relatively concentrated areas compared to the very dispersed biogenic VOC emissions, and 2) the biogenic VOC emissions are not accompanied by any significant NOx emissions, while anthropogenic VOC emissions occur in combination with very significant NOx emissions. This latter point is illustrated in a map of the VOC/NOx ratios which occur in the emission inventory, as shown in Figure 8. The ratios from the inventory have been calculated on a molar basis.

Further details concerning the development of the emission inventory are included in Appendix A.

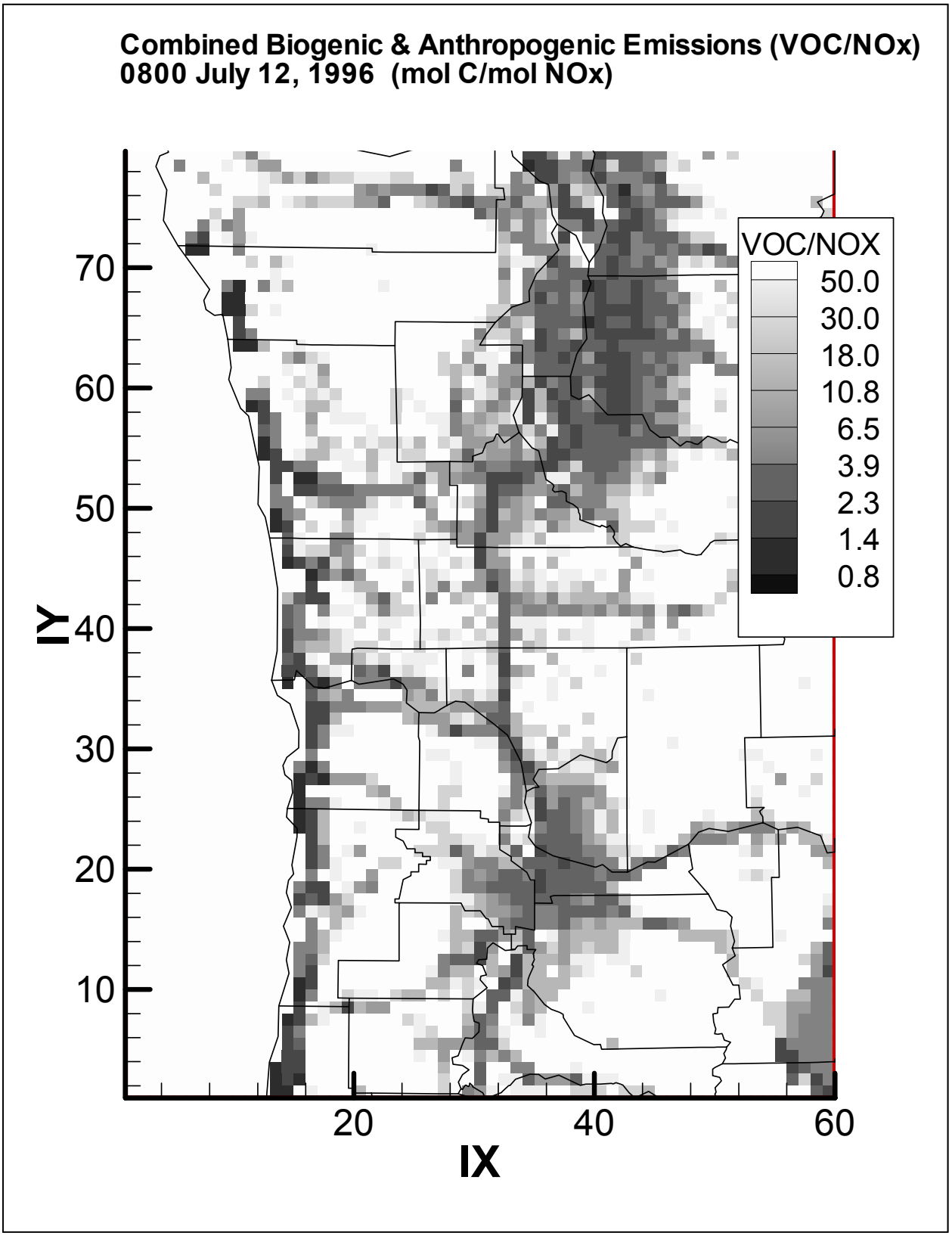
Combined Biogenic & Anthropogenic Emissions (VOC/NOx)
0800 July 12, 1996 (mol C/mol NOx)
VOC/NOX
50.0
30.0
18.0
10.8
6.5
3.9
2.3
1.4
0.8
IY
70
60
50
40
30
20
10
20
40
60
IX

Figure 8. Spatial distribution of total VOC/NOx molar ratios during 0800 on Friday, July 12, 1996.

Meteorology

Initially, the goal in the second phase of the model development was to run MM5 in FDDA mode (using gridded analysis) with a 5 km x 5 km horizontal grid resolution, and to use this wind field with minimal CALMET interpolation. Note that in the first phase of model development, archival forecast MM5 runs, with a 27 km grid resolution, were used as input to CALMET. After completing this fine-scale MM5 simulation, the MM5 surface winds were compared with observations. It was discovered that the predicted surface wind speeds were significantly higher than observed. This problem had been recently recognized by the University of Washington MM5 forecast group as well as other MM5 users. The UW team incorporated a modification to the wind/surface boundary code that effectively increased the surface drag within the model. With their assistance, this change was implemented in the WSU MM5 simulations. The result was improved agreement between the MM5 surface winds and observations.

Further analysis of the MM5 solution employed a "pass-through" approach with CALMET. In this pass-through approach, the MM5 wind field was incorporated into CALMET with no interpolation of the surface wind observations. However, this approach showed significant differences in wind direction patterns in some areas of the domain. This was particularly apparent in the Portland area. As shown in Figure 9, the CALMET pass-through case yields northerly flow through the Puget Sound and Portland areas. However, observations in the Portland region indicated that easterly flow from the Columbia River Gorge interacts with this northerly flow and produces areas of convergence which are not reproduced correctly in the CALMET pass-through solution.

Subsequently, a series of CALMET runs were initiated, where the surface observations were weighted relative to the MM5 solution to produce interpolated wind fields that combined aspects of MM5 and the observations. Different degrees of relative weighting of the observations with respect to the MM5 wind field were used in each run. In addition, different methods of extrapolating surface observations to upper levels of the model were tested. In some cases, selected surface stations were dropped from the list of monitoring sites, and a pseudo wind station was placed between Longview and Portland along the Columbia River. In addition, a comparison of observed vertical temperature profiles measured at Salem indicated a mid-day mixing height of approximately 1100 m. However, CALMET predicted mixing heights which reached as high as 2000 m. To address this problem of over estimating the mixing height, the maximum allowed mixing height in CALMET was set to 1200 m. Finally, two significant source code errors within CALMET were discovered and corrected. First, it was found that when MM5 data were input into CALMET, there was a unit conversion error that significantly changed the wind speed. Second, the extrapolation of surface winds to layers aloft was not correctly applied when the option of "user declared weighting factors" was invoked. Both of these errors were corrected prior to the execution of the base case and sensitivity simulations.

The strategy behind this iterative approach was to produce wind fields which agreed with wind observations and led to ozone predictions in good agreement with ozone observations in the Portland/Vancouver area. The end result of these iterative CALMET runs is shown in Figure 10 in terms of the predicted wind patterns in the 60 x 80 domain. The figure also includes the wind

vectors for each observation station during the selected hour. The corresponding ozone predictions will be presented in a later section.

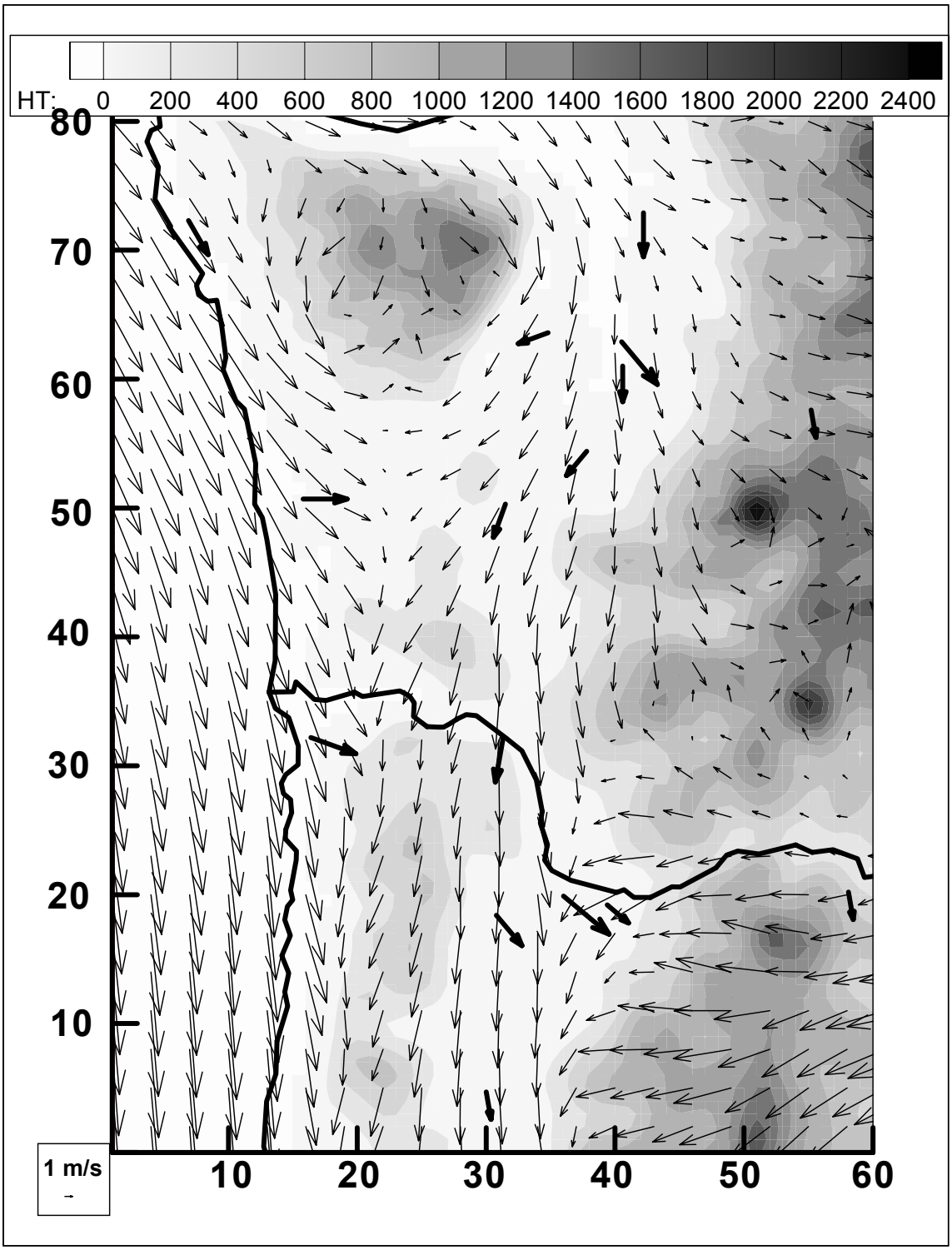

Figure 9. Surface wind patterns predicted from an MM5 solution passed through CALMET with no interpolation of surface wind observations for hour 1600 LST, 11 July 1996. Surface wind vectors from the available observation stations are shown as dark arrows. Shading indicates terrain heights (m).

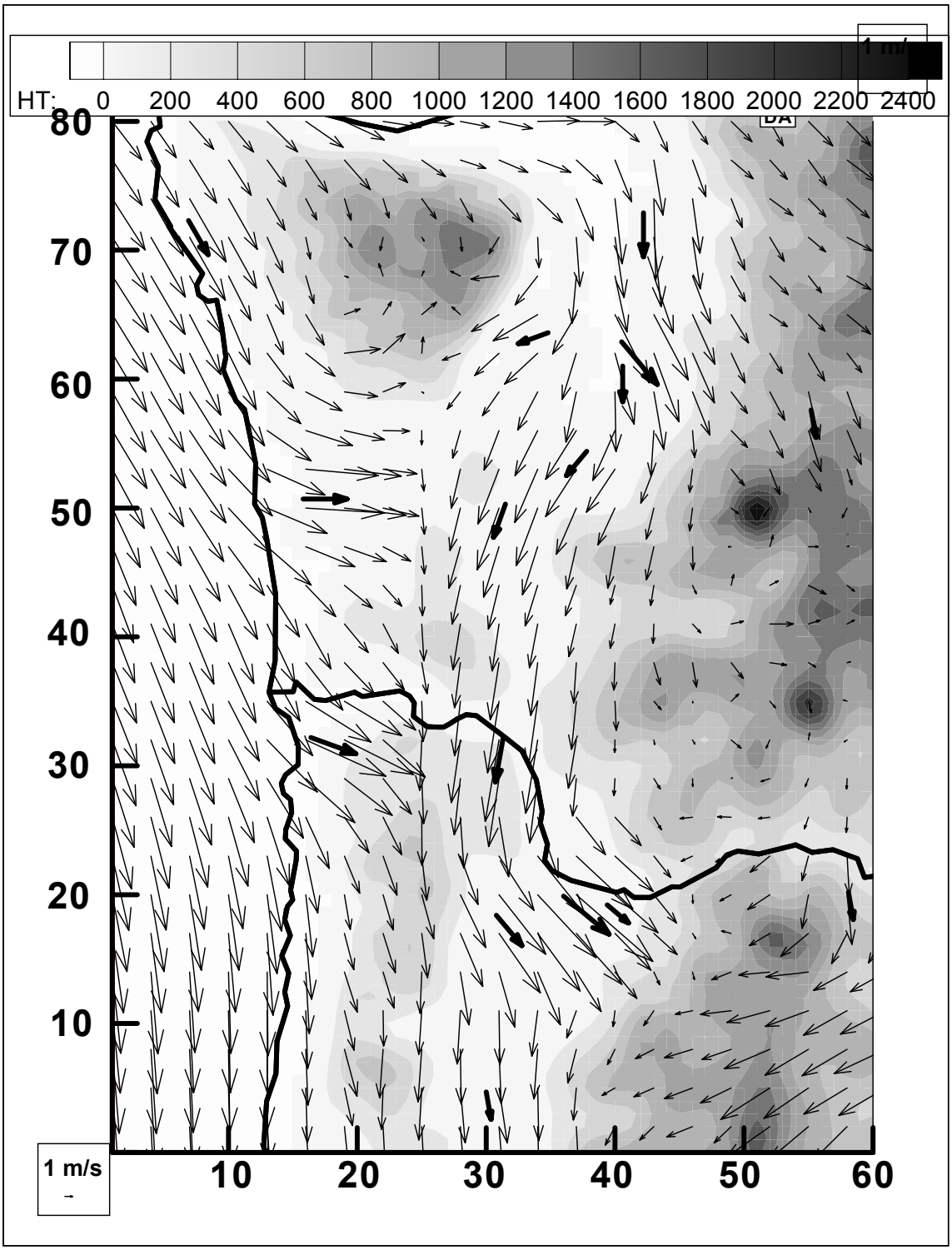

Figure 10. Surface wind patterns predicted from an MM5 solution modified by CALMET interpolation of surface wind observations for hour 1600 LST 11 July 1996. Surface wind vectors from the available observation stations are shown as dark arrows. Shading indicates terrain heights (m).

The meteorological time series for several stations are shown in Figures 11-13 in terms of predicted and observed surface wind speed, wind direction, and temperature. These results show that relatively close agreement can be achieved using CALMET to interpolate MM5 winds with available surface observations. However, it should be recognized that these results do not represent an independent test of the wind field model performance, since the observations are incorporated into the model solution. These results also show the difficulties which can occur if only the MM5 results are used without interpolation of observations. The MM5 wind speeds are in the correct range, but often diverge from the observed wind speed. For example, at Longview during the nighttime periods, MM5 wind speeds are 4 to 5 m/s, while the observed wind speeds decrease to near zero. Similarly, the MM5 wind directions at Lafayette exhibit a distinct diurnal cycle from northeast during the day to north-northwest at night, which is not reflected in the observations.

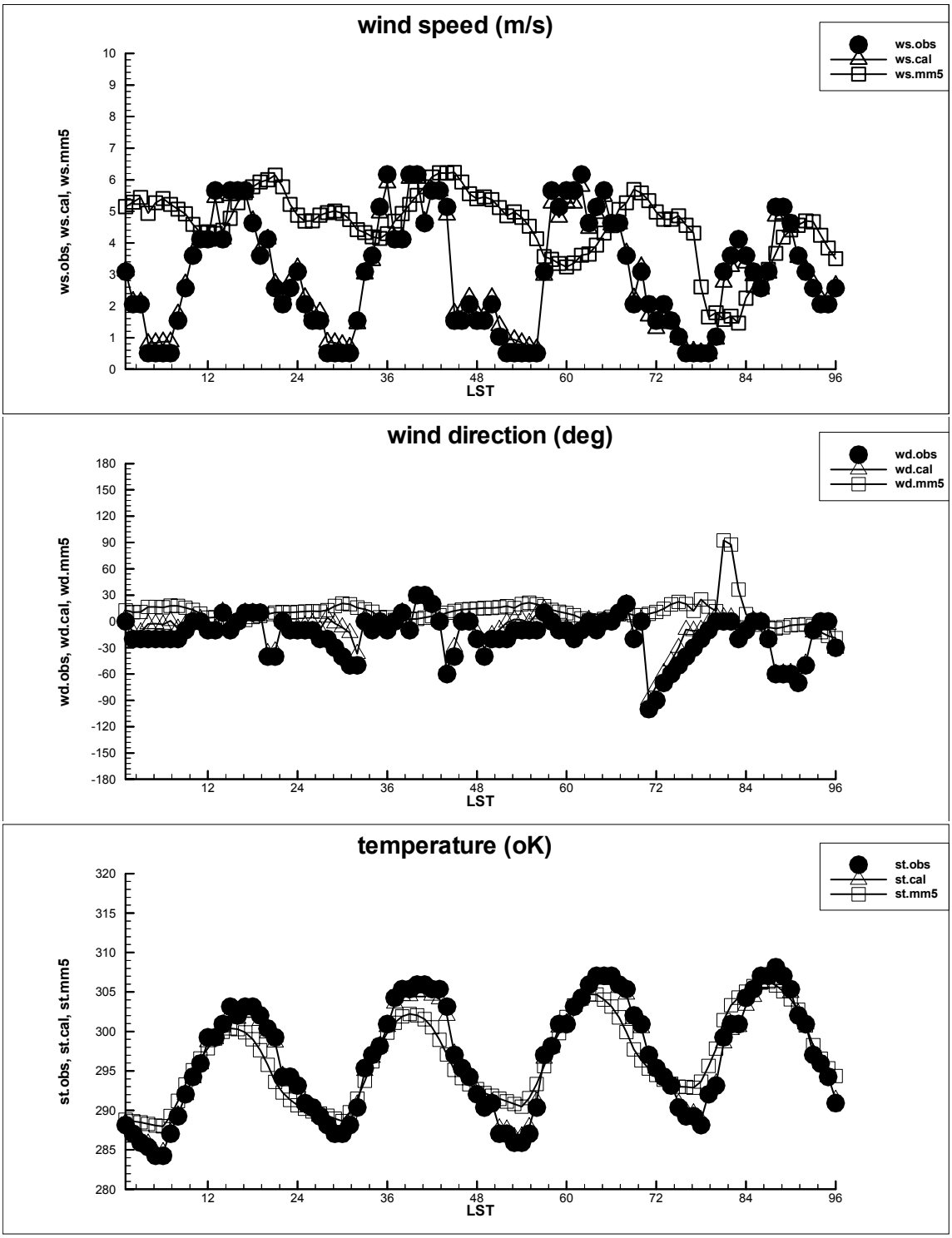

Figure 11. Observed and predicted times series of wind speed, wind direction, and temperature for the Longview site.

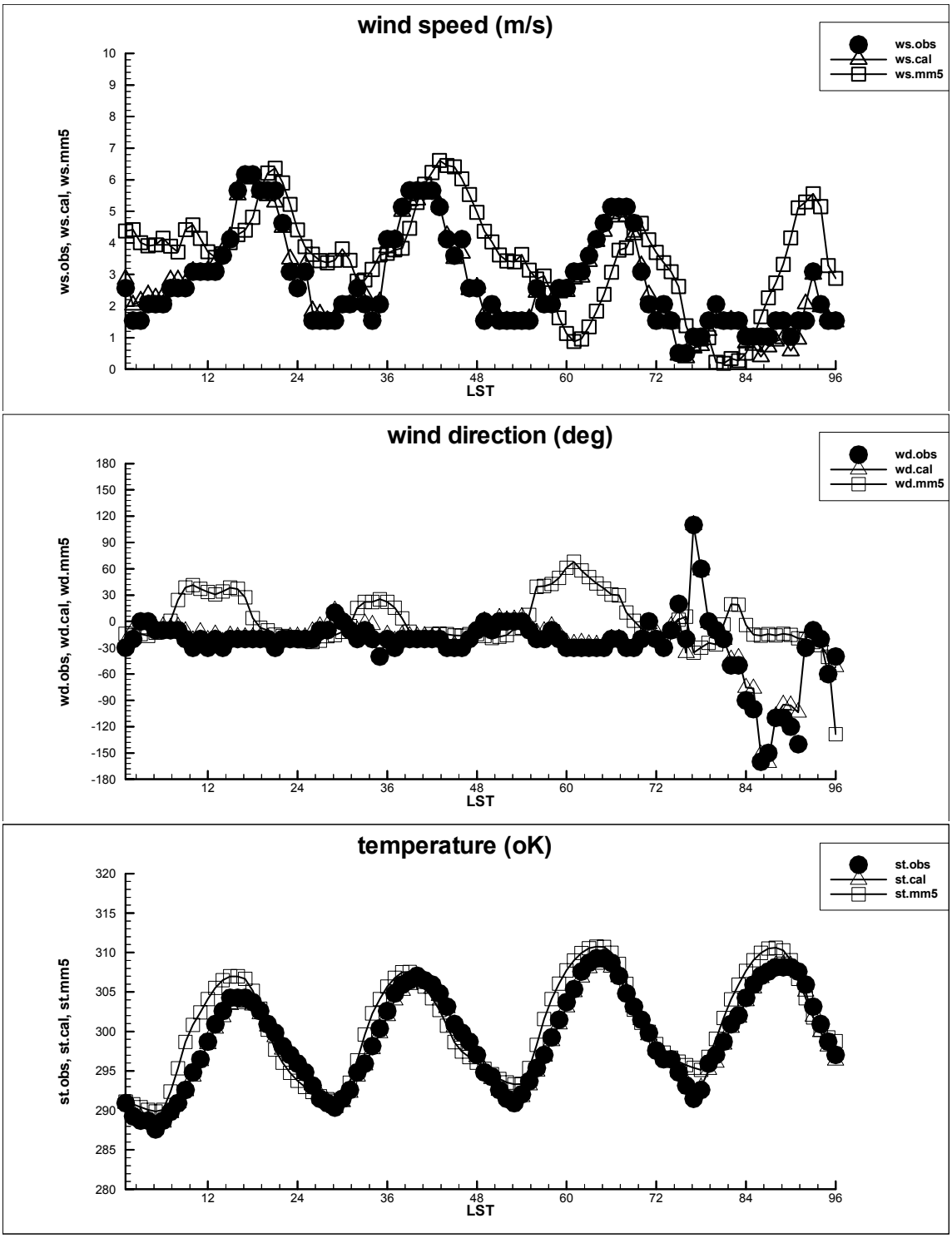

Figure 12. Observed and predicted times series of wind speed, wind direction, and temperature for the Lafayette site.

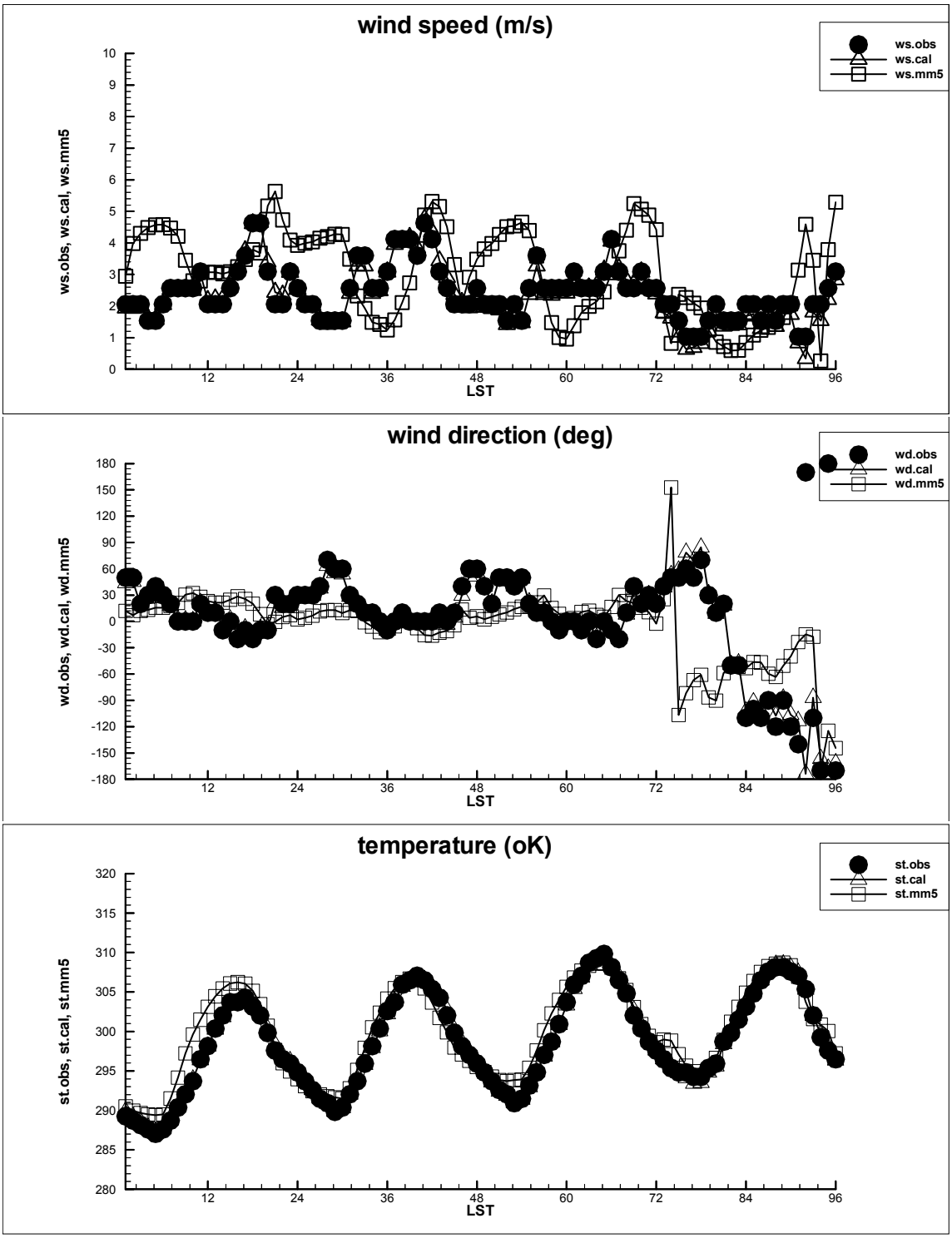

Figure 13. Observed and predicted times series of wind speed, wind direction, and temperature for the Carus site.

The fact that the MM5 solution did not yield better results in terms of predicted ozone concentrations, while discouraging, is not a unique experience. Recent work with the Urban Airshed Modeling system (UAM IV) applied to the complex topography in the Salt Lake City area produced results very similar to those obtained for the Cascadia region (Barickman and Swart, 1997). For Salt Lake City, output from a prognostic weather model (CSUMM) used with UAM IV yielded very poor agreement with ozone observations. The results were improved when surface and upper air data were interpolated using the UAM Diagnostic Wind Model (DWM). However, even in this case, the predicted ozone was as much as 50% less than the maximum observed hourly ozone concentrations. These results are very similar to the type of model performance observed in the first phase of the Cascadia model development and in the initial stages of the analyses conducted during this second phase of the model improvement.

In summary, a very considerable amount of effort was required to obtain a representative MM5 solution with reduced surface wind speeds at the 5 km grid scale. In turn, considerable work was also required to merge the MM5 solution with observations in CALMET to obtain wind fields which agreed with surface wind observations and which produced ozone concentration patterns in agreement with the available monitoring data in the Portland/Vancouver region. In both instances, the amount of effort was far more than originally anticipated. As a result, original plans to model two or even three separate ozone episodes were set back, and other model runs to investigate overall model sensitivity were greatly reduced. In the future, efforts to continue the development of the regional modeling system should seek to find the best methods for applying MM5 in a way that does not require substantial modification via CALMET. Three particular areas that need to be investigated include the use of a still finer MM5 grid (~ 1 km) in areas of strong convergence, use of a different planetary boundary layer scheme more appropriate to strongly convective boundary conditions, and the application of observational nudging within the inner MM5 domain.

CALGRID Simulations and Sensitivity Analyses

Boundary & Initial Conditions

Since the establishment of boundary conditions is crucial, it is important to keep the boundaries as far as possible from the regions of interest within the modeling domain. As indicated previously, an enlarged domain was selected so that the model solutions within western Washington would be less sensitive to the influence of boundary effects. The new domain measured 74 x 132 grids with a 5 km horizontal grid scale and was defined from south to north by UTMN 4900-5560 km (approximately 44 to 50 degrees north latitude), and from west to east by UTME 350-720 km (approximately 119-125 degrees west longitude).

The initial and boundary conditions required by CALGRID include the specification of ozone, NOx, and VOC concentrations for all cells for the initial hour and for all boundary cells (lateral and top boundaries) for all time steps. The same concentration levels were used for both initial and boundary conditions. These were determined from VOC measurements collected in 1995 at Wynoochee Dam on the Olympic Peninsula, and from the literature for clean Pacific maritime air

as described in Appendix C. The initial and boundary conditions are the same as used in the first phase of the model development.

As indicated previously, simulations were also conducted for a sub-domain. For these sub-domain runs, the initial and boundary conditions were left unchanged from the large domain simulations.

Model Simulations

When conducting sensitivity runs, it is necessary to determine what portion of the inventory will be modified for each of the runs. Since the objective of this investigation is to determine the impact of point sources located in Cowlitz County on Clark/Multnomah counties, the selection of which portion of the point source emission inventory to modify is straightforward.

The major industrial sources in Cowlitz County consist of two pulp mills (Longview Fibre and Weyerhaeuser), an aluminum smelter (Reynolds Metals), and a synthetic chemical manufacturing facility (B.F. Goodrich Kalama). Table 4 contains estimates of the annual emissions of sulfur dioxide (SO_2), nitrogen oxides (NO_x), volatile organic compounds (VOCs) and carbon monoxide (CO) for each of these facilities.

Table 4. Facility-wide emissions for the major point sources in Cowlitz County in tons/yr for 1996.

Facility	SO_2	NO_x	VOC	CO
Weyerhaeuser	994	2960	1265	3335
Longview Fibre	1260	2170	659	3485
B.F. Goodrich	21	103	159	1117
Reynolds Metals	56	54	436	19560

During the 11-14 July 1996 episode, the Longview Fibre facility was functioning at 60% of normal operating levels. The emission inventory reflected this situation. However, to address changes in emissions corresponding to possible control scenarios, it is appropriate to employ the normal operating emissions as the base case. Consequently, two different base case simulations were completed. The first base case reflected the actual conditions during the episode (Longview Fibre at 60% normal operating emissions). The results from this base case were used to evaluate model performance with respect to the available ozone observations. The second base case, or adjusted base case (reflecting normal operating emissions at Longview Fibre), was used for evaluating the control simulations.

Maps of ozone concentration contours for the actual (first) base case are shown in Figures 14-17 for four different hours on Sunday, 14 July 1996, which is when the highest ozone levels were observed. Early in the morning (0600 LST), ozone concentrations throughout the Portland/Vancouver area are quite low, in the range of 20 to 30 ppb, as shown in Figure 14. By

1000 LST (Figure 15), ozone levels have begun to increase throughout the area, with a maximum near 60 ppb to the southwest of Portland. During mid-afternoon (1400 LST, shown in Figure 16), elevated ozone concentrations exceeding 150 ppb are predicted to occur near the Carus monitoring station south of Portland. At 1800 LST, the predicted ozone concentrations have increased to more than 160 ppb, with the region of maximum ozone occurring approximately 65 km south of the Portland urban center.

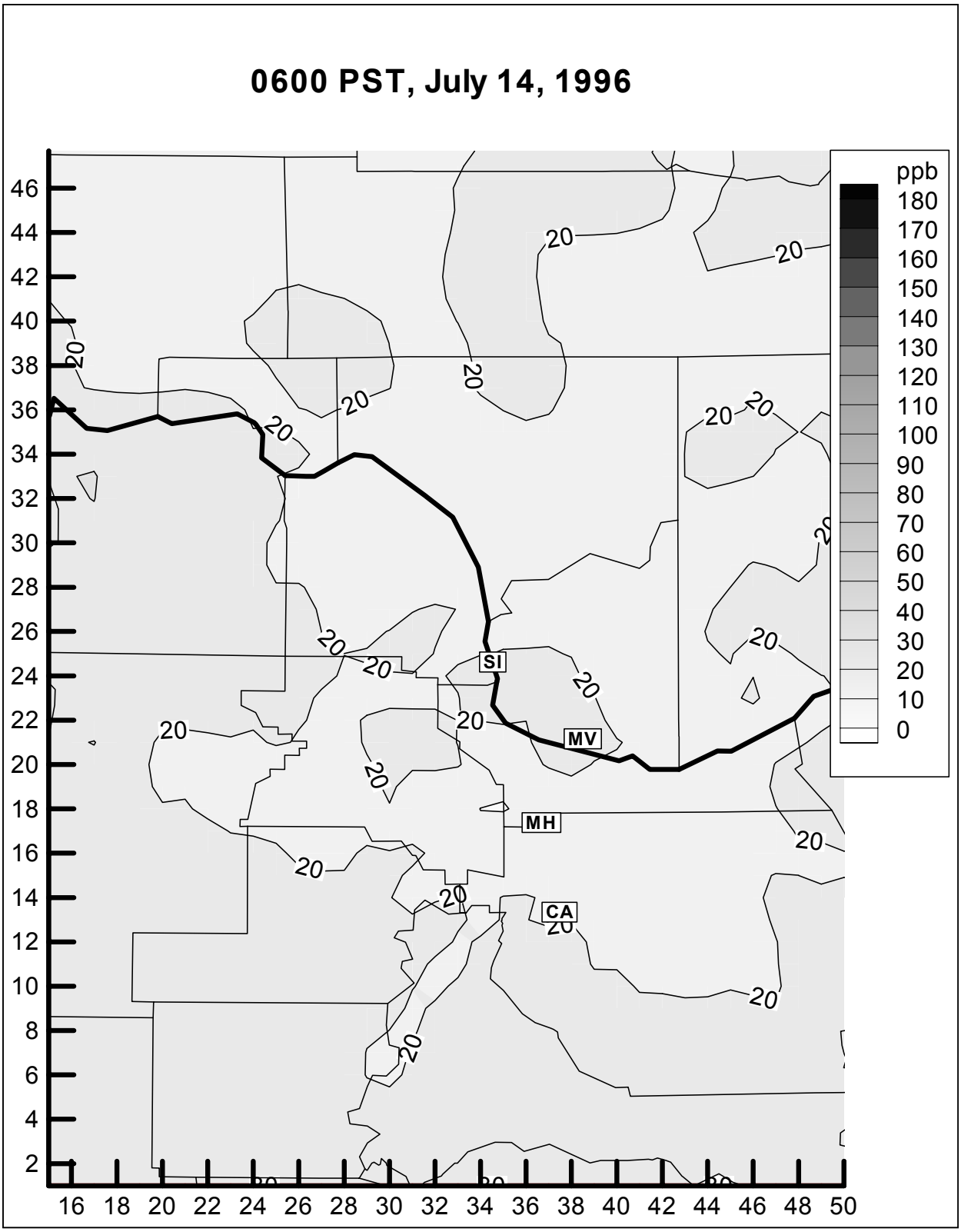

Figure 14. Predicted O_3 concentration patterns at 0600 on Sunday, July 14, 1996 in the Portland/Vancouver area.

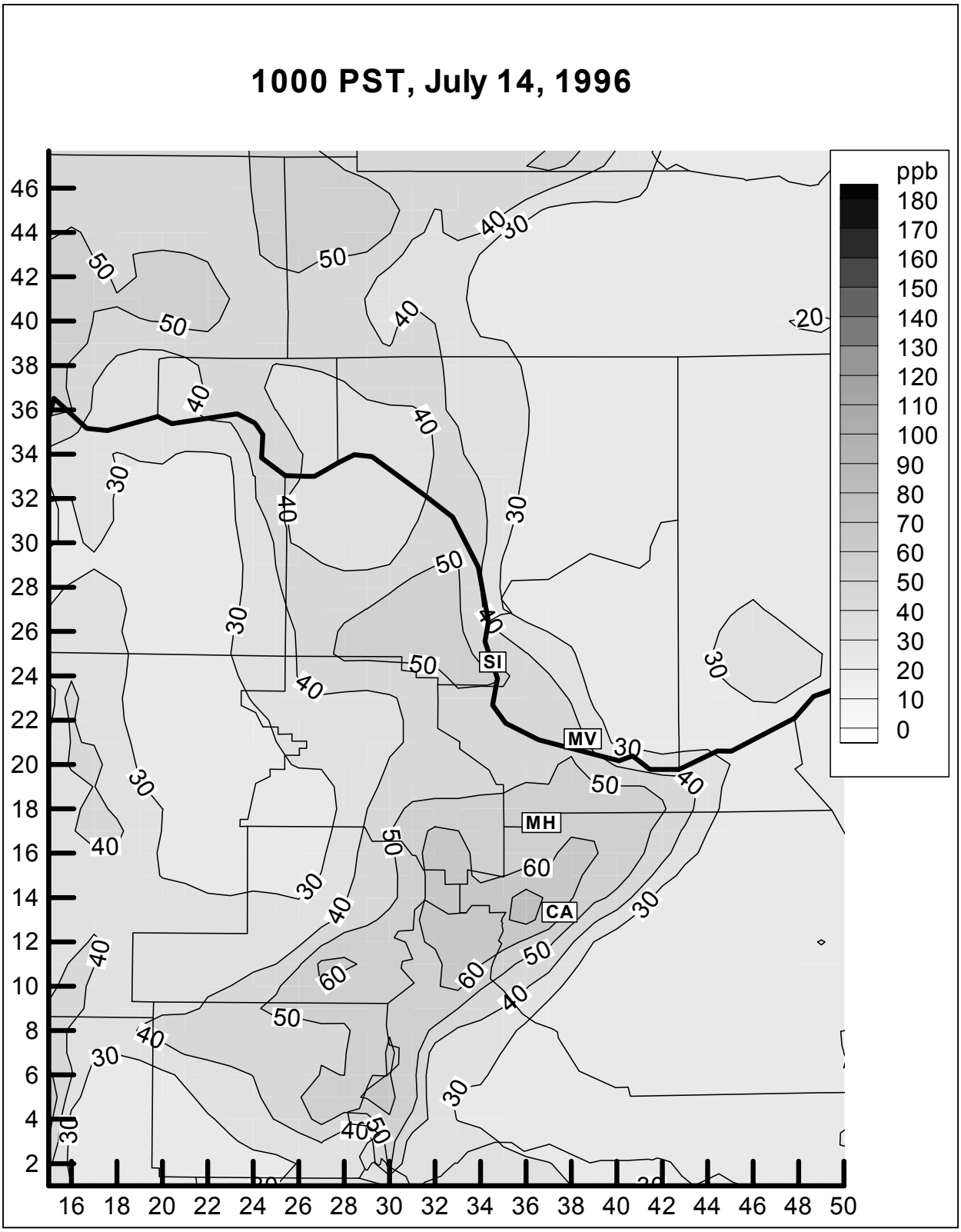

Figure 15. Predicted O_3 concentration patterns at 1000 on Sunday, July 14, 1996 in the Portland/Vancouver area.

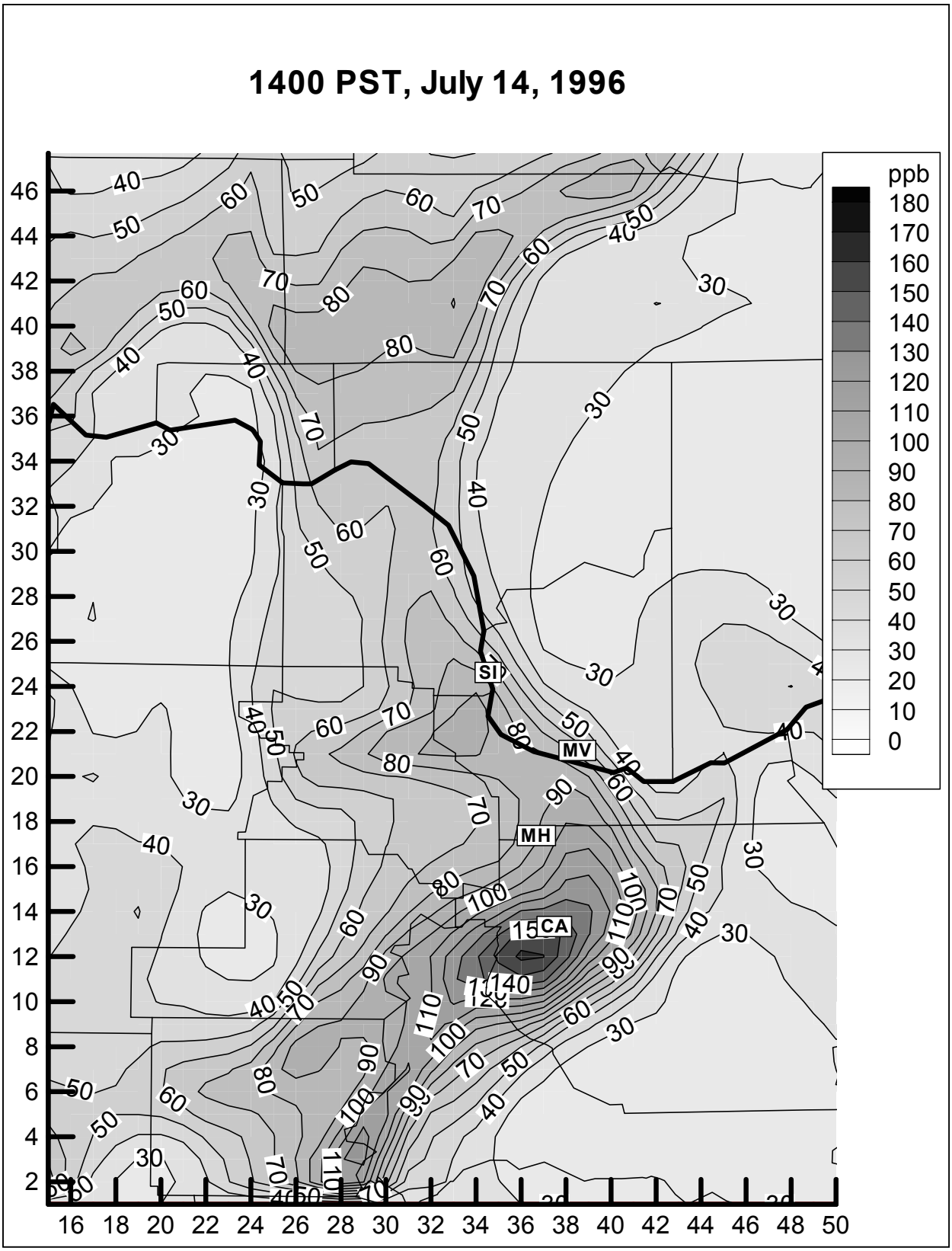

Figure 16. Predicted O_3 concentration patterns at 1400 on Sunday, July 14, 1996 in the Portland/Vancouver area.

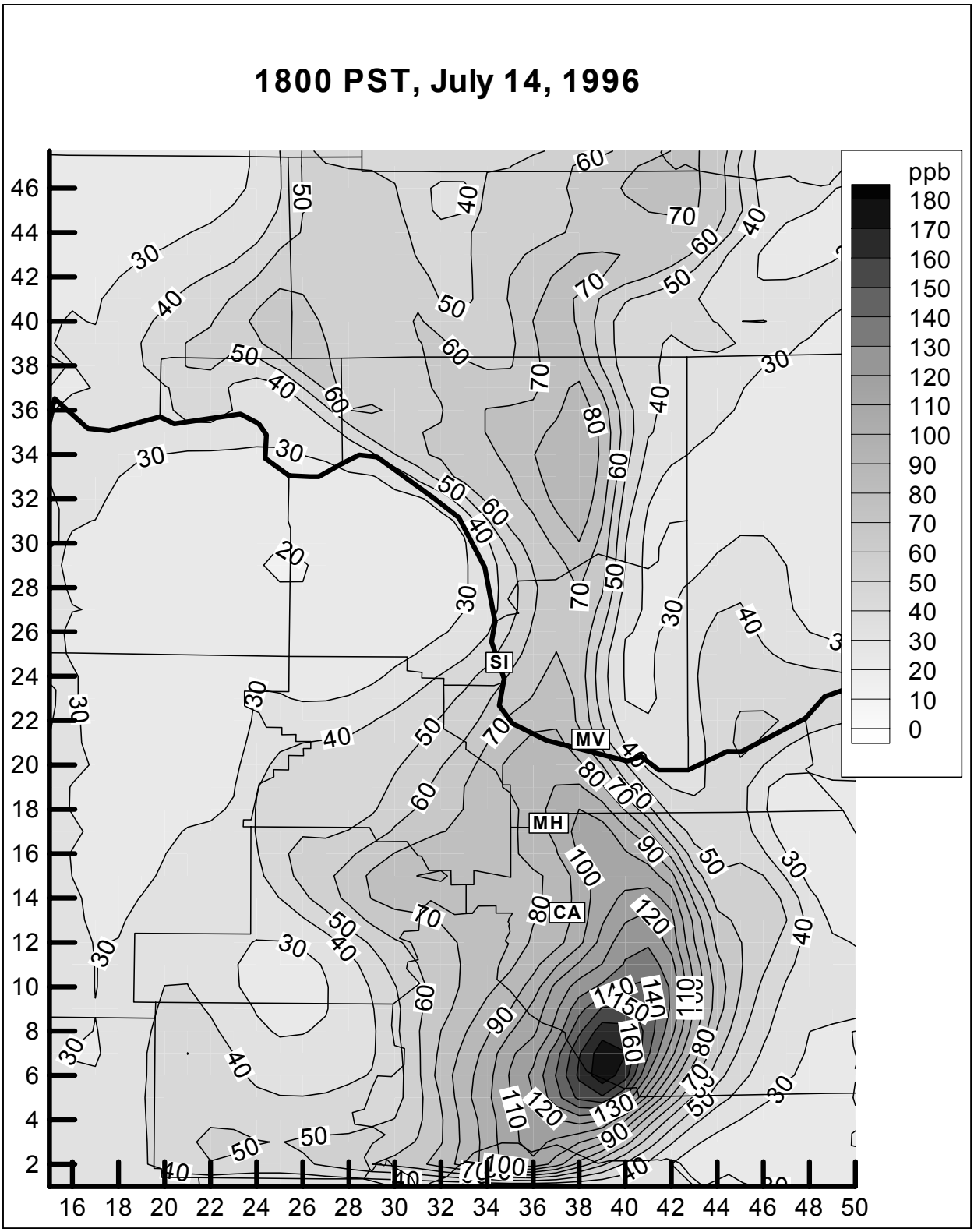

Figure 17. Predicted O_3 concentration patterns at 1800 on Sunday, July 14, 1996 in the Portland/Vancouver area.

In the second base case, emissions from Longview Fibre were increased to simulate normal operating conditions. This adjusted base case was then used as the basis for comparison to the following sensitivity runs:

1. Modification of point source VOC/CO emissions to reflect 90%, 80%, and 60% of actual emissions,
2. Modification of point source NOx emissions to reflect 90%, 80%, and 60% of actual emissions,
3. Modification of point source VOC/CO and NOx emissions to reflect 90%, 80%, and 60% of actual emissions, and
4. Modification of point source emissions to reflect zero NO_x emissions, zero VOC/CO emissions, and zero VOC/CO and NO_x emissions.

Thus, two base case runs and twelve sensitivity runs were completed for this study. The intent of these sensitivity runs was to provide an estimate of the change in ozone levels experienced in the ozone maintenance region as a result of changes in point source emissions in Cowlitz County. The results are presented in terms of the change in ozone from each sensitivity run compared to the adjusted base case run:

$$\Delta O_3 = O_3(\text{sensitivity run}) - O_3(\text{adjusted base case})$$

In this case, a negative ΔO_3 reflects a decrease in ozone levels due to a reduction in point source emissions. A positive ΔO_3 reflects an increase in ozone due to a reduction in point source emissions. The latter situation can occur when NO_x emissions are reduced, which reduces the titration of ozone by NO near NO_x sources. The sensitivity results can be viewed graphically with maps of the ΔO_3 for a given hour or in terms of a time series of ΔO_3 for a given location. In either case, it is important to compare the ΔO_3 to the corresponding base case ozone ambient concentration. A large ΔO_3 in a region with very little ambient ozone in the base case may not be considered as significant as a smaller ΔO_3 in a region with very high ambient O_3 concentrations.

Animations of the ΔO_3 maps were generated for each sensitivity run to see how the ΔO_3 patterns evolved in time and space. These animations were compared visually to predicted ambient O_3 concentrations in the corresponding base case movie. As an illustration of these results, the combined ΔO_3 map and base case ozone map are shown in Figure 18. In this figure, ΔO_3 contours reflect the sensitivity run with 60% of normal VOC/CO and NOx emissions (i.e., a 40% reduction) from the four major point sources at 1600 LST, 14 July 1996. This period corresponds to the time of maximum reduced (negative) ΔO_3 for this case. There are several features from the map which should be highlighted:

- Reducing VOC/CO and NOx emissions causes an increase in ozone concentrations as large as 5 ppb immediately downwind of the industrial sources. The increase is due to reduced NO titration of ozone. However, it occurs in an area with very low ambient ozone concentrations.
- The largest ΔO_3 for the 60% emissions reduction case equals a decrease of approximately 7 ppb in ambient O_3 levels.

- The location of the maximum ΔO_3 occurs approximately 80 km south of the Longview sources in a region where the ambient ozone levels are approximately 90 ppb.
- Maximum predicted ambient ozone levels during this period equal 172 ppb and occur approximately 50 km south of the Portland urban center.
- The location of the maximum ΔO_3 and the area of maximum ambient ozone do not coincide.

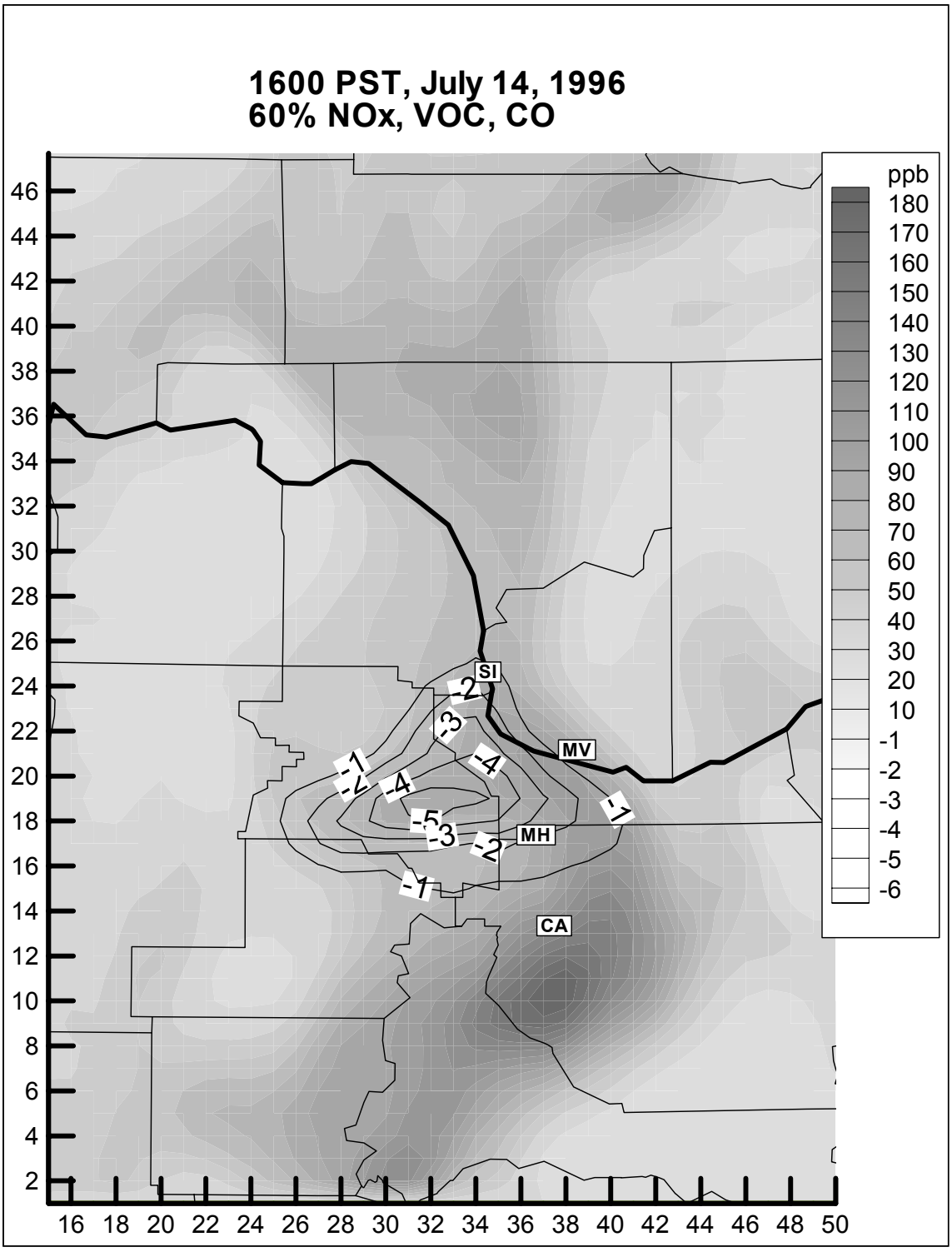

Figure 18. Map of ΔO_3 for the case with the largest reduction of O_3 due to 60% reduction of VOC/CO and NO_x from the four industrial sources. Shading represents the predicted ozone concentration for the base case.

For the sensitivity simulations with reduced NOx, but normal VOC/CO emissions, the results are very similar to those for both reduced NOx and VOC/CO, as shown in Figure 19 for the 60% NOx reduction runs. There is still an enhancement of ozone immediately downwind of the industrial facilities, but this occurs in an area with low ambient ozone levels. The largest reduction in ozone is approximately 6 ppb in an area with 90 ppb ozone, but the location of the maximum ΔO_3 does not coincide with the urban ozone plume downwind of Portland.

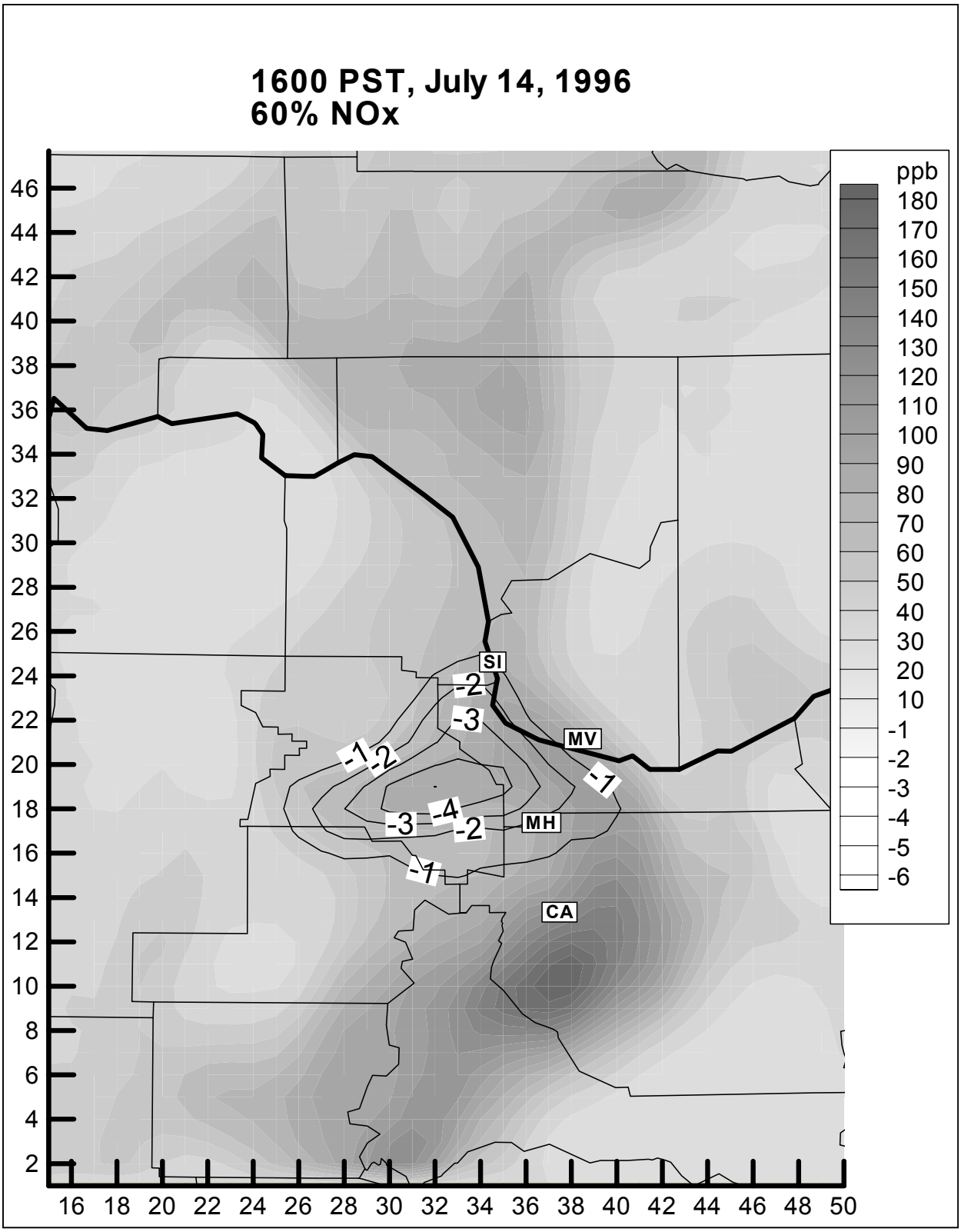

Figure 19. Map of ΔO_3 for the case with the largest reduction of O_3 due to 60% reduction of NO_x emissions from the four industrial sources. Shading represents the predicted ozone concentration for the base case.

In contrast, the sensitivity runs with reduced VOC/CO, but normal NOx emissions, showed very little change in ozone. The largest reduction in ozone for the 60% VOC/CO run was approximately 2 ppb, as shown in Figure 20. This difference between the reduced NOx simulation and the reduced VOC/CO simulation indicates that *for this episode and these sources*, the air mass is NOx limited with respect to ozone production. Changes in VOC emissions do not appear to have as large an effect as changes in NOx emissions with regard to ozone production.

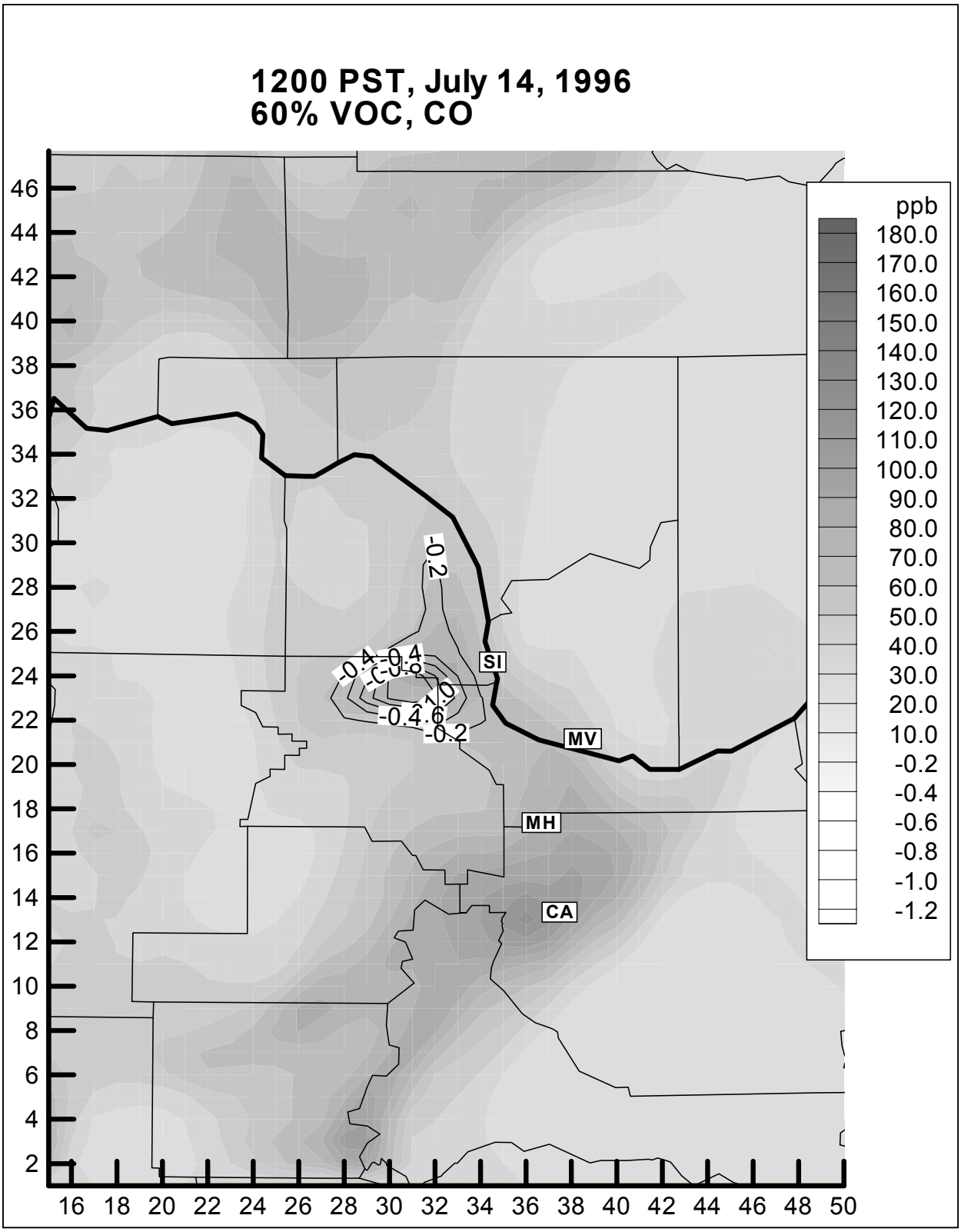

Figure 20. Map of ΔO_3 for the case with the largest reduction of O_3 due to 60% reduction of VOC and CO emissions from the four industrial sources. Shading represents the predicted ozone concentration for the base case.

Results for the 60% reduction cases are also shown in Figures 21-24 in terms of time series of ΔO_3 and ambient ozone at the Portland area monitoring stations. In this case, the ΔO_3 values are all quite low because the plumes from the point sources did not directly impact these monitoring sites, while ozone due to other urban sources did influence the sites to produce relatively high ozone during the latter two days of the event. There is a diurnal pattern in ΔO_3 in which ozone is slightly enhanced during the night when NO is titrating ozone, followed by a slight reduction in ozone during mid-afternoon periods.

Figure 21. Time series of ΔO_3 and predicted ambient O_3 concentrations for the Mountain View monitoring site.

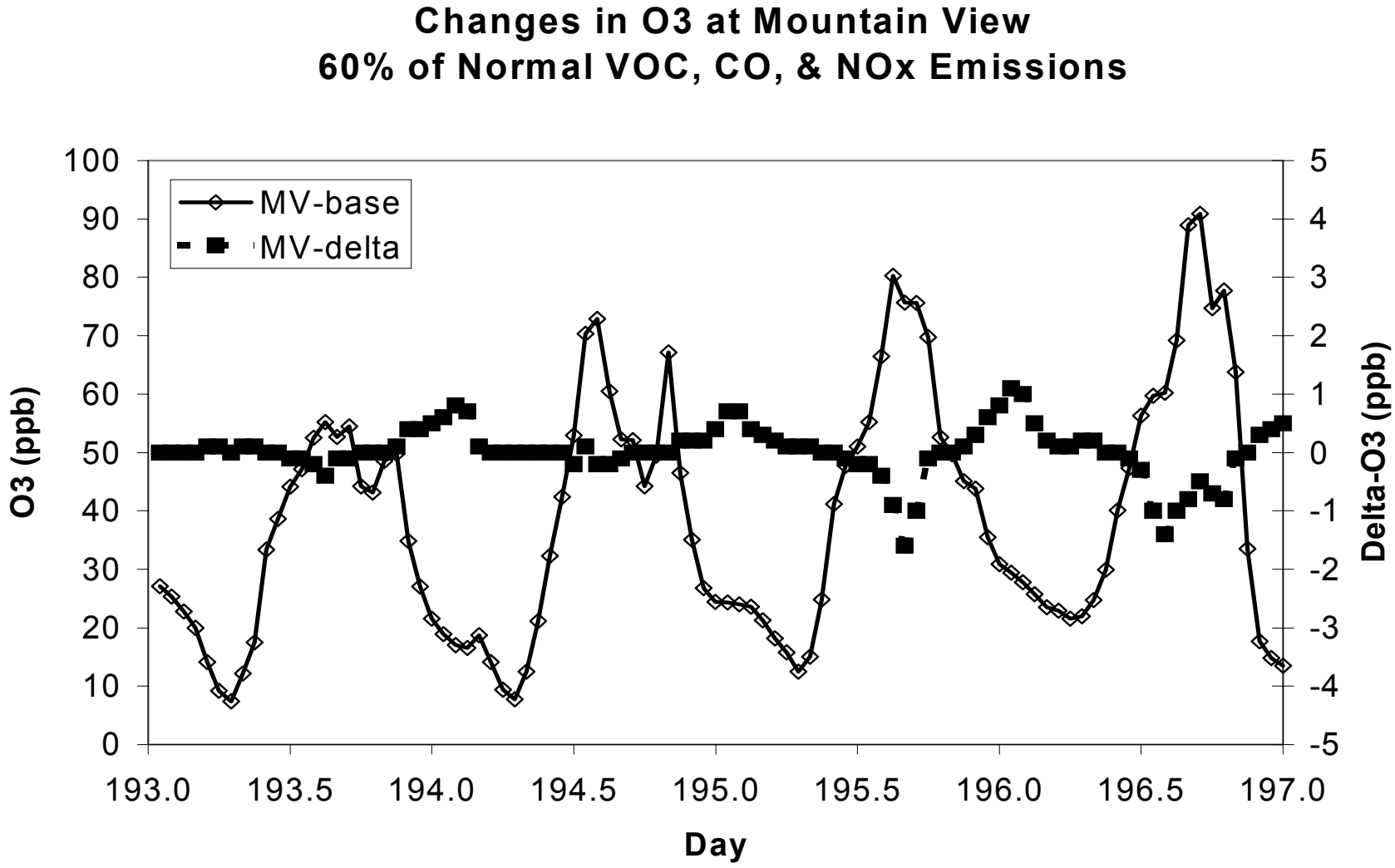

Figure 22. Time series of ΔO_3 and predicted ambient O_3 concentrations for the Sauvie Island monitoring site.

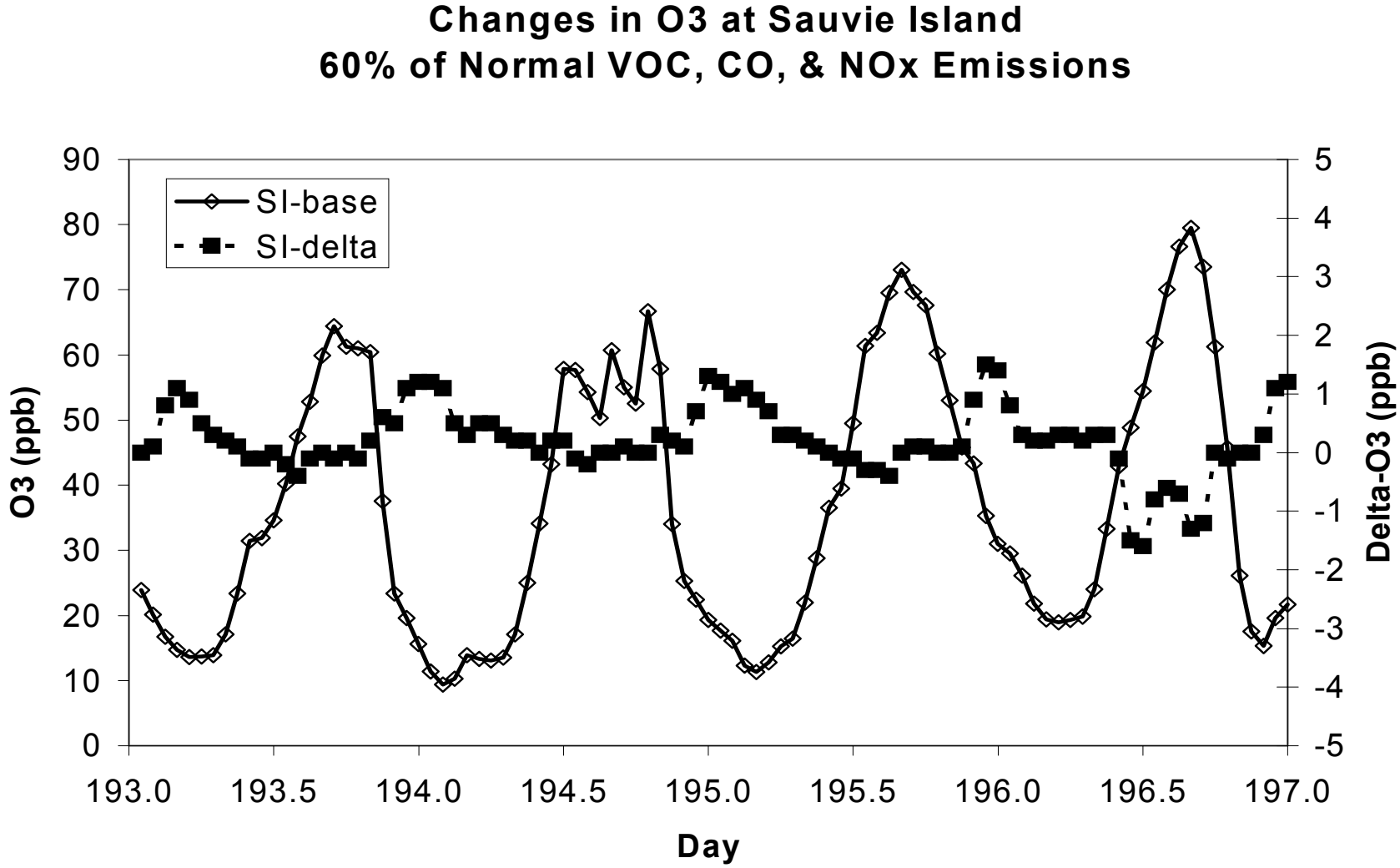

Figure 23. Time series of ΔO_3 and predicted ambient O_3 concentrations for the Milwaukee monitoring site.

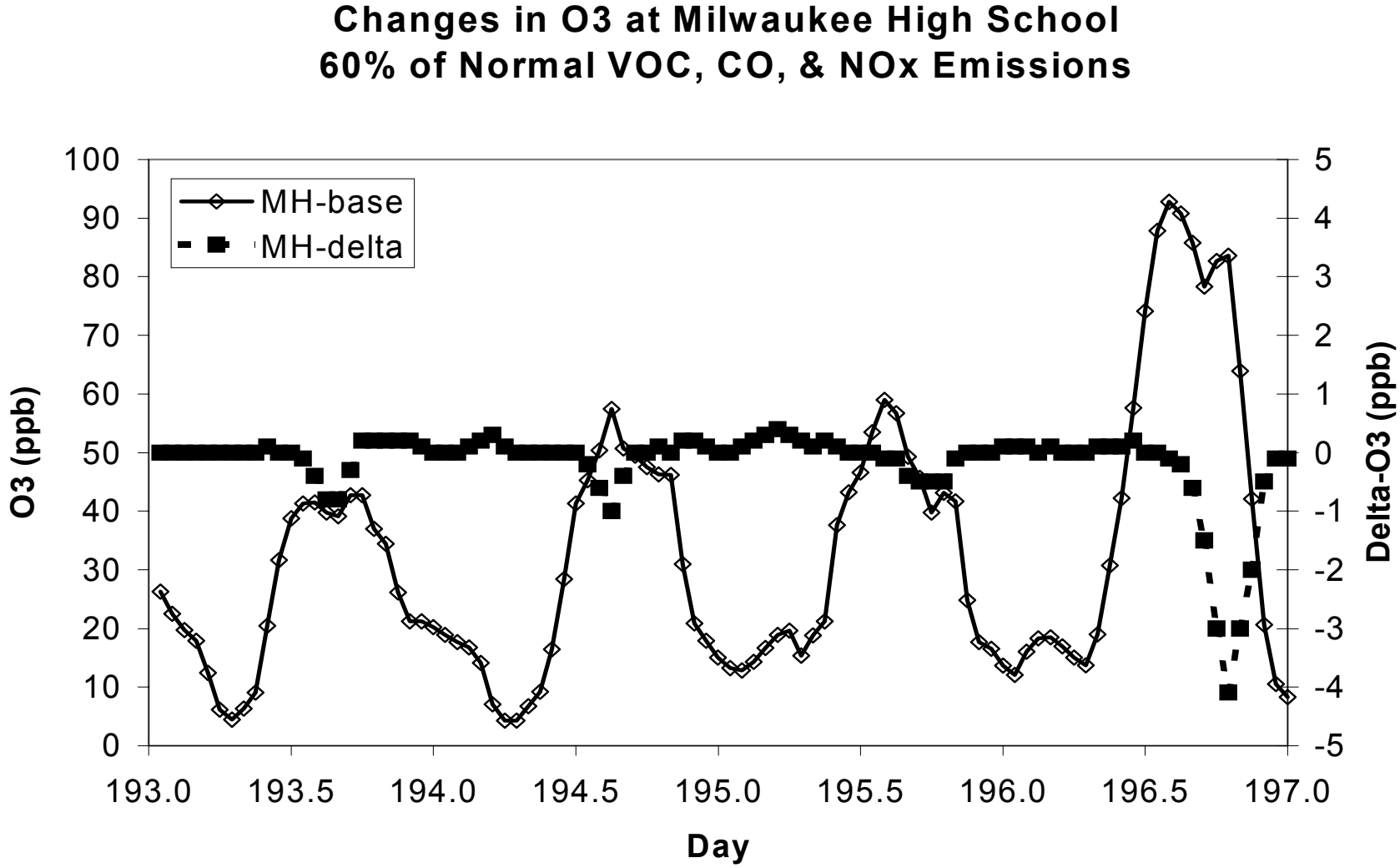

Figure 24. Time series of ΔO_3 and predicted ambient O_3 concentrations for the Carus monitoring site.

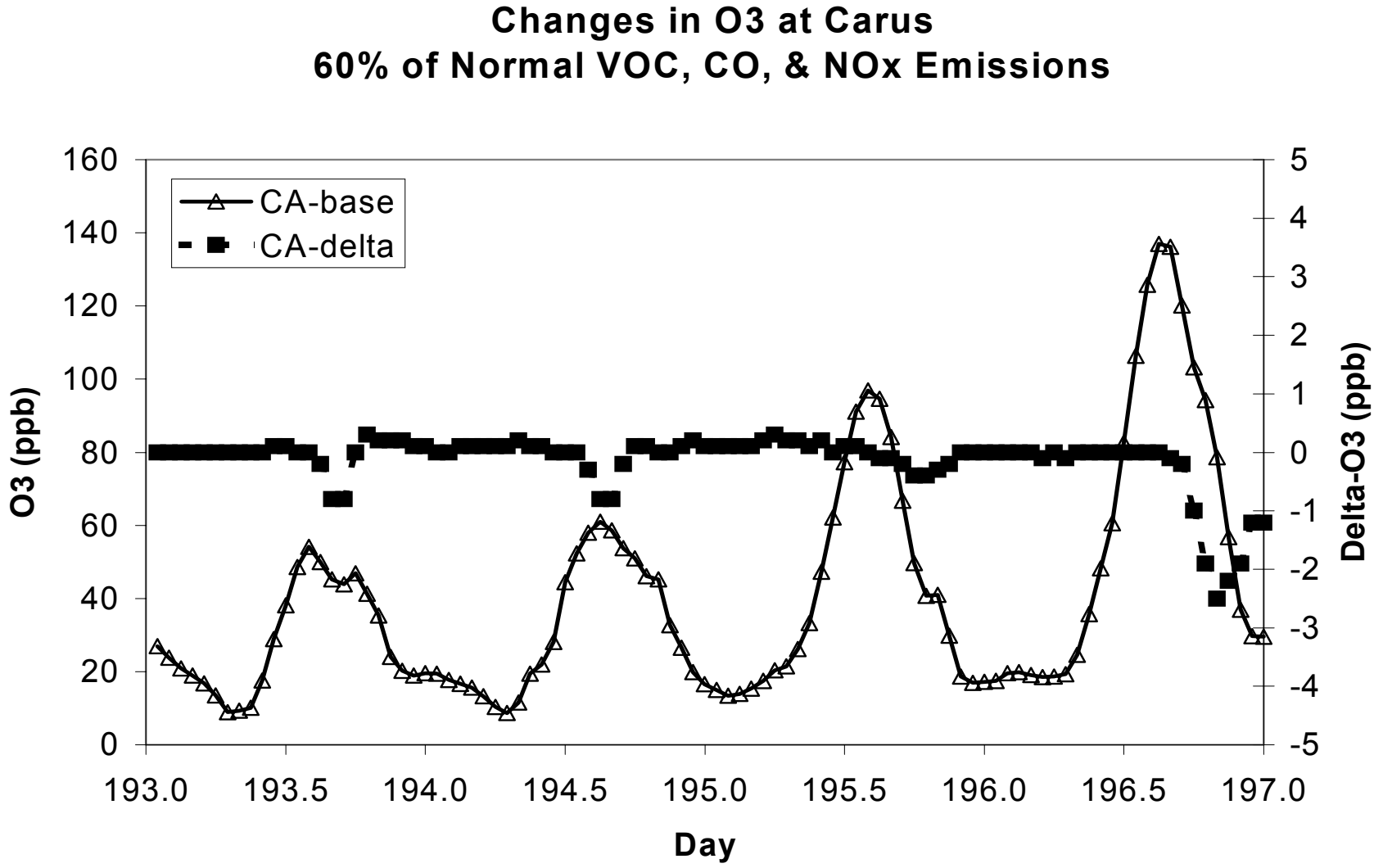

Time series of running eight hour averages are shown for the four monitoring stations in Figures 25-28. For the longer time average, the ambient ozone concentrations are decreased at each site compared to the one hour averages, and the ΔO_3 is also reduced on an eight hour average basis. The largest reduction in ozone, on an eight hour basis, occurs at the Milwaukee monitor and equals approximately 2 ppb during a period when the ambient ozone concentration is approximately 50 ppb.

Figure 25. Time series of 8-hr average ΔO_3 and predicted ambient O_3 concentrations for the Mountain View monitoring site.

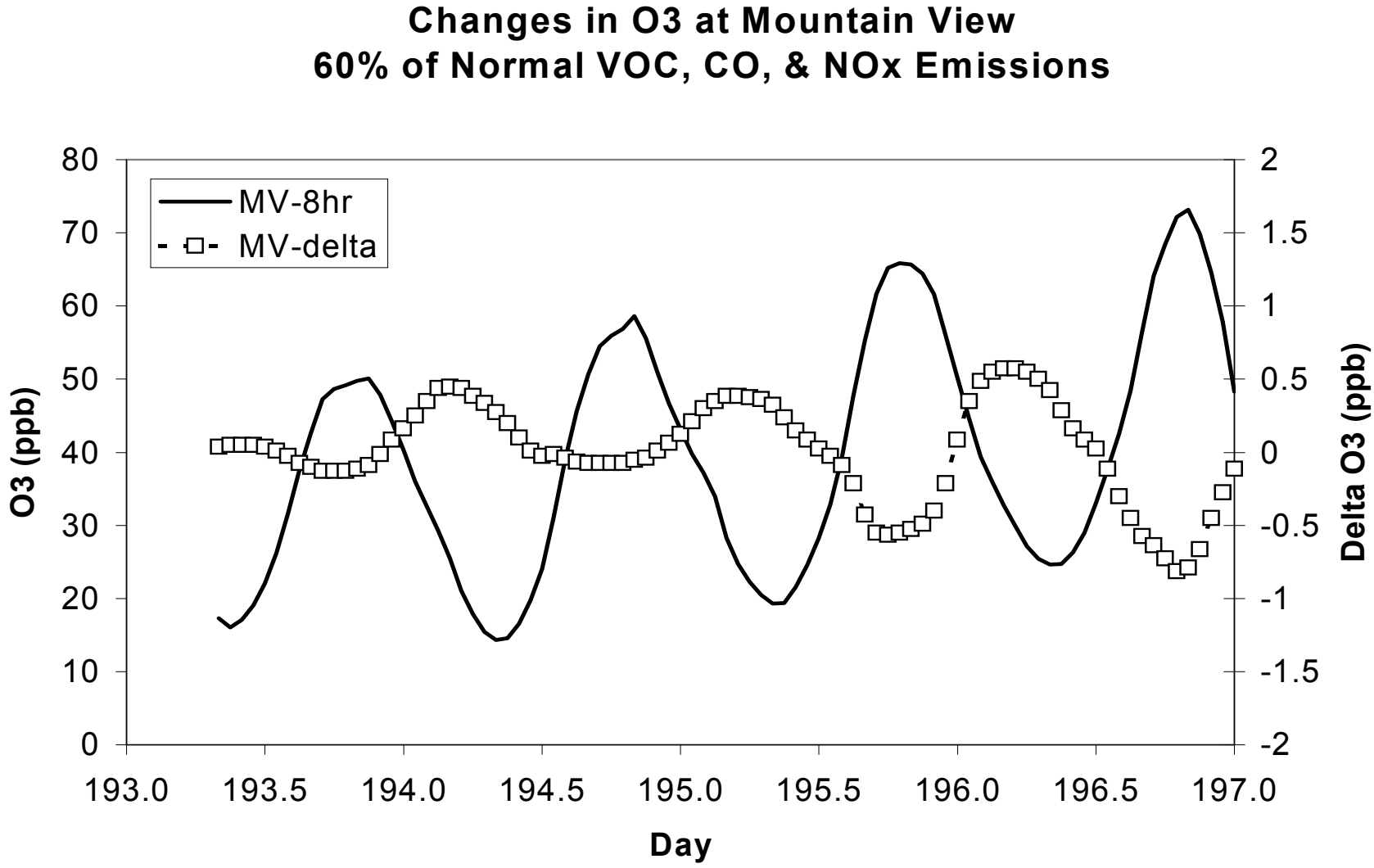

Figure 26. Time series of 8-hr average ΔO_3 and predicted ambient O_3 concentrations for the Sauvie Island monitoring site.

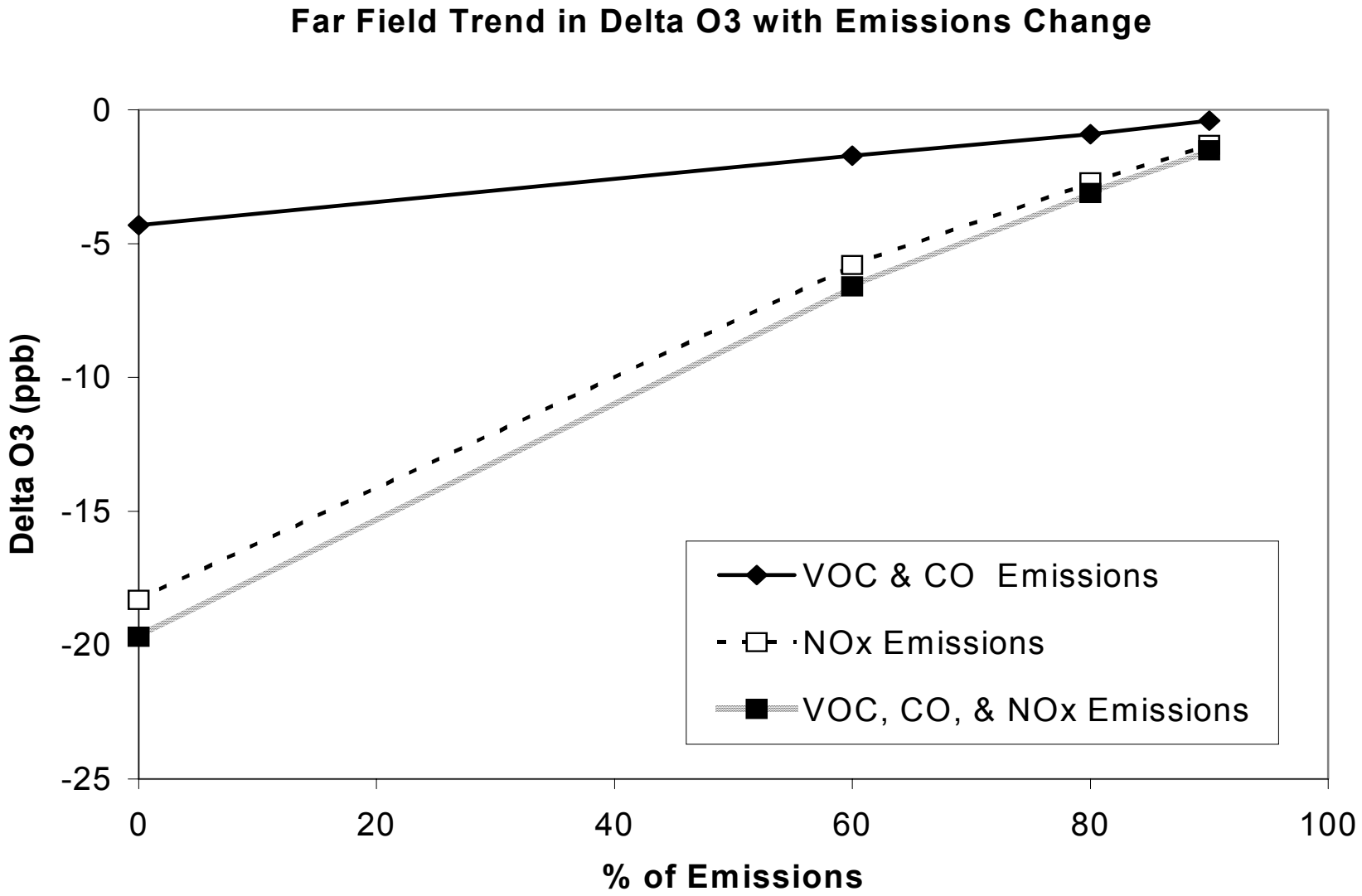

Figure 27. Time series of 8-hr average ΔO_3 and predicted ambient O_3 concentrations for the Milwaukee monitoring site.

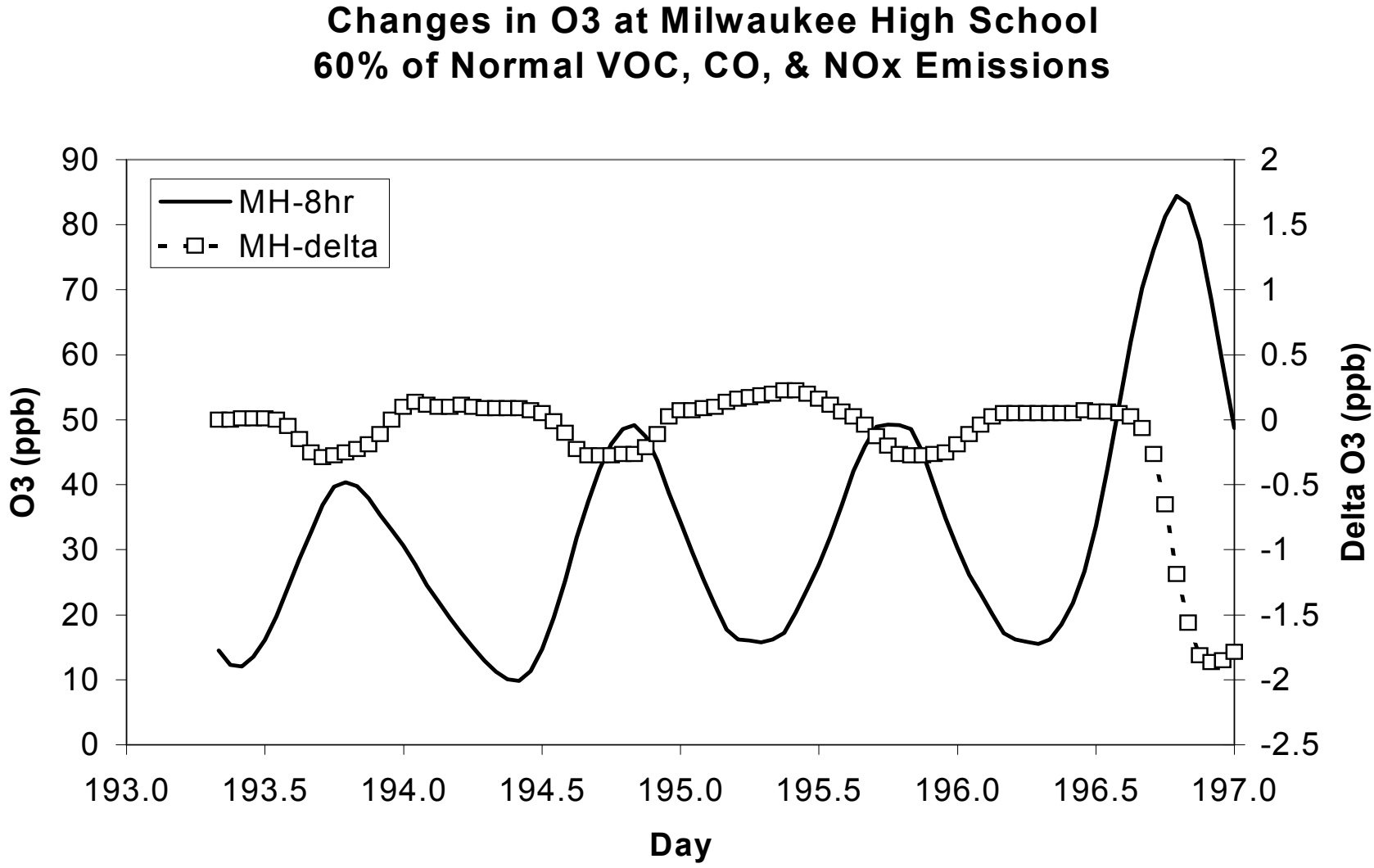

Figure 28. Time series of 8-hr average ΔO_3 and predicted ambient O_3 concentrations for the Carus monitoring site.

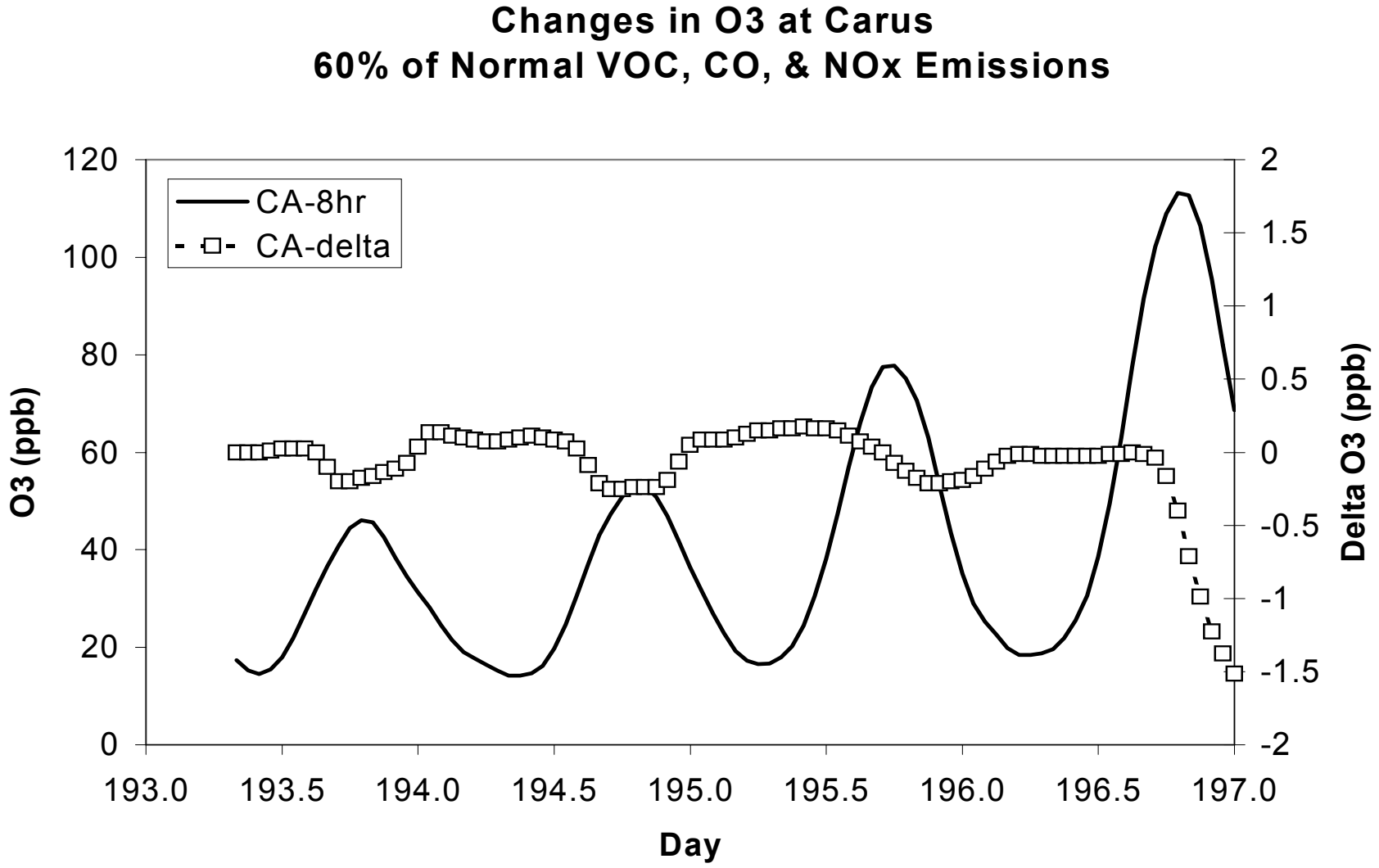

Results for all twelve of the sensitivity runs are summarized in Figures 29 and 30 in terms of the maximum and minimum ΔO_3 observed in each case, along with the coincident ambient ozone level at the location of the max/min ΔO_3. Similar results are shown in Figures 31-34 for each of the Portland area monitoring sites. The largest enhancements to ozone equal approximately 12 ppb and occur for the cases with zero NOx and with zero NOx, VOC/CO emissions. However, these enhancements exist at a location near the industrial sources at night when the ambient ozone concentration is approximately 20 ppb. For the other sensitivity runs with 60% to 90% of normal emissions, the enhancement in ozone is less than 5 ppb. The largest reduction in ozone equals approximately 19 ppb and occurs for the zero NOx, VOC/CO case and the zero NOx case. These reductions appear at locations further downwind, where ambient ozone levels are approximately 90 ppb. For the zero VOC/CO emission case, the largest reduction in ozone equals 4 ppb in an area with ambient ozone equal to 75 ppb. For all of the other sensitivity runs (60% to 90% of normal emissions), the reduction in ozone was less than 7 ppb. At the monitoring sites, the largest predicted enhancement is 5 ppb at Sauvie Island, while the largest reduction is 11 ppb at Milwaukee; these values represent the case with no emissions from the point Cowlitz Co. point sources.

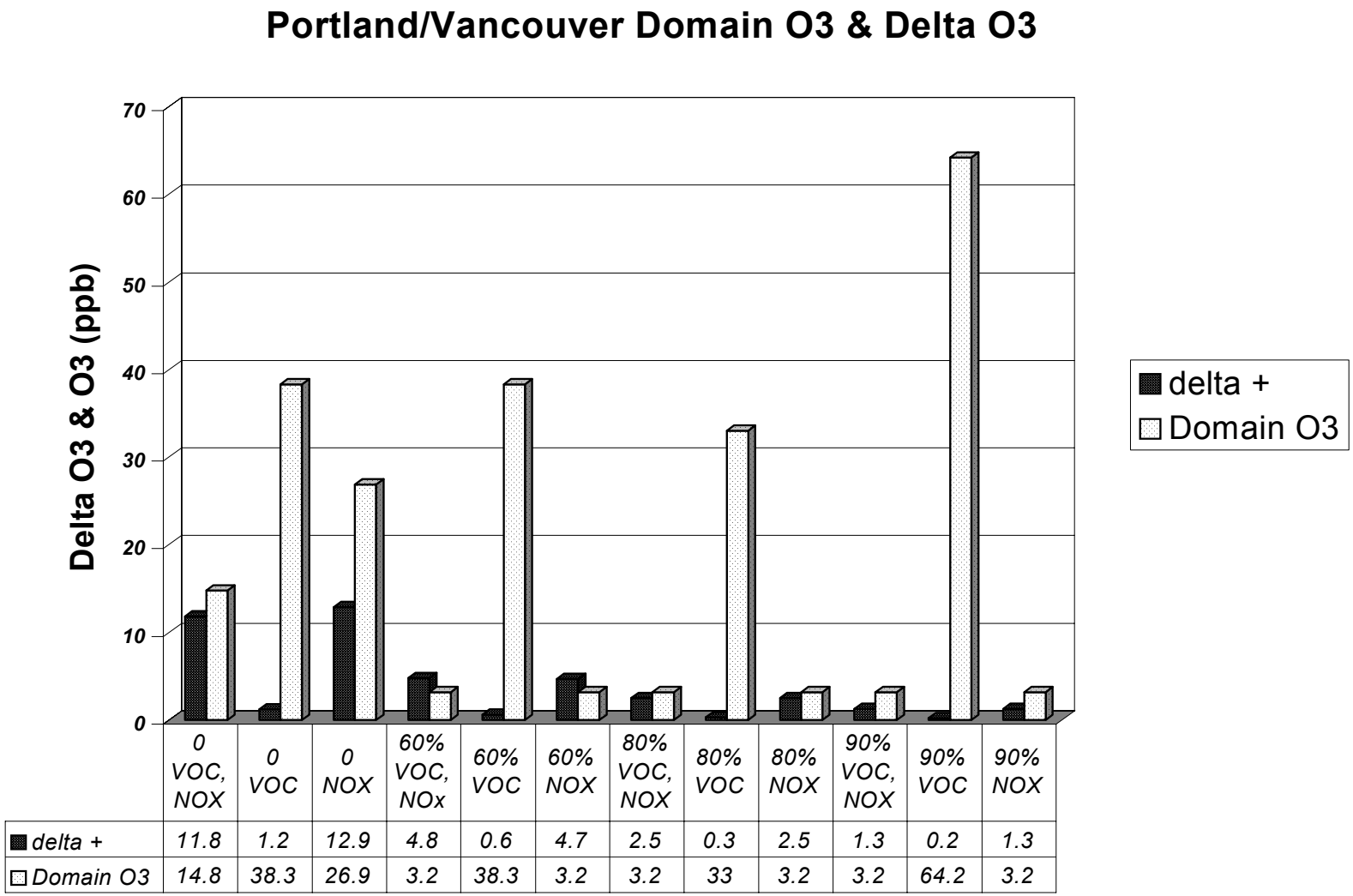

	0 VOC, NOX	0 VOC	0 NOX	60% VOC, NOx	60% VOC	60% NOX	80% VOC, NOX	80% VOC	80% NOX	90% VOC, NOX	90% VOC	90% NOX
delta +	11.8	1.2	12.9	4.8	0.6	4.7	2.5	0.3	2.5	1.3	0.2	1.3
Domain O3	14.8	38.3	26.9	3.2	38.3	3.2	3.2	33	3.2	3.2	64.2	3.2

Figure 29. Summary of maximum (delta +) ΔO_3 observed in the Portland/Vancouver area and the coincident ambient O_3 level for each sensitivity run.

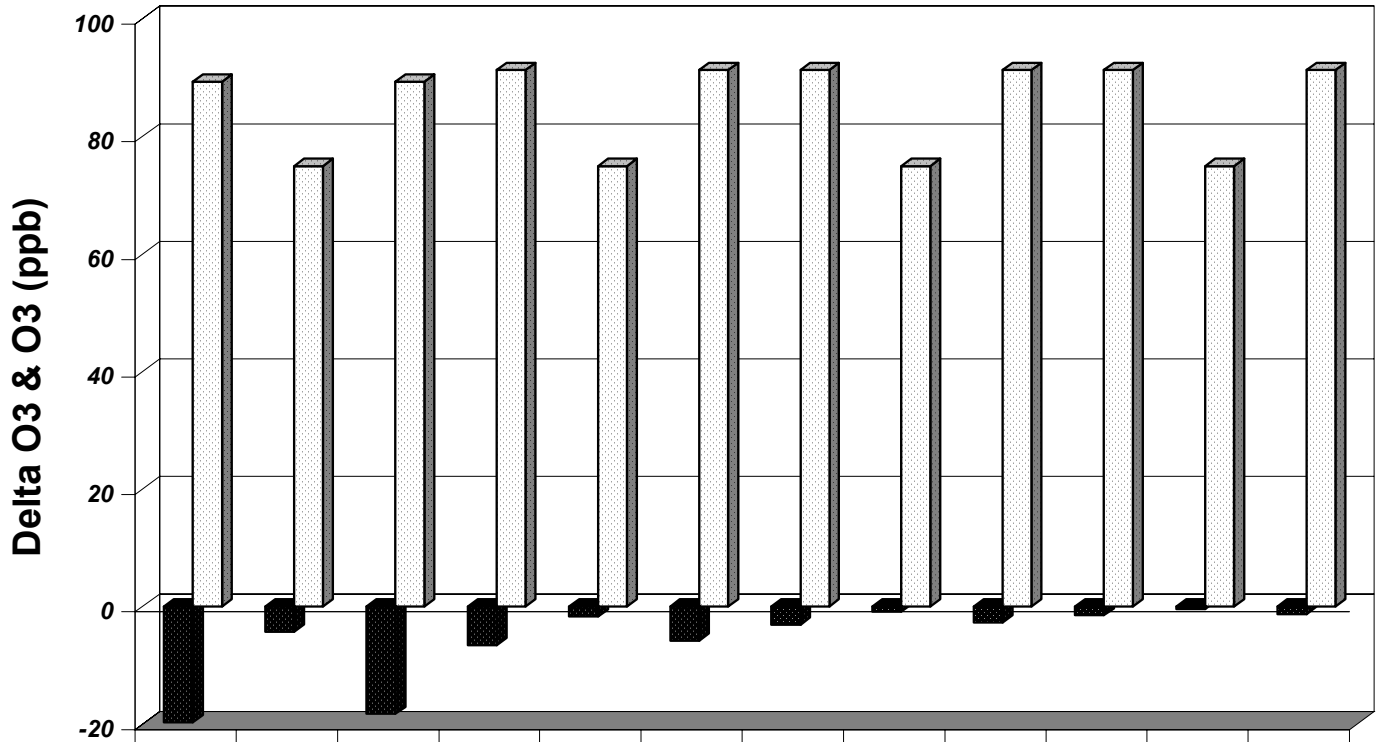

	0 VOC, NOX	0 VOC	0 NOX	60% VOC, NOx	60% VOC	60% NOX	80% VOC, NOX	80% VOC	80% NOX	90% VOC, NOX	90% VOC	90% NOX
delta -	-19.7	-4.3	-18.3	-6.6	-1.7	-5.8	-3.1	-0.9	-2.7	-1.5	-0.4	-1.3
Domain O3	89.3	75	89.3	91.3	75	91.3	91.3	75	91.3	91.3	75	91.3

Figure 30. Summary of minimum (delta -) ΔO_3 observed in the Portland/Vancouver area and the coincident ambient O_3 level for each sensitivity run for each sensitivity run

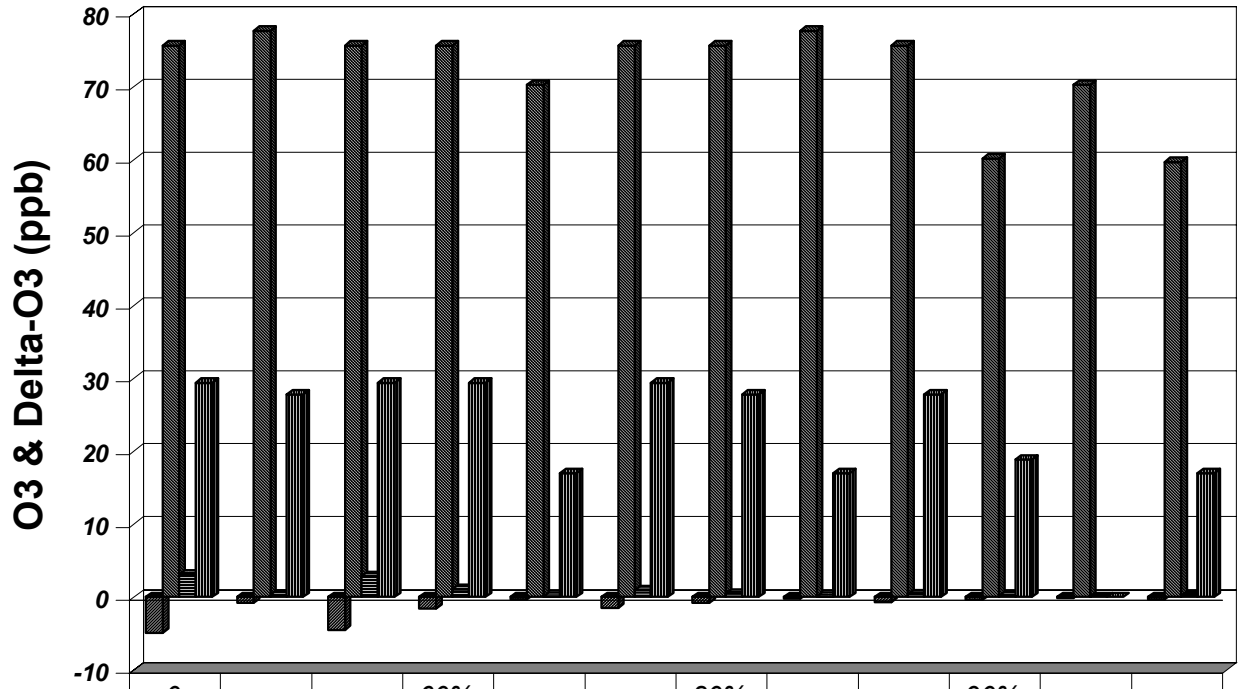

	0 VOC, NOX	0 VOC	0 NOx	60% VOC, NOx	60% VOC	60% NOX	80% VOC, NOX	80% VOC	80% NOX	90% VOC, NOX	90% VOC	90% NOX
delta -	-4.9	-0.8	-4.5	-1.6	-0.3	-1.5	-0.8	-0.2	-0.7	-0.4	-0.1	-0.3
MV -O3	75.7	77.7	75.7	75.7	70.3	75.7	75.7	77.7	75.7	60.2	70.3	59.7
delta +	3.1	0.3	2.9	1.1	0.1	1	0.5	0.1	0.4	0.2	0	0.2
MV +O3	29.4	27.8	29.4	29.4	17	29.4	27.8	17	27.8	18.9	0	17

Figure 31. Summary of max/min ΔO_3 and the coincident ambient O_3 level for each sensitivity run at the Mountain View monitoring site.

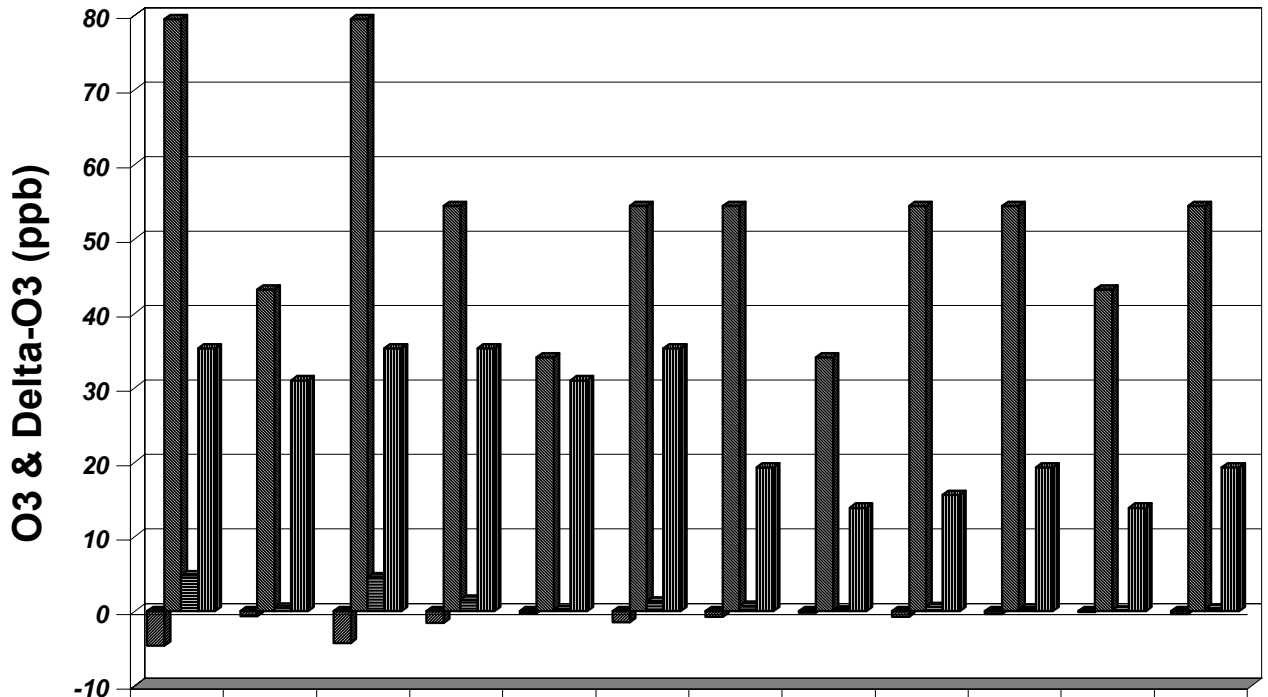

	0 VOC, NOX	0 VOC	0 NOx	60% VOC, NOx	60% VOC	60% NOX	80% VOC, NOX	80% VOC	80% NOX	90% VOC, NOX	90% VOC	90% NOX
delta -	-4.6	-0.7	-4.3	-1.6	-0.3	-1.5	-0.8	-0.2	-0.8	-0.4	-0.1	-0.4
SI -O3	79.5	43.2	79.5	54.4	34.1	54.4	54.4	34.1	54.4	54.4	43.2	54.4
delta +	4.8	0.5	4.6	1.5	0.2	1.3	0.7	0.1	0.6	0.3	0.1	0.3
SI +O3	35.3	31	35.3	35.3	31	35.3	19.3	13.9	15.6	19.3	13.9	19.3

Figure 32. Summary of max/min ΔO_3 and the coincident ambient O_3 level for each sensitivity run at the Sauvie Island monitoring site.

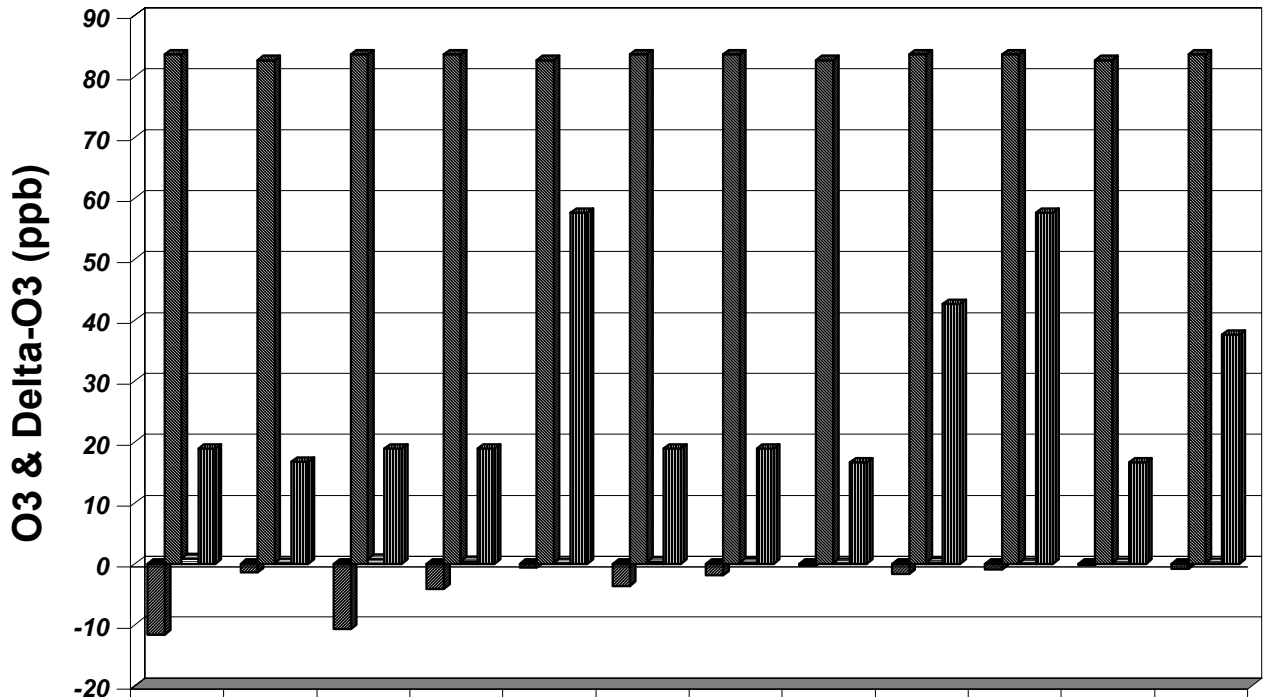

	0 VOC, NOX	0 VOC	0 NOx	60% VOC, NOx	60% VOC	60% NOX	80% VOC, NOX	80% VOC	80% NOX	90% VOC, NOX	90% VOC	90% NOX
delta -	-11.6	-1.4	-10.7	-4.1	-0.6	-3.6	-1.9	-0.3	-1.7	-0.9	-0.2	-0.8
MH -O3	83.6	82.7	83.6	83.6	82.7	83.6	83.6	82.7	83.6	83.6	82.7	83.6
delta +	0.9	0.1	0.8	0.4	0.1	0.3	0.2	0.1	0.2	0.1	0.1	0.1
MH +O3	18.9	16.8	18.9	18.9	57.6	18.9	18.9	16.7	42.7	57.6	16.7	37.6

Figure 33. Summary of max/min ΔO_3 and the coincident ambient O_3 level for each sensitivity run at the Milwaukee monitoring site.

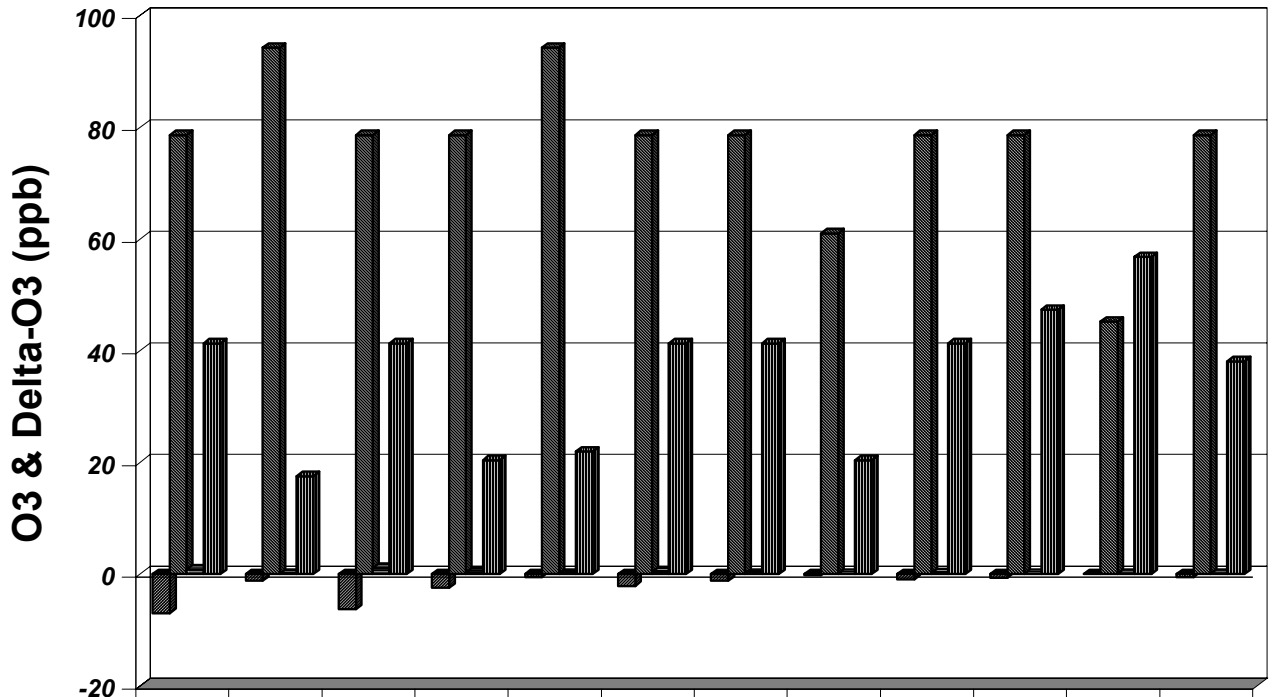

	0 VOC, NOX	0 VOC	0 NOx	60% VOC, NOx	60% VOC	60% NOX	80% VOC, NOX	80% VOC	80% NOX	90% VOC, NOX	90% VOC	90% NOX
delta -	-7	-1.2	-6.3	-2.5	-0.5	-2.1	-1.2	-0.2	-1	-0.6	-0.1	-0.5
CA -O3	78.6	94.2	78.6	78.6	94.2	78.6	78.6	61	78.6	78.6	45.2	78.6
delta +	0.8	0.1	1.1	0.3	0.1	0.4	0.1	0.1	0.2	0.1	0.1	0.1
CA +O3	41.3	17.5	41.3	20.4	21.9	41.3	41.3	20.4	41.3	47.3	56.8	38.1

Figure 34. Summary of max/min ΔO_3 and the coincident ambient O_3 level for each sensitivity run at the Carus monitoring site.

Trends in enhanced and reduced ozone can be examined with respect to percent changes in emissions and in terms of actual mass changes in emissions. With regard to percent changes in emissions, the trends for enhanced and reduced ozone, as a function of the magnitude of the emissions, are shown in Figures 35 and 36, respectively. For both the enhancement and reduction cases, the trend in ΔO_3 is essentially linear with changes in emissions. Ozone concentration is much more sensitive to changes in NOx emissions than to changes in VOC an d CO emissions. The trends are summarized in Table 5. The slope of the enhanced ozone curve is approximately 0.12 ppb for each percent reduction in NOx emissions, and only 0.01 ppb for each percent reduction in VOC/CO emissions. Thus, enhancements in ozone are approximately ten times more sensitive to NOx than to VOC emission changes on a percent basis. The slope of the reduced ozone curve is approximately -0.2 ppb for each percent reduction in NOx and -0.4 ppb for each percent reduction in VOC/CO. Therefore, reductions in ozone are approximately five times more sensitive to NOx than to VOC/CO emission changes on a percent basis. Again, it should be emphasized these trends reflect the modeled characteristics of only one ozone episode.

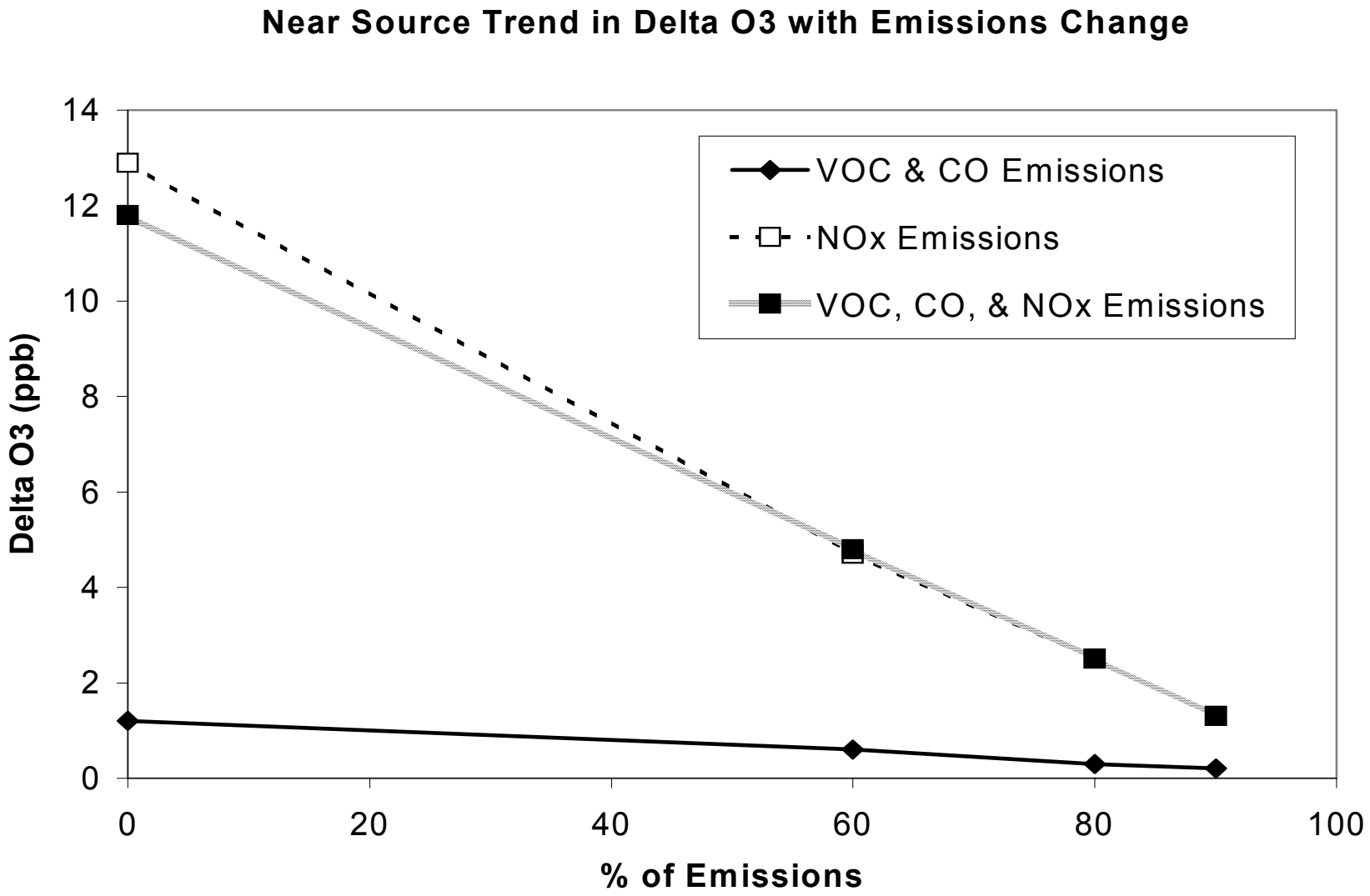

Figure 35. Trend in maximum enhancement of O_3 as a function of % change in industrial emissions.

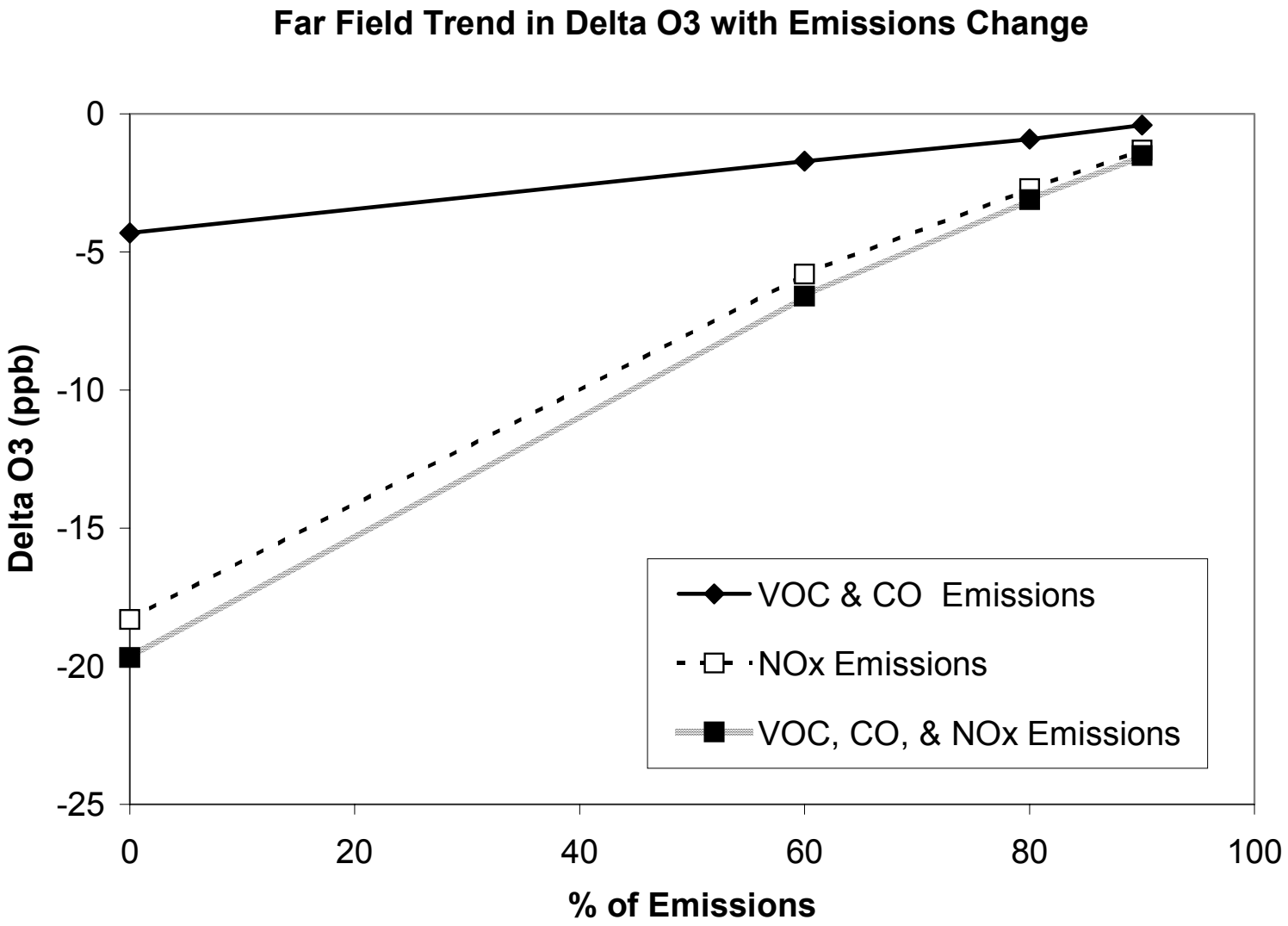

Figure 36. Trend in maximum reduction of O_3 as a function of % change in industrial emissions.

Table 5. Summary of slopes of ΔO_3 versus % emission changes for enhanced and reduced O_3 maxima within the Portland/Vancouver area.

	Enhanced O_3 cases	Reduced O_3 cases
Emissions change	Slope (ppb O_3/% emissions change)	Slope (ppb O_3/% emissions change)
VOC, CO, & NOx	0.12	-0.20
NOx	0.13	-0.19
VOC & CO	0.01	-0.04

Similar results are obtained when the change in ozone is examined with respect to the mass change in emissions. The trend for enhanced ΔO_3 with respect to mass emission change is shown in Figure 37 and the trend for reduced ΔO_3 with respect to mass emission change is shown in Figure 38. For these cases, the effects of CO are assumed negligible and the mass emission change is shown for only NOx or VOC emissions. The slopes of the ΔO_3 versus mass change of emissions are summarized in Table 6. In terms of mass change in emissions, ozone enhancements are approximately five time more sensitive to changes in NOx emissions compared to changes in VOC emissions, while ozone reductions are approximately two times more sensitive to changes in NOx emissions compared to changes in VOC emissions.

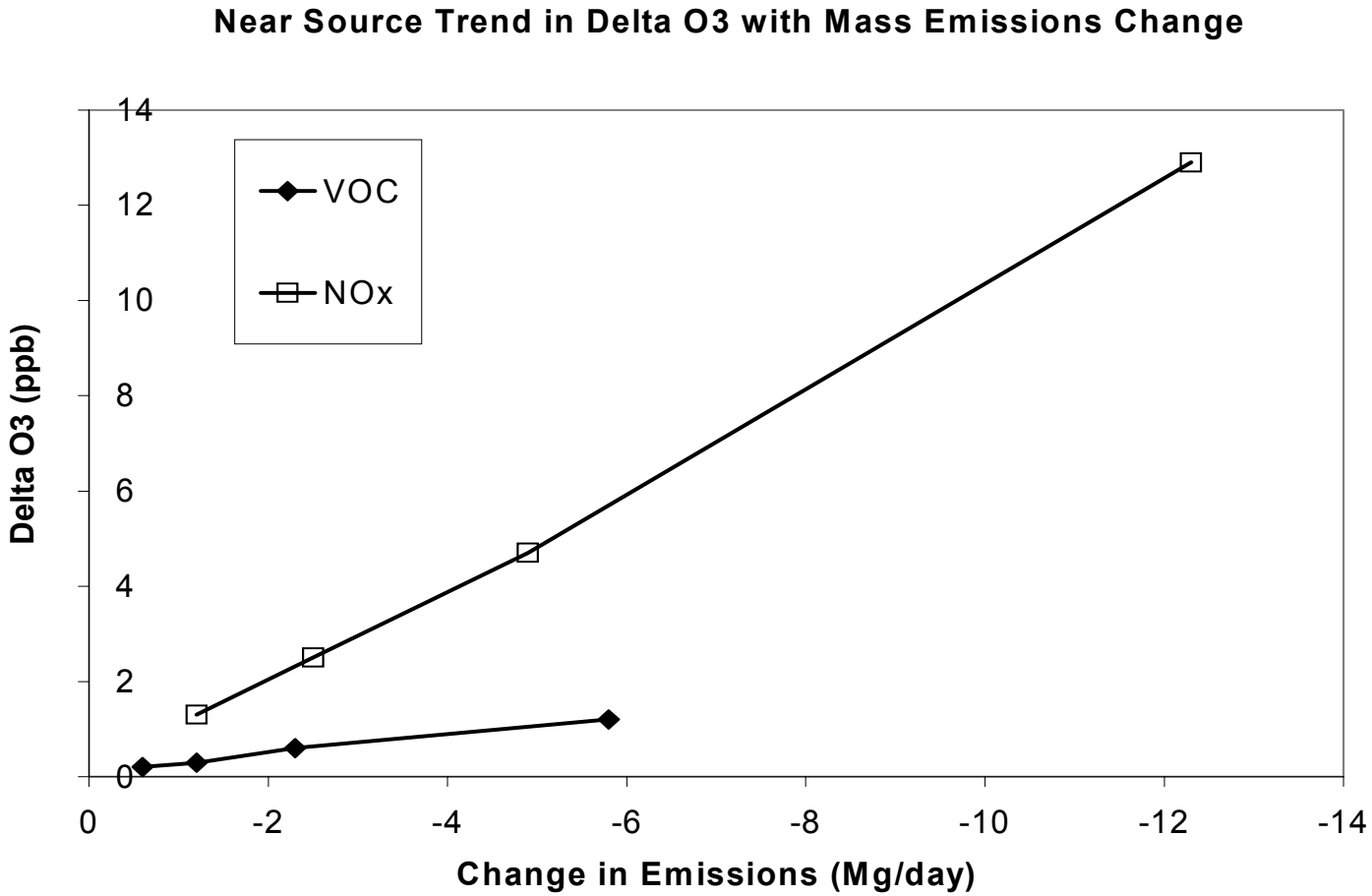

Figure 37. Trend in maximum enhancement of O_3 as a function of mass change in industrial emissions.

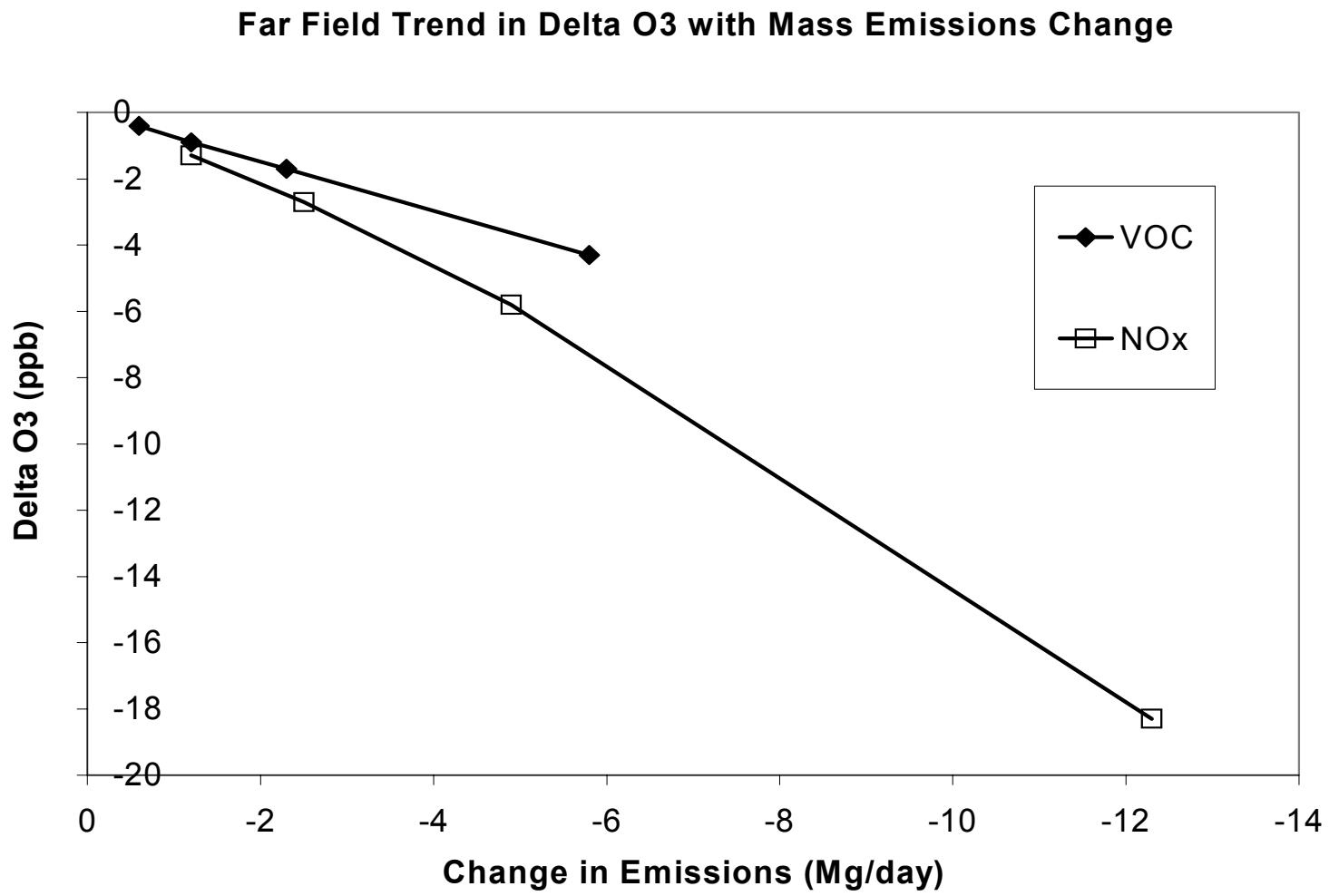

Figure 38. Trend in maximum reduction of O3 as a function of mass change in industrial emissions.

Table 6. Summary of slopes of ΔO_3 versus mass change in emissions for enhanced and reduced O_3 maxima within the Portland/Vancouver area.

	Enhanced O_3 cases	Reduced O_3 cases
Emissions change	Slope (ppb ΔO_3/(MT/day reduction)	Slope (ppb ΔO_3/(MT/day reduction)
VOC	0.19	-0.75
NOX	1.05	-1.56

In summary, the sensitivity runs for reduced emissions from the four industrial sources show that ozone levels can be increased due to reduced emissions immediately downwind of the sources. At the same time, however, ozone levels are reduced compared to the base case further downwind of the sources. It is significant that the reduced ozone levels do not occur in the region where the maximum ozone levels are predicted to occur. As a result, it does not appear from this analysis that changes in emissions at the industrial sources in Cowlitz County will have a significant impact upon the maximum levels of ozone produced in the Portland/Vancouver airshed. Since the Portland/Vancouver urban area and the industrial sources are separated by 90 km, it is not likely that the region of maximum ozone concentration produced by the urban plume will intersect the region of maximum impact from the industrial area for other cases.

Quality Assurance and Model Validation

Comparisons of the meteorological parameters and observations have been shown in a previous section. In this section, the performance of the model is evaluated in terms of predicted versus observed ozone concentrations.

The time series of predicted and observed ozone for all four monitoring sites in the 60 x 80 sub-domain are shown in Figure 39. Note that the predicted time series are taken from the first base case, with emissions from Longview Fibre reflecting the actual operating level during this episode. At Mountain View and Sauvie Island, the overall pattern of observed ozone concentrations are matched reasonably well by the predicted ozone concentrations, although the maximum observed concentration on Sunday at Mountain View is underestimated by 19% and the maximum concentration at Sauvie Island is underestimated by 22% on Saturday. The poorest model performance is exhibited at Milwaukee, where the model underestimates the observed ozone on each day of the simulation. The maximum observed concentrations at Milwaukee are underestimated by approximately 35% on both Saturday and Sunday. At Carus, the model also underestimates the observed ozone concentrations, except on Sunday, when the model prediction exceeds the maximum observed value by approximately 13 ppb.

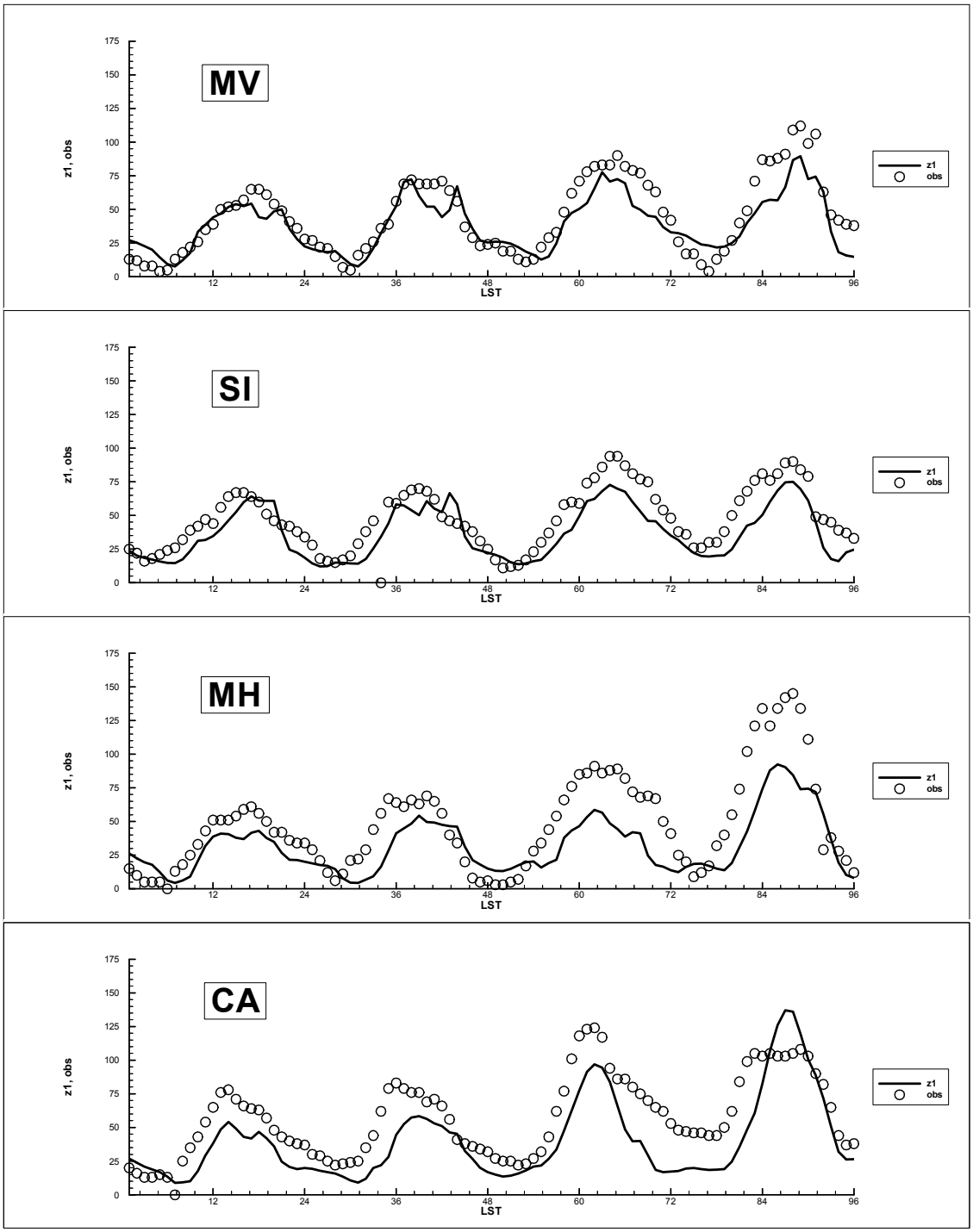

Figure 39. Time series of predicted (solid line) and observed (open circle) surface ozone concentrations at the Mountain View (MV), Sauvie Island (SI), Milwaukee (MH), and Carus (CA) monitoring sites.

Model performance statistics are summarized in Table 7. The model index of agreement is greater than 0.8 for all four stations, which suggests an acceptable level of agreement. The normalized mean bias ranges from –7% to –41% at the four sites, which indicates an overall tendency for the model to underestimate the observed ozone concentrations. This tendency to underestimate ozone is also reflected in the differences between the average observed and predicted concentrations and in the slope of the regression curve of predicted versus observed ozone. A scatter diagram of predicted versus observed ozone for the latter three days at all four sites is shown in Figure 40. The normalized gross error ranges from 26% to 41%. For comparison, the California Air Resources Board (CARB) guidelines for typical photochemical model performance include a normalized bias within ± 15% and a normalized gross error within ± 35% (DaMassa et al., 1992). The standard deviations of observed and predicted concentrations are similar, which indicates that the model matches variations in observed ozone. Differences in the three day average of the maximum observed and predicted daily ozone concentrations are approximately 10% for the Sauvie Island, Carus, and Mountain View monitors, and 30% for the Milwaukee monitor. The CARB guidelines for peak prediction accuracy, unpaired in space and time, are ± 20%. Note that the results for peak predictions in Table 7 are paired in space, but not in time.

Table 7. Summary of model performance statistics based upon observed and predicted O_3 concentrations by monitoring site.

	CA	MH	MV	SI
Average Observed O_3 (ppb)	58	48	45	47
Average Predicted O_3 (ppb)	40	32	39	37
Standard Deviation of Observations (ppb)	30	36	28	23
Standard Deviation of Predictions	30	22	21	20
Slope	0.86	0.52	0.67	0.77
Intercept (ppb)	-9.1	7.3	8.6	0.1
RMSD	24	26	14	15
Index of Agreement	0.85	0.81	0.92	0.88
Normalized Gross Error	0.36	0.37	0.26	0.29
Normalized Bias	-0.07	-0.20	-0.20	-0.18
Ave. Max Obs.	105	102	91	85
Ave. Max Pred.	98	70	81	73
% Difference	7	30	10	13

Given the complicated terrain and associated wind patterns in the area, the model performance appears to be within the acceptable range, although it is clear that the model has a tendency to underestimate observed ozone concentrations. As indicated previously, one objective of this work was to improve the overall performance of the regional modeling system. This was accomplished through changes in the method used to generate the input meteorological fields. No changes in the emission inventory were required to obtain a reasonable level of agreement between observed and predicted ozone concentrations, which suggests that the emission inventory is not in significant error. In future work on the regional modeling system, a more rigorous method of modeling the meteorology should be identified. Also, further analysis of other pollutants, in comparison to available observations, should be completed. Finally, more ozone episodes should be evaluated, and a more complete uncertainty analysis conducted, to better understand photochemical air pollution in the Cascadia region of the Pacific Northwest.

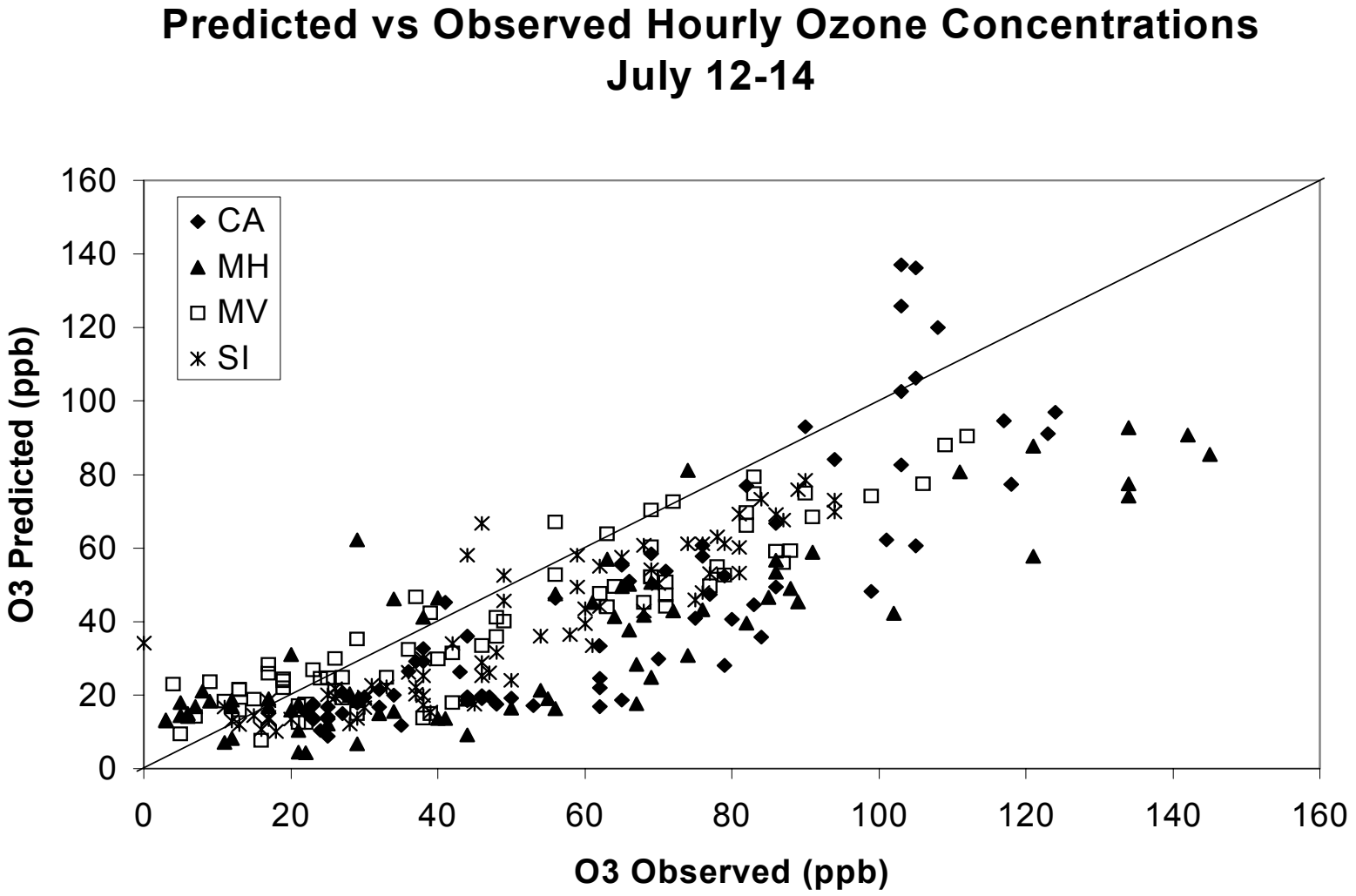

Figure 40. Predicted versus observed ozone concentrations for all four sites during July 12-14, 1996.

References

Barickman, P. and R. Swart, 1997. Status Report on the Wasatch Front Ozone Study, UDAQ Document DAQT-078-97, Division of Air Quality, Department of Environmental Quality, State of Utah, 150 N. 1950 West, Salt Lake City, UT 84116-3085.

DaMassa, J., 1992. Technical Guidance Document: Photochemical Modeling, California Air Resources Board, P.O. Box 2815, Sacramento, CA 95812.

Appendix A
Preparation of the Emission Inventory

Emissions inventories were developed as input for the CALGRID model to simulate ozone production during two ozone episodes occurring July 12-14, and July 24-28, 1996. A "spin-up" day was added to the beginning of each event to initialize the model. Hourly emissions were estimated for each day, and allocated to five kilometer grids over the modeling domain bounded by (in UTM zone 10 coordinates) 4900 to 5560 north and 350 to 720 east. This is roughly Vancouver, BC to Eugene, OR; and the Pacific Ocean to just east of the Cascade ridge.

The inventory documentation is divided into five major sections. The first through third sections describe the methodology used to estimate emissions from point, area and nonroad, and biogenic sources. The fourth section is a summary of Washington and Oregon emissions. The fifth section describes the process of nitrogen oxide and hydrocarbon speciation in preparation for photochemical modeling.

I. Point Sources

An emissions inventory was developed for major stationary sources for western Washington, Oregon, and British Columbia. To develop an emissions inventory for point sources, two types of data are needed: 1) emission rates and 2) physical source characteristics. Both of these data types are described below for major stationary sources. For the purposes of this report, a *point source* is defined as each unit within a facility.

1. Emission Rates

To develop an emissions inventory for point sources, emissions were limited to those sources that met one of the following criteria: VOC, NOx or SO_2 greater than 40 tons per year; or CO greater than 100 tons per year. These point sources were determined by using the Washington Emission Data System (WEDS)[1] and through contact with the Oregon Department of Environmental Quality and the National Resource Council of Canada.

For this study, hourly emission rates were determined by one of three methods: 1) continuous emission monitoring (CEM) data, 2) amount of raw materials consumed, or 3) reported annual emission rate using a facility operating schedule. An attempt was made to provide the most accurate data possible for the period in question. However, it was not possible to get continuous emission monitoring (CEM) data from every facility.

Washington Point Sources

CEM data or other daily estimates were obtained for most of the sources regulated by Ecology (pulp mills and aluminum smelters) and some of the sources regulated by the

Northwest Air Pollution Authority (oil refineries).[2 - 19] Those sources that did not provide CEM data provided either amount of raw materials consumed or an operating schedule for the study period. Raw material data was used with emission factors from AP-42[20] and National Council for Air and Stream Improvement (NCASI) Technical Bulletins to determine actual emissions.[21] Operating schedules were used with the WEDS data to determine more accurate emission rates.

Emissions for Washington point sources where CEM or daily estimates were not available were obtained from the WEDS. The annual hours of operation are also reported to WEDS and these numbers were used with the annual emission rates to determine an average hourly emission rate.

For the Centralia Power Plant, annual operation was used to determine emissions during upset conditions. The annual reporting showed that upset conditions only occurred over only three hours during the year. In the modeling, the emissions were inadvertently used for all hours, resulting in higher emissions than actually occurred. This mainly affected SO2 emissions, and to a lesser extent, NOx emissions. This will be corrected in any future modeling exercises. The summaries shown in section IV reflect one hour of possible upset on each day.

Oregon Point Sources

1996 emissions for 44 facilities in Oregon were provided by the Oregon Department of Environmental Quality. No data were provided for hours of operation, therefore, each facility was assumed to operate 24 hours a day for the full year.

Canada Point Sources

Emissions were supplied by the Canadian National Research Council for a specific weekly event (Sunday – Friday) in 1993. Average Monday through Friday emissions were used as estimates for all weekdays. Sunday estimates were used for weekend days.

Table A-1. Number of Point Sources by Category

Category	WA	OR	Canada
External Combustion Engines	72	30	9
Internal Combustion Engines	21	6	0
Chemical Manufacturers	4	1	3
Food and Agriculture	5	0	0
Primary Metal Production	15	8	1
Secondary Metal Production	2	3	0
Mineral Products	15	4	3
Petroleum Industry	50	0	2
Pulp and Paper and Wood Products	47	39	19
Rubber and Miscellaneous Plastics Production	5	1	1
Surface Coating Operations	38	8	0
Bulk Terminals/Plants	1	3	0
Printing/Publishing	0	0	0
Transportation and Marketing of Petroleum Products	5	3	0
Solid Waste Disposal	6	2	1
Other	11	6	11
Total Number of Western Washington Sources	***297***	***114***	***50***

2. Physical Site Characteristics

To develop an emission inventory for point sources, physical site characteristics are needed in addition to emission rates. These characteristics include point source location and stack parameters such as height, diameter, exit velocity, and temperature.

Point Source Location

To determine the location of a point source, coordinates and elevation are needed. The WEDS, Oregon, and Canada emission inventories provided UTM coordinates for each point source or facility. Sources with missing coordinates were assigned coordinates using their location address. In some cases, estimates were based on the county and city of location.

Stack Parameters

Some of the point sources did not have stack data either because the sources do not have a stack or because the data was not available. To get estimates of stack parameters for these sources, averages of available stack parameters were calculated by industrial process (defined by Source Classification Category codes). For those processes where stack parameters were not available, stack parameters from similar processes were used. These average stack parameters were applied to these sources dependent on process. For fugitive sources, the following stack parameters were used:

Temperature = 303 K (30 degrees C)
Height = 0 m
Diameter = 1 m
Velocity = 0.1 m/s

II. Area and Mobile Sources

In order to prepare an inventory suitable for modeling, four basic tasks were completed for each source category: 1) estimate an activity level, 2) adjust/allocate the activity (emissions) temporally, 3) allocate the activity (or emissions) spatially, and 4) estimate emission rates per the activity level. Each of these tasks is described below for point sources, on-road mobile sources, stationary anthropogenic area sources, and non-road mobile sources.

On-road Mobile Sources

1. Activity Level - Vehicle Miles Traveled

The Washington and Oregon Departments of Transportation (WSDOT, ODOT) and several local transportation planning agencies provide information on the average daily number of vehicle miles traveled (ADVMT). Wherever possible, local agency VMT spatially resolved by roadway segment (link) was obtained to accurately model mobile source emissions. [22, 23, 24, 25] Where spatially resolved local agency was not available, state transportation department link data for state route ADVMT was utilized. [26, 27]

The state route link ADVMT data was adjusted to account for county and city jurisdiction ADVMT. To do this, summary ADVMT information was obtained. Both WSDOT and ODOT provided Highway Performance Monitoring System (HPMS) data, which is summary VMT over several urban and rural areas.[26, 28] HPMS differs from the state route link ADVMT because it also includes county and city VMT. WSDOT also provided estimates of total ADVMT by county. The estimates were based in part on actual traffic counts, and are normally used for general informational purposes.[26] In Washington, the state route link ADVMT was increased by multiplying the link ADVMT by the ratio of total county HPMS ADVMT to county state route ADVMT. In Oregon, the state route link ADVMT was increased by multiplying the link ADVMT by the ratio of total state HPMS ADVMT to state route ADVMT.

Table A-2 lists the final sources of ADVMT used in this inventory. The following abbreviations are used for the local agencies: PSRC (Puget Sound Regional Council), SWWRTC (Southwest Washington Regional Transportation Council), TRPC (Thurston Regional Planning Council), and METRO (transportation planning agency for Portland, OR).

Table A-2. ADVMT Sources

Agency	Area	Year of ADVMT
WSDOT	All WA counties except those listed below	1995
ODOT	All OR areas except METRO's planning area	1996
PSRC	King, Kitsap, Pierce, Snohomish Counties – WA	1995
SWWRTC	Clark County – WA	1994
TRPC	Thurston County – WA	1994
METRO	Greater Portland, OR area	1994

2. Temporal Adjustments

Annual

All 1994 ADVMT was projected to 1995 using the ratio of 1995 to 1994 summary HPMS ADVMT. 1996 HPMS ADVMT for most areas was not available when the ADVMT estimates were finalized. To project to 1996, WSDOT, PSRC and SWWRTC ADVMT projections were examined.[29, 30, 31] In general, PSRC had the lowest growth rates and WSDOT the largest. The average of PSRC and SWWRTC growth rates (2%) was used to linearly project 1995 ADVMT to 1996 for all areas. 1996 ADVMT is listed in table A-3. The ADVMT listed in the eastern-most counties represents the ADVMT occurring within the modeling domain (west of UTM coordinate 720 km), not the whole county.

Other adjustments

Monthly, daily and hourly adjustments were made to the ADVMT based on traffic recorder statistics supplied by WSDOT.[32, 33] July traffic is approximately 7% higher than the annual average. Daily variation shows an increase in traffic beginning with Monday and peaking on Friday. The lowest traffic occurs on the weekend, with Sunday traffic lower than Saturday traffic. Hourly variation shows morning and evening peaks during the weekdays. On weekends, the traffic increases from morning until peaking at about 5 pm.

Table A-3. County 1996 Average Daily Vehicle Miles

Washington			Oregon	
County	ADVMT		County	ADVMT
Chelan	1,742,772		Benton	1,246,658
Clallam	1,368,402		Clackamas	6,217,754
Clark	5,240,672		Clatsop	1,339,824
Cowlitz	2,378,082		Columbia	1,396,362
Douglas	379,869		Crook	294,318
Grays Harbor	1,733,797		Deschutes	595,790
Island	919,493		Hood River	1,063,887
Jefferson	755,524		Jefferson	1,033,630
King	42,239,815		Lane	69,954
Kitsap	5,315,901		Lincoln	1,608,478
Kittitas	2,062,030		Linn	3,778,930
Klickitat	774,754		Marion	6,283,545
Lewis	2,652,498		Multnomah	10,273,247
Mason	883,885		Polk	1,333,984
Okanogan	121,219		Sherman	408,368
Pacific	636,317		Tillamook	894,375
Pierce	16,509,856		Wasco	1,182,707
Skagit	2,751,168		Washington	6,492,085
Skamania	859,342		Yamhill	2,022,717
Snohomish	15,260,340			
Thurston	6,209,522			
Wahkiakum	145,604			
Whatcom	3,655,237			
Yakima	3,821,669			
Total	***118,417,768***		***Total***	***47,536,613***

3. Spatial Allocation

Roadway link geographic coordinates were used to spatially allocate ADVMT to the modeling grid system.

4. Emission Rates

The EPA's MOBILE model (version 5b) was used to generate emission rates for nitrogen oxides (NOx), carbon monoxide (CO), and total organic compounds (TOG) in grams per mile.[34] Sulfur dioxide (SO_2) emission factors were generated from a similar EPA model called PART5.[35]

EPA used data collected from different categories of vehicles under different operating conditions to develop the model. The model is continuously updated as new information is gathered. The model may be tailored to account for local conditions (such as fleet registration mix, temperature, fuel parameters, vehicle inspection and maintenance programs (I/M), and speeds). The model can output results for several classes of gasoline and diesel powered vehicles. Organic emissions can be output both in total and with a detailed evaporative and exhaust emission breakdown.

Local parameters were used for speed, inspection and maintenance (I/M) programs, anti-tampering programs, Reid vapor pressure (RVP), hourly temperatures, and the vehicle fleet age distribution. Each will be described below.

It should be noted that emission rates calculated for the first ozone event (July 11-14) were calculated in a prior modeling effort to assess the effects of stage II vapor recovery at gasoline service stations. The emission rates were not re-calculated for this study. Because the emission rates for the two events were not made at the same time, there are minor differences in the way they were calculated. Differences are not expected to have a great effect on the results; they are noted below where appropriate.

Speed

To simplify modeling of the roadway network of approximately 50,000 links, a single speed that would produce emissions representative of the area was utilized for each pollutant. To determine the speed appropriate for each pollutant, an analysis of link-specific speeds and corresponding emission rates was conducted using the Puget Sound traffic network (13,000 links). Emissions in grams were calculated for each link and summed for an area-wide total. The total emissions were divided by the total number of ADVMT to obtain an average emission rate in grams per mile. The average rates were compared to emission rates calculated using the MOBILE model, and the speeds producing emission rates closest to the area-wide average emission rates were chosen. The speeds were 27 mph for CO, 29 mph for TOG, and 49 mph for NOx. Speed has no effect on the SO2 emissions produced by the PART5 model.

Inspection and Maintenance (I/M), Anti-Tampering Programs

Vehicle I/M programs are in place in the Puget Sound, Vancouver, and Portland areas. The Portland area also operates an anti-tampering program. Parameters appropriate for each area were used in the MOBILE modeling files.[36, 37, 38] The parameters include program start year, stringency (percent of vehicles failing the initial test), vehicles and model years required to take the test, type of test(s), waiver rates, program compliance rates, and passing emissions cutpoints. Washington runs a loaded-idle test. Due to the smaller sample size used to determine credits for this type of test in the MOBILE model, there is actually less credit given to it than is given to the 2500/idle test. For this reason, and at the recommendation of OMS,[39] the test type was run as 2500/idle.

Table A-4. I/M Program Parameters

Parameter	Puget Sound Seattle	Puget Sound Tacoma, Everett	Portland	Vancouver
test type	2500-idle	2500-idle	2500-idle	2500-idle
start year	1982	1993	1975	1993
stringency	32%	32%	47%	36%
model yrs tested	1968-1995	1968-1995	1975-1994	1968-1995
pre '81 waivers	9%	9%	0%	6%
post '80 waivers	17%	17%	0%	14%
compliance rate	90%	90%	90%	90%
cutpoints	test default	test default	test default	test default

For areas with an inspection and maintenance (I/M) program, emission factors with and without the I/M program were weighed according to the percentage of vehicles entering the I/M area from areas where I/M is not required. For the Puget Sound the percentage was 82.9% I/M, for Vancouver 70.1% I/M, and for Portland 84.1% I/M.[40], [41]

Reid Vapor Pressure (RVP)

In 1992, the legal summertime RVP limits were 7.8 for Oregon, and 9.0 for Washington.[42] Based on fuel surveys, the Washington RVP was adjusted according to geographic area. For the first event, the RVP was lowered to 8.7,[43] for the second event, it was lowered to 8.2 in the Puget Sound area, and lowered to 8.9 in the rest of Washington.[44] Gasoline used in Clark County, WA was assumed to come from Oregon suppliers, and thus have an RVP of 7.8.[45]

Hourly Temperatures

Hourly temperatures for the first event were obtained from the Sand Point meteorological station in north Seattle.[46] The Sand Point temperatures were used for all mobile source emissions calculations. The same temperatures were used for each day since they were very similar. For the second event, hourly temperatures became more easily available from other meteorological stations. SeaTac temperatures were used for all of Washington except Clark County, and Portland temperatures were used for Clark County, WA and all of Oregon.[47]

Table A-5. Maximum and Minimum Temperatures in Fahrenheit

Day(s)	Sand Point		SeaTac		Portland	
	min	max	min	max	min	max
7/11-14	63	87	na	na	na	na
7/23	na	na	64	85	67	97
7/24	na	na	65	88	68	93
7/25	na	na	61	91	63	95
7/26	na	na	64	88	67	94
7/27	na	na	62	89	66	94
7/28	na	na	62	83	67	76

Vehicle Fleet Age Distribution

Fleet age distributions (curves depicting the number of vehicles 1, 2, 3, …, 25 years old) were constructed using vehicle licensing information from the Washington State Department of Licensing. For the first event, a distribution was constructed from 1995 registration records. For the second event, 1996 registrations were used.[48]

Area Sources – Gasoline Service Stations

Gasoline service station emissions were the focus of a prior CALGRID modeling effort of the same ozone event (July 11-14, 1996). In Washington, emissions estimates were made using gasoline throughput and control equipment records from local air authority registration program records.[49, 50, 51, 52, 53] In Oregon, gasoline throughput estimates were made using total ADVMT, assuming an average fuel economy of 20 miles per gallon. Controls in place were assumed similar to Washington.

VOC emissions were calculated using a combination of emission factors from AP42[54] and MOBILE5b.

Gasoline service station emissions were very small in comparison to other sources.

Area Sources – Stationary Anthropogenic Sources

Using the ozone maintenance plans from PSAPCA and SWAPCA, the larger sources of total organics (TOG) were inventoried.[30, 31] Some smaller sources were also inventoried. The categories were:

- Architectural Surface Coating

- Commercial/Consumer Products
- Graphic Arts
- Autobody Surface Coating
- Industrial Surface Coating
- Surface Cleaning

1. Activity Level - Population

Population was used to estimate emissions from these sources. Census block population estimates for Washington from the 1990 Population Census were projected to 1996 using Washington State Office of Financial Management 1996 to 1990 county population ratios.[55, 56, 57] Spatial population for Oregon was obtained and projected to 1996 using Bureau of Census 1996 to 1990 county population ratios.[58, 59]

2. Temporal Adjustments

Seasonal and hourly adjustments were made using EPA adjustment factors.[60]

Table A-6. Area Source Adjustments

Category	Adjustments
Architectural Coating	33% summer, uniform hours 06-18, 7 d/w
Commercial/Consumer Solvents	80% hrs 06-18, 20% hrs 19-23, 7 d/w
Graphic Arts	90% hrs 06-18, 10% hrs 19-23, 6 d/w (used commercial fuel use as surrogate)
Autobody Refinishing	80% hrs 06-18, 20% hrs 19-23, 6 d/w (used degreasing as surrogate)
Industrial Surface Coating	80% hrs 06-18, 20% hrs 19-23, 6 d/w (used degreasing as surrogate)
Surface Cleaning	80% hrs 06-18, 20% hrs 19-23, 6 d/w

3. Spatial Allocation

The Census block population was allocated to the 5 km grid system using geographical information system methods.[57]

4. Emission Rates

No area specific information was gathered. All sources' emissions were based on national per capita factors.[60, 61] The per capita factors were multiplied by population estimates to calculate emissions. Table A-7 lists the factors in grams per person-yr.

Table A-7. Total Organic Compound Per Capita Emission Factors

Category	Factor
Architectural Surface Coating – Solvent	1036
Architectural Surface Coating – Water	611
Commercial/Consumer Solvents	3556
Graphic Arts	590
Autobody Refinishing	1043
Industrial Surface Coating	3992
Surface Cleaning	3266

Nonroad Mobile Sources

Using the ozone maintenance plans from PSAPCA and SWAPCA, most of the larger sources of VOC and NOx were inventoried.[30, 31] Locomotives and ships were fairly large sources of NOx, but due to difficulties in obtaining necessary information, they were not inventoried. Some smaller sources were also inventoried. The categories were:

- Boats
- Construction Equipment
- Commercial Equipment
- Industrial Equipment
- Lawn and Garden Equipment
- Recreational Vehicles

1. Activity Level - Population

Population was used to estimate emissions from these sources. Methods and sources were identical to those described previously under "Stationary Anthropogenic Sources."

2. Temporal Adjustments

Hourly adjustments were made using EPA adjustment factors.[60] The seasonal adjustments were taken from EPA's 1990 Non-road Study.[62]

Table A-8. Non-Road Mobile Adjustments

Category	Adjustments
Boats	57% summer, 30% M-F, 70% S-S, hours 06-18, 7 d/w (added one hour to the evening)
Construction Equipment	38% summer, uniform hrs 06-18 M-F, 06-11 Sat
Commercial Equipment	38% summer, uniform hrs 06-18 M-F, 06-11 Sat (used construction equipment as surrogate)
Industrial Equipment	25% summer, 80% hrs 06-18, 20% hrs 19-23, 6 d/w
Lawn and Garden Equipment	40% summer, 50% M-F, 50% S-S, hours 08-18
Recreational Vehicles	43% summer, 30% M-F, 70% S-S, hours 08-18

3. Spatial Allocation

The Census block population was allocated to the 5 km grid system using geographical information system methods.[57]

4. Emission Rates

Emission factors in grams per person-year were calculated using EPA's 1990 Non-road Study for the Seattle-Tacoma ozone nonattainment area.[62, 63, 64] Emission factors were calculated for each equipment type in each category above CO, NOx, HC, and SOx.

For future years' calculations, a November 24, 1994 EPA memorandum was used to calculate emissions reductions/increases.[65] The memorandum included percent reductions/increases in NOx and HC emissions for future years that could be applied to emissions inventories. For HC, the reductions had to apply to both exhaust and evaporative emissions, since no distinction was made.

Incorporation of Canadian Inventory

Information for on-road mobile and area sources for southern British Columbia were obtained from the Canadian National Research Council. The emissions were adjusted from their base year of 1993 to 1996 using population, vehicle miles traveled, and vehicle emission rate projections. The August 4th, 1993 Canadian on-road mobile file was adjusted, and used for all 1996 case days because the temperature range for that day was close to the temperature ranges experienced in the 1996 episodes. The Canadian area files were matched with 1996 case days based on day of week, and then adjusted for population growth between 1993 and 1996 by multiplying by 1.05 (ratio of 1996 to 1993 Washington State population).[55]

III. Biogenic Sources

In the program Biogenic Emissions Inventory System 2 (BEIS2), VOC emissions are calculated for isoprene, the sum of monoterpenes, and other VOC (OVOC). For each compound class, the following formulation is used to calculate the emission flux (mass/area/time) for a given landuse or vegetation class:

$$F = Fs*CL*CT$$

where Fs is the class specific emission flux for the specified compound class at 30°C and 1000 μmol/m^2/s PAR (photosynthetically active radiation), CL is a light correction factor and CT is a temperature correction factor. For this inventory, BEIS2 standard emission factors were used as given below.

Table A-9. BEIS2 Standard Emission Fluxes for 30°C and PAR=1000 μmol/m^2/s.

species/landuse	Flux in ug/m2-hr				% land area
	Isoprene	Terpenes	Other VOC	Soil NO	
grassland	37.8	94.5	56.7	57.8	36
conif. forest	524.2	1672	1781.2	3.5	16
Douglas fir	170	2720	2775	4.5	14
desert	65	94.5	56.7	57.8	5
western hemlock	79.3	158.7	1295	4.5	4
red alder	42.5	42.5	693.7	4.5	4
agriculture	7.6	19	11.4	12.8	3
rangeland	37.8	94.5	56.7	57.8	3
mixed ag & forest	265.9	845.5	896.3	8.1	2
ponderosa pine	79.3	2380	1295	4.5	2
lodgepole pine	79.3	2380	1295	4.5	2
western red cedar	170	1020	2775	4.5	1
bigleaf maple	42.5	680	693.7	4.5	1
Pacific Silver Fir	170	5100	2775	4.5	1
Oregon white oak	29750	85	693.7	4.5	1
Grand Fir	170	5100	2775	4.5	1
fir	170	5100	2775	4.5	0
hickory	42.5	680	693.7	4.5	0
hemlock	79.3	158.7	1295	4.5	0
black cottonwood	29750	42.5	693.7	4.5	0
urban	1022.45	402.1	502.15	31.15	0
sitka spruce	23800	5100	2775	4.5	0
spruce	23800	5100	2775	4.5	0
Sub-alpine fir	170	5100	2775	4.5	0
Noble fir	170	5100	2775	4.5	0

species/landuse	Flux in ug/m2-hr				% land area
	Isoprene	Terpenes	Other VOC	Soil NO	
mountain hemlock	79.3	158.7	1295	4.5	0
unknown	7.6	19	11.4	12.8	0
tundra	2411.7	120.6	150.7	0.2	0
Englemann spruce	23800	5100	2775	4.5	0
aspen	29750	42.5	693.7	4.5	0
cherry	42.5	42.5	693.7	4.5	0
Oregon ash	42.5	42.5	693.7	4.5	0
western larch	42.5	42.5	693.7	4.5	0
western white pine	79.3	2380	1295	4.5	0
Alaskan cedar	79.3	1269.3	1295	4.5	0
Pacific maldrone	42.5	42.5	693.7	4.5	0
ponderosa pine	79.3	2380	1295	4.5	0
paper birch	42.5	85	693.7	4.5	0
Pacific dogwood	42.5	680	693.7	4.5	0
Pacific yew	42.5	1275	693.7	4.5	0
paper birch	42.5	85	693.7	4.5	0
balsam poplar	29750	42.5	693.7	4.5	0
whitebark pine	79.3	2380	1295	4.5	0
gold chinkapin	42.5	42.5	693.7	4.5	0
ice	0	0	0	0	0
white alder	42.5	42.5	693.7	4.5	0
birch	42.5	85	693.7	4.5	0
apple	42.5	42.5	693.7	4.5	0
wetland	1050	660	770	0.2	0
California black oak	29750	85	693.7	4.5	0
White Fir	170	5100	2775	4.5	0
western juniper	79.3	476	1295	4.5	0
sub-alpine larch	42.5	42.5	693.7	4.5	0
larch	42.5	42.5	693.7	4.5	0
tamarack	42.5	42.5	693.7	4.5	0
white spruce	20400	5100	2775	4.5	0
black spruce	30600	5100	2775	4.5	0
willow	14875	42.5	693.7	4.5	0
Alaska paper birch	42.5	85	693.7	4.5	0

The formulations for CL and CT are given in BEIS2. For terpenes and OVOC, there is no light effect and CL is equal to 1. In the WABEIS model, microclimate solar radiation levels and leaf temperatures are estimated as a function of height within the canopy using a simple forest canopy model and leaf energy balance as described by Lamb et al. (1993). During daylight hours, the effects are to attenuate solar radiation downward through the

canopy, to increase leaf temperatures in the upper, exposed section of the canopy, and to decrease leaf temperatures due to shading in the lower sections of the canopy. In BEIS2, solar radiation is attenuated through the canopy, but leaf temperatures are assumed to equal above canopy temperatures. Hourly meteorological information from SeaTac and Portland International Airports was used to calculate CL and CT.[47] SeaTac data was used north of UTM 5140 km, and Portland data south of UTM 5140 km. In general, Portland temperatures were warmer, resulting in higher emissions.

Recent US Forest Service tree inventory data were obtained for western Washington, and these data were used to determine the distribution of forest species within Washington. These data included tree inventory information for approximately 2,000 plots within the state. For each plot, the data included number of trees, species types, tree sizes, and crown area. Plots represented approximately 3 mi. x 3 mi. areas and thus were approximately equal in size to a modeling grid. The information from the plots were used to determine the species distributions for each grid where a plot occurred and to determine the fraction of the grid area accounted for by the total crown area. The overall averages of these plot data are listed below:

Table A-10. Tree Species Distribution

Code	Genus	Examples	Percent of Crown Area
11	Abies	(fir)	5.3
17	Abies	(fir)	1.6
22	Abies	(fir)	0.2
42	Larix	(larch)	0.0
98	Picea	(spruce)	0.9
108	Pinus	(pine)	0.2
119	Pinus	(pine)	0.0
122	Pinus	(pine)	2.5
202	Pseudotsuga	(douglas fir)	38.5
231	Taxodium	(cypress)	0.0
242	Thuja	(W.red cedar)	5.9
263	Tsuga	(Eastern hemlock)	21.5
264	Tsuga	(Eastern hemlock)	0.7
312	Acer	(maple)	4.3
351	Alnus	(European alder)	14.3
361	Alnus	(European alder)	1.2
376	Betula	(birch)	0.8
492	Cornus	(dogwood)	0.0
542	Fraxinus	(ash)	0.2
746	Populus	(aspen)	0.0
747	Populus	(aspen)	1.2
760	Prunus	(cherry)	0.2
815	Quercus	(oak)	0.1

Code	Genus	Examples	Percent of Crown Area
999	Misc	crops	0.2

The gridded plot data were then combined with gridded land use obtained from the National Research Council of Canada for the photochemical modeling domain. These data were the dominant land use type in each grid for the land uses listed below. This list includes the overall distribution of land use types within the domain:

Table A-11. Land Use Distribution

Land use	Code	Percent Distribution
urban	1100	
agriculture	1200	6.6 (combined ag & urban)
irrigated agriculture	-1200	
rangeland	1300	20.6
forest	1400	34.4
water	1500	37.0
wetland	1600	0.0
barren	1700	0.9
tundra	1800	0.4
ice	1900	0.2

To combine the land use and species plot data, for each grid with a plot, the species distribution was used directly and the balance of the land area within the grid was represented by the land use. These plot data were then interpolated using an inverse distance squared routine where the existing land use type in a grid was modified according to the interpolation results for that grid. For example, given a grid with land use type equal to rangeland, the areal contribution of species from nearby plots is calculated and the rangeland area is reduced proportionally. The interpolation scheme is essentially identical to that used in the CALMET wind field interpolation. The weighting factor was taken to equal 5 km and the maximum distance for interpolation was 40 km.

The gridded areal distributions, the environmental correction terms from the canopy model, and the BEIS2 standard emission fluxes were combined to yield gridded fluxes of isoprene, terpenes, and OVOC for each hour of the selected modeling day. Soil NO emissions were also calculated as part of this method.

IV. Emissions Summaries for Washington and Oregon

Table A-12. Carbon Monoxide Emissions in Pounds per Day

Category	7-11 (Thu)	7-12 (Fri)	7-13 (Sat)	7-14 (Sun)
NRM Diesel	161,596	161,596	83,087	5,641
NRM Gasoline	2,212,574	2,212,574	4,826,911	4,359,668
ORM diesel	234,387	257,736	209,414	173,951
ORM gasoline	8,518,151	9,366,702	7,542,783	6,265,442
Longview Point	142,374	142,757	142,988	142,811
Other Point	1,177,064	1,181,342	1,189,377	1,188,303
TOTAL	***12,446,147***	***13,322,708***	***13,994,561***	***12,135,815***

Category	7-23 (Tue)	7-24 (Wed)	7-25 (Thu)	7-26 (Fri)	7-27 (Sat)	7-28 (Sun)
NRM Diesel	161,596	161,596	161,596	161,596	83,087	5,641
NRM Gasoline	2,212,574	2,212,574	2,212,574	2,212,574	4,826,911	4,359,668
ORM diesel	228,958	230,550	232,213	253,421	205,850	171,025
ORM gasoline	8,885,342	8,916,638	9,123,359	9,848,042	7,956,314	6,270,492
Longview Point	151,488	154,882	144,148	150,818	155,120	155,128
Other Point	1,185,788	1,181,374	1,184,262	1,187,458	1,189,662	1,189,662
TOTAL	***12,825,747***	***12,857,614***	***13,058,153***	***13,813,909***	***14,416,943***	***12,151,615***

Table A-13. Nitrogen Oxides Emissions in Pounds per Day

Category	7-11 (Thu)	7-12 (Fri)	7-13 (Sat)	7-14 (Sun)
Biogenics	107,377	120,377	129,614	132,515
NRM Diesel	289,192	289,192	159,441	19,512
NRM Gasoline	19,460	19,460	40,447	27,377
ORM diesel	414,799	456,120	370,604	307,844
ORM gasoline	905,072	995,232	803,409	667,355
Longview Point	27,825	26,631	26,994	27,227
Other Point	214,506	225,169	237,649	242,144
TOTAL	***1,978,230***	***2,132,181***	***1,768,158***	***1,423,974***

Category	7-23 (Tue)	7-24 (Wed)	7-25 (Thu)	7-26 (Fri)	7-27 (Sat)	7-28 (Sun)
Biogenics	123,007	123,767	122,643	123,338	123,038	106,222
NRM Diesel	289,192	289,192	289,192	289,192	159,441	19,512
NRM Gasoline	19,460	19,460	19,460	19,460	40,447	27,377
ORM diesel	419,377	422,292	425,339	464,184	377,049	313,262
ORM gasoline	914,136	918,313	926,443	1,008,333	815,009	691,400
Longview Point	21,584	24,469	23,245	24,322	28,537	28,413
Other Point	237,360	247,667	251,661	251,766	253,993	254,856
TOTAL	***2,024,116***	***2,045,160***	***2,057,985***	***2,180,595***	***1,797,514***	***1,441,041***

Table A-14. Sulfur Dioxide Emissions in Pounds per Day

Category	7-11 (Thu)	7-12 (Fri)	7-13 (Sat)	7-14 (Sun)
NRM Diesel	24,853	24,853	13,334	1,476
NRM Gasoline	1,428	1,428	4,113	3,834
ORM diesel	12,439	13,678	11,114	9,232
ORM gasoline	35,311	38,828	31,549	26,206
Longview Point	19,212	20,676	21,389	19,195
Other Point	559,399	638,091	708,725	717,306
TOTAL	***652,642***	***737,556***	***790,222***	***777,250***

Category	7-23 (Tue)	7-24 (Wed)	7-25 (Thu)	7-26 (Fri)	7-27 (Sat)	7-28 (Sun)
NRM Diesel	24,853	24,853	24,853	24,853	13,334	1,476
NRM Gasoline	1,428	1,428	1,428	1,428	4,113	3,834
ORM diesel	12,355	12,441	12,531	13,675	11,108	9,229
ORM gasoline	35,072	35,316	35,571	38,820	31,533	26,198
Longview Point	16,739	16,782	15,664	16,230	17,187	19,205
Other Point	712,572	772,838	799,015	710,379	721,427	746,388
TOTAL	***803,020***	***863,659***	***889,062***	***805,385***	***798,701***	***806,330***

Table A-15. Volatile Organic Compound Emissions in Pounds per Day

Category	7-11 (Thu)	7-12 (Fri)	7-13 (Sat)	7-14 (Sun)
Area sources	677,276	680,941	673,625	258,235
Biogenics	8,396,762	10,052,215	11,426,482	11,662,996
NRM Diesel	36,652	36,652	20,712	3,129
NRM Gasoline	284,944	284,944	886,816	857,405
ORM diesel	53,441	58,765	47,747	39,661
ORM gasoline	1,012,180	1,113,010	907,116	753,499
Longview Point	12,486	13,008	13,008	13,008
Other Point	144,120	144,247	144,291	144,333
TOTAL	***10,617,862***	***12,383,783***	***14,119,797***	***13,732,267***

Category	7-23 (Tue)	7-24 (Wed)	7-25 (Thu)	7-26 (Fri)	7-27 (Sat)	7-28 (Sun)
Area sources	677,439	677,697	678,047	681,245	674,334	257,727
Biogenics	10,549,814	10,436,225	10,325,375	10,395,777	10,414,243	8,055,583
NRM Diesel	36,652	36,652	36,652	36,652	20,712	3,129
NRM Gasoline	284,944	284,944	284,944	284,944	886,816	857,405
ORM diesel	55,924	56,313	56,719	61,899	50,280	41,774
ORM gasoline	1,040,354	1,046,883	1,091,629	1,161,240	951,939	713,388
Longview Point	12,842	13,406	13,018	13,239	13,416	12,804
Other Point	144,667	144,613	144,763	144,793	155,000	155,000
TOTAL	***12,802,636***	***12,696,734***	***12,631,146***	***12,779,790***	***13,166,741***	***10,096,811***

V. Nitrogen Oxide and Hydrocarbon Speciation

Hydrocarbon and nitrogen oxide emissions had to be speciated according to the chemical lumping mechanism in CALGRID.

1. Hydrocarbon Speciation

Speciation was accomplished in one of four ways:

- profiles from the SPECIATE database[66]
- profiles from NCASI Technical Bulletin No. 701, Tables 3, 5, 8, 12A, 13A, 15A, 17, and 19A.[21]
- profiles provided by the facility (point sources)
- profiles from the Emission Inventory Improvement Program documents[61]

Emissions obtained from the WEDS database was assumed to be "as total VOC", unless otherwise specified.

For sources where no specific information on speciation was available, profiles from EPA's SPECIATE database were used. Pollutant percents were queried from the whole set of profiles chosen, and all that were less than one percent of every profile were eliminated. Gasoline marketing proved to have the largest percentage removed (8.5%). Profiles were then recalculated with the remaining pollutants to total 100%.

Each pollutant in a profile was assigned a SAROAD code according to the lumping scheme provided by the National Research Council (NRC) in Ottawa, Canada. Pollutants that did not match a specific SAROAD code were assigned to a SAROAD code of a closely related compound or group of compounds.

2. Nitrogen Oxides Speciation

NOx emissions from combustion sources were assumed to be comprised of 90% nitrogen oxide (NO) and 10% nitrogen dioxide (NO_2)

1. Washington Emissions Data System, 1994 and 1995.

2. John Michaelson, Intalco Aluminum Corp., facsimile October 30, 1996.

3. Steven Mrazek, Vanalco, Inc., written correspondence October 23, 1996.

4. Tom Dickey, Reynolds Metals, phone conversation October 22, 1996.

5. Paul Schmeil, Kaiser Aluminum, facsimile November 12, 1996.

6. Richard Abrams, Kimberly-Clark, written correspondence October 28, 1996.

7. Kip Whitehead, Georgia-Pacific, written correspondence.

8. McCollister, James River Corporation, written correspondence November 1, 1996.

9. Greg Narum, Simpson Tacoma Kraft Co., written correspondence November 5, 1996.

10. Al Gould, Port Townsend Paper Corporation, written correspondence October 16, 1996.

11. James W. Yount, Weyerhaeuser Company, written correspondence December 2, 1996.

12. Steven D. DuVall, Longview Fibre Company, written correspondence October 31, 1996.

13. Timothy R. Gould, Southwest Air Pollution Control Authority, written correspondence November 19, 1996, phone conversation June 30 - July 1, 1997.

14. Bryan Alexander, Tenaska Ferndale Cogeneration Facility, written correspondence October 22, 1996.

15. Flagg, Texaco Refining and Marketing, Inc., written correspondence to Axel Franzmann of Northwest Air Pollution Control Authority October 31, 1996.

16. Walter O. Williamson, ARCO Products Company, written correspondence to Axel Franzmann of Northwest Air Pollution Control Authority November 4, 1996.

17. Russell L. Knepper, Calpine (SUMAS Cogeneration Project), written correspondence to Axel Franzmann of Northwest Air Pollution Control Authority October 21, 1996.

18. Sandy Paris, TOSCO Ferndale Refinery, facsimile to Axel Franzmann of Northwest Air Pollution Control Authority October 31, 1996.

19. Axel Franzmann, Northwest Air Pollution Control Authority for March Point Cogeneration Company, facsimile November 26, 1996.

20. AP42. Fifth Edition, January 1995.

21. National Council for the Paper Industry for Air and Stream Improvement, Inc., Compilation of 'Air Toxic' and Total Hydrocarbon Emissions Data for Sources at Chemical Wood Pulp Mills, Technical Bulletin No. 701: Volumes 1 and 2, October 1995.

22. Puget Sound Regional Council, ADVMT via Sierra Research.

23. Regional Transportation Council. 1351 Officers' Row; Vancouver, Washington 98661. Steve Kelley.

24. Thurston Regional Planning Council. 2404 Heritage Court Southwest #B; Olympia, Washington 98502-6031. Paula Reeves.

25. METRO. 600 Northeast Grand Avenue; Portland, Oregon 97232-2736. Cindy Peterson and Jean Alleman.

26. Washington State Department of Transportation. ADVMT data from TRIPS, HPMS and GIS systems. Elizabeth Church (TRIPS), Pat Whitaker (HPMS), Marci Mitchell and Ron Cihon (GIS), Lloyd Fergestrom (MPO liaison).

27. Oregon Department of Transportation. ADVMT from ArcView shape file of the Oregon state highway system. Janet Shearer and Roxann Rivord.

28. Oregon Department of Transportation. "Daily Vehicle Miles Traveled." 1996 ADVMT. Available through ODOT Internet homepage.

29. "Forecast of Fuel, Vehicles, and Related Data Through 2015 (Forecast 9506)." Washington State Department of Transportation. Rick Judd.

30. Supplement to the State Implementation Plan for Ozone (O3) in Vancouver, WA, Redesignation request for Portland/Vancouver as Attainment for Ozone. Southwest Air Pollution Control Authority. June 1996.

31. Central Puget Sound Region Redesignation Request and Maintenance Plan for the National Ambient Ozone Standard. Puget Sound Air Pollution Control Agency. November 1995.

32. "Adjustment Factors for Vehicle Miles Traveled." Washington State Department of Transportation. Barbara Hertzog and Hank Borden. July 1992.

33. Annual Traffic Report. Washington State Department of Transportation. Pages XVI - XX (monthly traffic count data).

34. MOBILE5b. Model and User's Guide. Environmental Protection Agency, Office of Mobile Sources. September 1996.

35. PART5. Model and User's Guide. Environmental Protection Agency, Office of Mobile Sources. February 1995.

36. "Department of Ecology (Vehicle Emissions) Test Results for June 1 – December 31, 1994." Washington State Department of Ecology. February 1, 1995.

37. "Audit of Vehicles with September, 1990 Expiration Date." Department of Ecology Air Quality Program.

38. Personal conversation with Stan Sumich, Oregon Department of Environmental Quality.

39. Personal conversation with David Brzezinski, USEPA Office of Mobile Sources.

40. Supplement to the State Implementation Plan for Ozone (O3) in Vancouver, WA, Redesignation request for Portland/Vancouver as Attainment for Ozone. Southwest Air Pollution Control Authority. June 1996.

41. 1987 Compliance Survey, Bellevue and Spokane. Washington State Department of Ecology.

42. 40 CFR 80.27.

43. Motor Vehicle Manufacturing Association National Gasoline Survey. Seattle 1990 survey data.

44. "Motor Vehicle Fuel Properties." Washington State Department of Agriculture. 1994.

45. Personal conversation with Jennifer Brown, Southwest Air Pollution Control Authority.

46. Hourly temperature data from meteorological station at Sand Point, WA, 1996.

47. Hourly meteorological data from SeaTac and Portland International Airports, 1996. Available through the University of Washington.

48. "Motor Vehicle Registrations by Year W/N Class." Washington State Department of Licensing. July 1994 – June 1996.

49. Puget Sound Air Pollution Control Agency gasoline station database.

50. Olympic Air Pollution Control Authority gasoline station database.

51. Northwest Air Pollution Authority gasoline station database.

52. Southwest Air Pollution Control Authority gasoline station database.

53. Washington State Department of Ecology Northwest Regional Office gasoline station database.

54. AP42. Fifth Edition, January 1995. Table 5.2-7 (Evaporative Emissions from Gasoline Service Station Operations).

55. Population Trends. State of Washington Office of Financial Management, Forecasting Division. Table 4. October 1996.

56. METRO. 600 Northeast Grand Avenue; Portland, Oregon 97232-2736. 1995 Population Density Map. Bob Knight.

57. Population Census gridded into 5 km grids. Tom Schuettke, Washington State Department of Ecology.

58. Spatial population data for Oregon. State Service Center for Geographic Information Systems (GIS). 1990 population.

59. Bureau of the Census Internet homepage. Oregon population data by county for 1996.

60. Procedures for the Preparation of Emission Inventories for Carbon Monoxide and Precursors of Ozone. Volume I, tables 4.3-4 and 5.8.1; and Volume II, table 6-11. EPA-450/4-91-016, May 1991 (vol. I), EPA-454/R-92-026, March 1992 (vol. II).

61. Area Source Chapter documents. Prepared by Radian Corporation for Area Sources Committee of the STAPPA-ALAPCA Emission Inventory Improvement Program (EIIP): Architectural Surface Coating (Final Draft 11/95), Consumer and Commercial Solvents (Final 8/96), Auto Body Refinishing (External Draft 7/96), Graphic Arts (Final 11/96), Industrial Surface Coating (External Draft 7/96).

62. Non-road Engine Emission Inventories for CO and Ozone Nonattainment Boundaries Seattle-Tacoma. Energy and Environmental Analysis, Inc. Arlington, Virginia. Inventory (A+B)/2. Spreadsheets dated Aug. 25 and 26, 1992.

63. Procedures for Emission Inventory Preparation, Vol. IV: Mobile Sources. EPA-450/4-81-026d (Revised), Section 4.0.

64. Non-road Engine and Vehicle Emissions Study - Report. USEPA, Office of Air and Radiation (ANR-433), Washington DC, 20460. 21A-2001, November 1991.

65. "Future Non-road Emission Reduction Credits for Court-Ordered Non-road Standards." Memorandum dated November 28, 1994 from Philip A. Lorang, Director Emission Planning and Strategies Division, US Environmental Protection Agency.

66. SPECIATE database. USEPA.

Appendix B
Meteorological Modeling

Introduction

Wind, temperature, and turbulence fields were developed using predicted winds and temperatures from the MM5 mesoscale prognostic model, along with upper air and surface observations, as input into the CALMET diagnostic meteorological model. Output from the CALMET model were used directly as input to the CALGRID air quality model.

MM5 Output

MM5, developed by Pennsylvania State University and the National Center for Atmospheric Research, was applied to the Cascadia region to provide an initial hourly wind field for CALMET. MM5 solves the non-hydrostatic prognostic equations describing the atmospheric boundary layer.

The largest domain, D1, consists of a 100 rows and 76 columns with a horizontal grid resolution of 45km. The intermediate domain, D2, contains 76 rows and 76 columns with a grid resolution of 15km. Finally, the innermost domain, D3, encompasses most of Oregon and Washington, and contains 148 rows and 76 columns with a grid resolution of 5km. High resolution terrain and landuse data (grid scale of approximately 1 km) were aggregated to the appropriate grid scales for MM5's three nested domains. In the vertical dimension, thirty-two sigma layers are specified, with the first eight layers existing within the first kilometer of the boundary layer. The three MM5 domains are shown in Figure B-1.

One-way nesting, the medium range forecast (MRF) planetary boundary layer (PBL) scheme (Hong and Pan, 1996), a multi-layer soil temperature model, and the Kain-Fritsch cumulus parameterization scheme (Kain and Fritsch, 1993) were employed in the MM5 simulation. The MRF PBL scheme is suitable for a high-resolution description of the boundary layer. The five layer soil model responds to time scales less than the diurnal cycle to allow for a rapid surface temperature changes. The Kain-Fritsch cumulus parameterization is applied during convectively unstable conditions when sufficient vertical motion and cloud depths prevail.

Four-dimensional data assimilation (FDDA) was applied to the outer (D1) domain. This methodology applies Newtonian relaxation, or *nudging*, to the solution by adding artificial tendency terms to one or more of the prognostic equations to relax the model to the gridded analysis or observations. Specifically, gridded analysis nudging (vs. observational nudging) was applied to the outer domain. Analysis nudging involves nudging the entire solution toward gridded analyses that are based on synoptic observations, and differs from observational nudging which nudges the solution towards individual observations in the vicinity of the observation. The nudging coefficient was $2.5(10^{-4})$. Stauffer and Seaman (1994) conducted a study regarding the best application of FDDA methods and found that analysis nudging on the meso-alpha scale coupled with observational nudging on the finest scale offered the best simulation solution. Future MM5 simulations will incorporate both gridded analysis nudging and observational nudging. The MM5 results were obtained from simulations conducted at WSU.

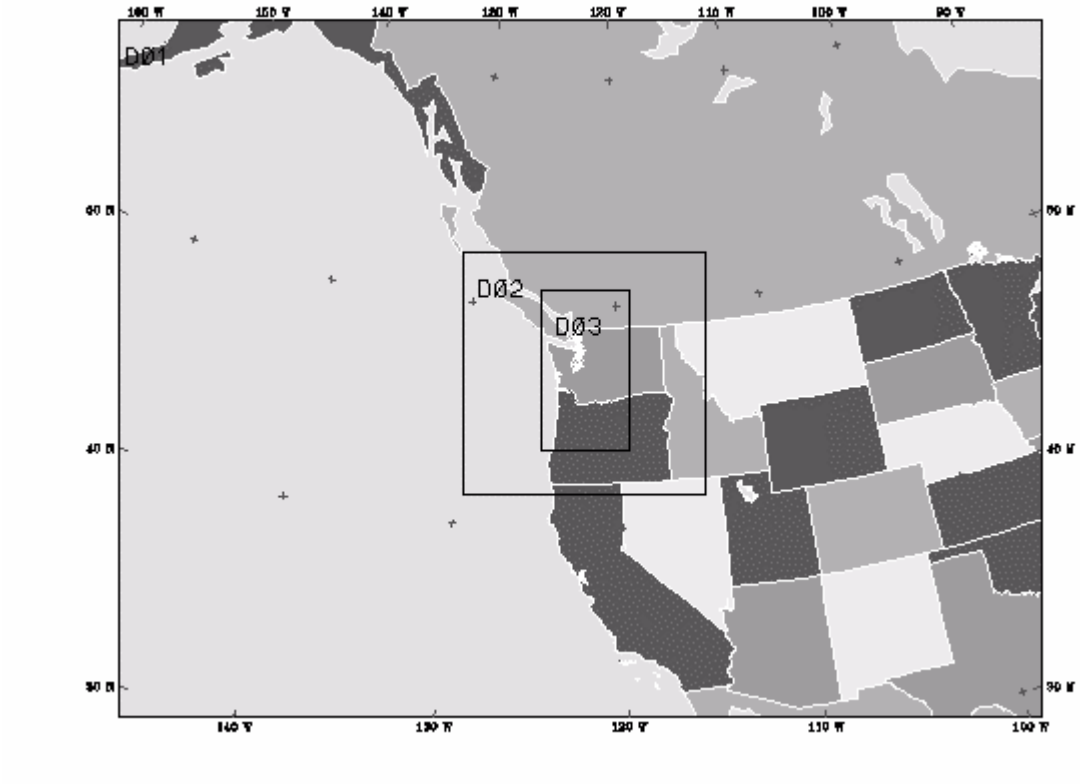

Figure B-1. Nested MM5 domains with 45 km, 15 km, and 5 km grid resolution.

CALMET Application

The diagnostic meteorological model CALMET was developed by Sigma Research Corp. for the California Air Resources Board (CARB), and can be coupled directly with both the Eulerian photochemical model CALGRID and the Lagrangian puff model Calpuff. CALMET consists of two components: a diagnostic wind field module that generates a description of the surface and upper level winds, and a micrometeorological module that calculates various components of overland and overwater boundary layers (e.g., temperature, mixing depth, PGT stability class).

CALMET develops the wind field using a three step process (Scire et al, 1995). First, an "initial guess" wind field is created, either by applying upper air observations to the entire domain, or through the introduction of prognostic model data, e.g., an MM5 solution. Next, the "step 1" wind field is calculated by adjusting the initial guess wind field for kinematic effects of terrain, slope flows, and terrain blocking (based on the local Froude number). Finally, observational data are introduced through an objective analysis procedure to create the "step 2" wind field. CALMET's objective analysis feature forces the predicted wind field towards the observations, with the relative weighting factor of the observations vs. the step 1 wind field specified by the user.

Two methods were used to introduce the 5 km MM5 wind field to CALMET. The first method treated the MM5 data as "psuedo-observations." One psuedo-observation was available for each CALMET node. The real observations were withheld from the solution and used for model validation. This resulted in CALMET merely passing through the MM5 wind field without modification, and rearranging the data in a format suitable for CALGRID. The second method assigned the MM5 wind field as CALMET's initial guess wind field. Again, one MM5 value was assigned to each CALMET node. The terrain corrections applied in the formulation of the step 1 wind field were not invoked. CALMET's objective analysis feature was used to force the predicted wind field towards the observations. A small subset of the surface meteorological sites were withheld from the objective analysis process to be used for validation of the surface wind field. It should be noted that in either case, the MM5 data input into CALMET only influenced the wind field prediction, and had no influence on the CALMET boundary layer module.

Although it was originally intended to operate CALMET using the first method described above (a pass through of the MM5 wind field without alteration), it became apparent that applying the objective analysis feature would be desirable in several portions of the domain. As a result, a series of CALMET runs was conducted to obtain an optimal wind field where the comparison with surface wind observations and surface ozone observations was used to judge the suitability of each iterative solution. The results presented in the remainder of this paper are based on the final wind fields obtained through this iteration of CALMET predictions. While this approach yields good model performance in terms of ozone predictions, the empirical nature of the iterative method is not a preferred method.

The CALMET and CALGRID domains are equivalent. The domain extends 660 km north-south by 370 km east-west, and covers western Washington, northwestern Oregon, and a small portion of southwestern British Columbia. The horizontal grid resolution is 5 km, resulting in 74 columns by 132 rows. Ten vertical layers are employed as indicated in Table B-1.

Table B-1. Layer Center Height

Layer	Height Above Surface (m)
1	10
2	50
3	120
4	190
5	335
6	535
7	930
8	1700
9	2900
10	4300

Land use and terrain data for the CALMET domain were taken from the University of Washington MM5 1 km data sets. Historical surface and upper air observations were incorporated into the model during execution. Data from 25 surface stations and 1 upper air station were incorporated into the model.

These data were screened for missing hours in the modeling interval. When an hour was missing, wind speed, direction, and temperature were interpolated in time from the existing data. Because CALMET requires at least one surface station to have pressure and cloud cover data at each hour, the observations for Seattle-Tacoma AP were modified to meet this requirement. Where data were missing, the value was interpolated in time from the nearest data available.

The Quillayute sounding was used to determine the lapse rate and the Seattle-Tacoma AP station was used for the surface temperature. A summary of all of the model input and control parameters is given in Table B-2.

Table B-2. Base case model control and input parameters for CALMET.

Model Parameter	Base Case Input Value	Comments
CALMET Parameters		
horizontal grid scale	5 km	
number of x grids	74	east-west
number of y grids	132	north-south
origin (x,y)	350E, 4900 N km	UTM Zone 10
number of vertical layers	10	
vertical face heights	see Table B-1	
number of surface stations	25	hourly average data
number of upper air stations	1	twice daily observations
MM5 initialization	Same inner domain as for CALMET, 5 km grid size	
time step	1200 s	
wind field adjustments	No terrain adjustments	
	surface obs extrapolated to upper layers using a power law method	
radius of influence of met stations	50 km	
radius of influence of terrain	5 km	
weighting distance where surface obs = upper air obs	25 km	
divergence criteria	5×10^{-6}	

The modeling period begins at midnight LST on July 11th, 1996, and covers 96 hours terminating at midnight LST on July 14th, 1996. The CALMET model was run on an HP 9000-C100 workstation. For this event, the required CPU time was 26,272 seconds and required 41,963 seconds to execute.

Appendix C
CALGRID Simulations

Introduction

The CALGRID air quality model predicts gridded, hourly concentrations for specified pollutants. Several input files are required for operation; these files specify the meteorology, surface emissions, initial and boundary conditions, and the chemistry mechanism. In addition, a user control file, CALGRID.INP, declares the various run-time options for CALGRID (e.g., duration of the simulation, domain specifications, dry deposition parameters, treatment of horizontal/ vertical diffusion, output options, etc.). CALGRID Version 1.6/S90 was used for this study.

CALGRID Input Files

Seven input files were used during CALGRID simulations conducted for this study. These files contain the following information:

- model control and operation (CALGRID.INP),
- meteorology (CALMET.DAT; described in Appendix C)
- initial/boundary concentrations (ICON.DAT)
- area and point source emissions (AREM.DAT and PTEMARB.DAT, respectively; described in Appendix B)
- chemistry mechanism definition and parameters (COND2243.MOD and CD2243V2.RXP, respectively)

A summary of each file is given in Table C-1.

Table C-1. CALGRID Input Files

Input File Name	Description	Format
CALGRID.INP	User control file (described above)	formatted
CALMET.DAT	Geophysical data: surface roughness length land use categories terrain elevations leaf area index Gridded hourly meteorological data: u,v,w wind components air temperature surface friction velocity mixing height convective velocity scale Monin-Obukhov length	unformatted

Input File Name	Description	Format
	PGT stability class Surface station hourly meteorological data: air density air temperature short-wave solar radiation relative humidity	
ICON.DAT	Initial and boundary concentrations	formatted
AREM.DAT	Gridded hourly emissions for anthropogenic and biogenic area sources	unformatted
PTEMARB.DAT	Gridded hourly emissions data for anthropogenic point sources	unformatted
COND2243.MOD	Chemical mechanism definition file for the SAPRC 90 chemistry mechanism	formatted
CD2243V2.RXP	Emission-specific chemical data file for the SAPRC 90 chemistry mechanism	formatted

Model Domain

The CALGRID model domain was the same as described for CALMET in Appendix B. The domain measured 74 x 132 grids horizontally with a 5 km grid resolution and 10 vertical layers. The vertical layers have variable spacing and extend to 5000 m above the surface.

Chemistry Mechanism

The CALGRID chemistry mechanism is based on the widely used SAPRC90 system developed by Carter for California's Statewide Air Pollution Research Center (SAPRC). The SAPRC90 system generates two input files (COND2243.MOD and CD2243V2.RXP) and three mechanism-specific subroutines to be incorporated into CALGRID (BLDUP, CONSTR, and DIFUN). The chemistry mechanism is defined in the COND2243.MOD input file. COND2243.MOD contains 54 chemical species and 129 reactions. A description of the volatile organic compounds (VOC's) is shown in Table C-2.

Table C-2. Volatile Organic Compounds Included in the SAPRC90 Chemistry Mechanism

SAPRC90 Model Species Name	Description
ETHE	Ethene
MEOH	Methanol
ETOH	Ethanol
MTBE	Methyl t-butyl ether
HCHO	Formaldehyde

SAPRC90 Model Species Name	Description
CCHO	Acetaldehyde
RCHO	Propionaldehyde and higher aldehydes
MEK	Methyl ethyl ketone and higher ketones
CRES	Cresols and other alkyl phenols
MGLY	Methyl glyoxyl
ALK1	1st lumped group of alkanes (k_{OH} < 1.0 E4 ppm^{-1} min^{-1})
ALK2	2nd lumped group of alkanes (k_{OH} > 1.0 E4 ppm^{-1} min^{-1})
ARO1	1st lumped group of aromatics (k_{OH} < 2.0 E4 ppm^{-1} min^{-1})
ARO2	2nd lumped group of aromatics (k_{OH} > 1.0 E4 ppm^{-1} min^{-1})
OLE1	1st lumped group of anthropogenic alkenes (k_{OH} < 7.5 E4 ppm^{-1} min^{-1})
OLE2	2nd lumped group of anthropogenic alkenes (k_{OH} > 7.5 E4 ppm^{-1} min^{-1})
OLE3	3rd lumped group of primarily biogenic alkenes (iosprene, terpenes)

Emissions-weighted kinetic and mechanistic parameters for the seven lumped VOC's are specified in the CD2243V2.RXP file. CD2243V2.RXP was developed by the National Research Council of Canada (NRC) using Carter's software for a CALGRID application to the Lower Fraser Valley of southwestern British Columbia. It was assumed that the emissions profile used to develop the parameters in CD2243V2.RXP was similar to the one used in this study, and hence would better describe the lumped VOC behavior as compared to the default parameter file. For example, both the NRC study and this study were conducted in the Pacific Northwest, where a sizable portion of the VOC emissions are attributed to biogenic production; this would be directly reflected in the rate constants calculated for OLE3. In contrast, the default parameter file that is shipped with CALGRID is based on emissions data collected during the South Coast Air Quality Study (SCAQS), which are probably much less representative of the Pacific Northwest emissions profile.

Initial and Boundary Conditions

The initial and boundary concentrations of each model species were specified in the ICON.DAT file. It was assumed that the CALGRID model domain was large enough to encompass all significant urban pollution sources, and hence the model boundary could be described as a relatively clean, rural atmosphere. Ambient VOC measurements collected at Wynoochee Dam on Washington's Olympic Peninsula, along with trace gas concentrations stated in the literature, were used to determine the initial and boundary concentrations in ICON.DAT. An extra day was added at the beginning of each simulation to "wash out" the effects of the initial concentration field. The initial and boundary concentrations are shown in Table C-3.

Table C-3. Initial and boundary concentrations specified in ICON.DAT

	Model Species	Initial/boundary concentration (ppbV)
Ozone	O3	30
Nitric Oxide	NO	0
Nitrogen Dioxide	NO2	0.2
Lumped Alkane Group 1	ALK1	5.75
Lumped Alkane Group 2	ALK2	0.97
Lumped Aromatic Group 1	ARO1	1.52
Lumped Aromatic Group 2	ARO2	3.17
Methanol	MEOH	0
Ethanol	ETOH	0
Methyl t-butyl ether	MTBE	0
Ethylene	ETHE	0.3
Lumped Olefin Group 1	OLE1	0.33
Lumped Olefin Group 2	OLE2	0
Lumped Olefin Group 3	OLE3	0.86
Formaldehyde	HCHO	0.31
Acetaldehyde	CCHO	0.32
Higher Aldehydes	RCHO	0
Methyl Ethyl Ketone	MEK	0.39
Cresols	CRES	0
Methyl Glyoxal	MGLY	0
Aromatic Fragments	AFG2	0
NO_3 Radicals	NO3	0
N_20_5	N2O5	0
Nitric Acid	HNO3	0.1
Nitrous Acid	HONO	0
Peroxynitric Acid	HNO4	0
HO_2 Radical	HO2.	0
Carbon Monoxide	CO	200
Hydrogen Peroxide	HO2H	2
Sulphur Dioxide	SO2	0
Alkyl Peroxy Radical	RO2.	0
Peroxy Acetyl Radical	CCO-O2.	0
Higher Peroxy Radicals	C2CO-O2.	0
Hydroperoxy Group	-OOH	0
Lumped Organic Nitrates	RNO3	0
Peroxy Acetyl Nitrate	PAN	0
Peroxy Propionyl Nitrate	PPN	0

Dry Deposition of Gases

Five gases were dry deposited during CALGRID simulations: ozone, nitrogen dioxide, nitric acid, peroxy acetyl nitrate, and hydrogen peroxide. The surface layer dry deposition flux is calculated as

$$F_{dd} = v_d C_s$$

where

F_{dd} = dry deposition flux at the surface (g m^{-2} s^{-1})
v_d = vertical deposition velocity (m s^{-1})
C_s = pollutant concentration (g m^{-3})

The vertical deposition velocity can be specified by the user in the VD.DAT input file or calculated using a resistance model. All simulations performed for this study used the resistance model. The resistance model defines the deposition velocity as the inverse of the sum of three resistances that exist at the surface:

$$v_d = (r_a + r_d + r_c)^{-1}$$

where
r_a = atmospheric resistance through the surface layer
r_d = deposition layer resistance
r_c = vegetation layer resistance

r_a, r_d, and r_c are defined in the CALGRID User's Manual. r_c requires several user-supplied parameters (specified in CALGRID.INP); these are given in Table D-4.

Table C-4. Vegetation Layer Deposition Parameters

Species Name	Diffusivity (cm^2 s^{-1})	Alpha Star	Reactivity	Mesophyll Resistance (cm s^{-1})	Henry's Law Coefficient (dimensionless)
O3	0.1594	10.00	15.0	4.0	2.0
NO2	0.1656	1.00	8.0	5.0	3.5
HNO3	0.1628	1.0	18.0	0	8.0 E-8
HO2H	0.2402	1.00	12.0	0.0	4.0 E-7
PAN	0.1050	1.00	4.0	1.0	1.0 E-2

Previous applications of CALGRID at Washington State University indicated that there was an error in the implementation of the dry deposition removal process. To correct this, the original implicit Crank-Nicholson scheme was modified to explicitly account for mass removal at the surface. This modification resulted in very close agreement between the CALGRID-predicted

deposition loss and the predicted deposition loss calculated using a mass balance for each cell volume.

Horizontal and Vertical Diffusion

Turbulent diffusion processes in CALGRID were treated using simplified K-theory closure, i.e.

$K_h = K_{xx} = K_{yy}$
$K_v = K_{zz}$

where K_h and K_v are the horizontal and vertical eddy diffusivity coefficients, respectively, and K_{xx}, K_{yy} and K_{zz} are the diagonal terms of the eddy diffusivity tensor.

Horizontal Diffusion

CALGRID uses a combination of two methods to calculate K_h. The first uses the simplified Smagorinsky formulation, which defines the eddy diffusivity coefficient as a function of the stress in the horizontal wind field. Using the Smagorinsky formulation, the non-dimensionalized, horizontal eddy diffusivity coefficient, K_a, is defined as

$$K_a = \alpha_o^2 D \Delta t$$

where

$\alpha_o \cong 0.28$, an empirical constant
Δt = time step (s)

$$D = \left[\left(\frac{\partial v}{\partial x} + \frac{\partial u}{\partial y} \right)^2 + \left(\frac{\partial u}{\partial x} + \frac{\partial v}{\partial y} \right)^2 \right]^{1/2} \ (s^{-1})$$

D characterizes the stress in the wind field and can be computed directly from the existing u, v component supplied by CALMET.

The second method for calculating K_h uses parameterizations developed by Briggs, where the horizontal eddy diffusivity coefficient is defined as a function of the atmospheric stability. This second method is necessary when a uniform horizontal wind field exists (D = 0). The constants shown in Table C-5 are multiplied by the mean horizontal wind speed to determine the horizontal eddy diffusivity coefficient.

Table C-5. Horizontal Eddy Diffusivity Parameters Defined by Atmospheric Stability Class

Atmospheric Stability Class	Suggested Diffusivity Constant ($m^2 s^{-1}$ / u ($m s^{-1}$))
A	224
B	96
C	32
D	0
E	0
F	0

During stable conditions (classes D - F), K_h is not calculated.

Vertical Diffusion

Calculations for vertical diffusion in CALGRID were based on convective scaling theory for the daytime boundary layer and local (or z-less) scaling theory for the nighttime boundary layer. Calculating the vertical eddy diffusivity coefficient required CALMET data for the mixing height, surface friction velocity, Monin-Obukhov length, and convective scaling height. Using these data, CALGRID defines K_z for the three cases of the convective, stable and neutral boundary layer. These formulations are described in the CALGRID User's Manual.

Computer Requirements

All CALGRID simulations were performed on a Hewlett-Packard 9000/C100 workstation with a 100 MHz PA-RISC 7200 processor and 128 MB of memory. A typical CALGRID run required approximately 15 minutes of CPU time for each simulated hour. Between 0.5 and 1 GB of storage space was required to archive each CALGRID simulation.